Universitat Autònoma de Barcelona

Promoting Autotrophic Sulfate Reduction and Elemental Sulfur Recovery in Bioelectrochemical Systems

Enric Blázquez Ribas

Universitat Autònoma de Barcelona

Escola d'Enginyeria

Departament d'Enginyeria Química, Biològica i Ambiental

Promoting Autotrophic Sulfate Reduction and Elemental Sulfur Recovery in Bioelectrochemical Systems

PhD Thesis

Programa de Doctorat de Ciència i Tecnologia Ambientals

Institut de Ciència i Tecnologia Ambientals

Enric Blázquez Ribas

Abril 2019

GENOCOV
Departament d'Enginyeria Química
Escola d'Enginyeria
Universitat Autònoma de Barcelona
Tel: 93 5811587

JUAN ANTONIO BAEZA i LABAT, ALBERT GUISASOLA i CANUDAS i DAVID GABRIEL i BUGUÑA, professors agregats del Departament d'Enginyeria Química, Biològica i Ambiental de la Universitat Autònoma de Barcelona,

CERTIFIQUEM:

Que l'ambientòleg ENRIC BLÁZQUEZ RIBAS ha realitzat sota la nostra direcció el treball amb títol "Promoting Autotrophic Sulfate Reduction and Elemental Sulfur Recovery in Bioelectrochemical Systems" que es presenta en aquesta memòria i que constitueix la seva Tesi per optar al Grau de Doctor per la Universitat Autònoma de Barcelona.

I per a què se'n prengui coneixement i consti als afectes oportuns, presentem a l'Escola d'Enginyeria de la Universitat Autònoma de Barcelona l'esmentada Tesi, signant el present certificat a

Bellaterra, 9 d'abril de 2019

Dr. Juan Antonio Baeza i Labat	Dr. Albert Guisasola i Canudas	Dr. David Gabriel i Buguña

Agraïments

Aquest és l'últim capítol que escric dins d'aquest manuscrit. És potser el més fàcil d'escriure perquè surt de mi, no dels experiments. Però alhora és complicat. Són moltes emocions les que et passen pel cap. Molts moments viscuts durant aquesta muntanya russa que és la tesi doctoral. Però considero que he tingut sort, i així ho vull agrair en les següents pàgines a totes les persones que han compartit aquest camí amb mi.

Primer de tot vull agrair als meus directors. Gràcies Juan, Albert i David. Encara recordo quan al principi del treball final de màster vaig comentar a en Juan que volia fer la tesi i em vas respondre que amb les meves notes era difícil aconseguir una beca, que hi havia molta competència. I finalment, gràcies a un calaixet d'en David vaig poder començar una tesi amb els tres. Tot i que m'he queixat molt, m'he pogut desfogar amb vosaltres amb una cervesa i us he pogut demanar consell amb moltíssimes coses. Em sento molt afortunat d'haver-vos tingut com a directors. Especialment en els moments de *coaching* i per la confiança que heu dipositat en mi i que sempre m'heu demostrat.

En segon lloc vull agrair a dues persones que han sigut els meus pilars a l'ombra a nivell tan científic com personal. Gràcies Javi i Mabel per tot, de veritat. Els inicis sempre son durs i més quan no tens ni idea del que tens entre les mans, i vosaltres hi heu sigut quan més al fons m'he trobat. Javi, et vas convertir en una persona imprescindible tan dins com fora de la universitat. Gràcies a tu he donat molts passos endavant en molts àmbits. Aquest viatge sense tu, de segur, no l'hauria gaudit tant. Mabel, tu ets una persona que enriqueixes la vida dels que t'envolten. M'has ensenyat tant i m'has fet gaudir tant de tot que no sé ni com descriure-ho. I no parlo només de ciència (que també), has sigut psicòloga, companya, amiga,... Desitjo que aviat tornem a estar colze a colze.

D'altres persones també he après molt. La bioelectroquímica no va ser (ni és) senzilla per mi, però les estones dedicades amb la Laura i la Yolanda van valdre or. Moltes gràcies a les dues per dedicar-me temps en els moments de més estrés. També vull agrair a la resta de membres de GENOCOV per les ensenyances en els seminaris i en els laboratoris. Especialment als grups de BES (Mireia, Pili, Jesús, Antonella i Mira) i gasos (Dani, Eva, Xudong, Deivid, Mabel, Francesco, Luís i Tercia). Dono les gràcies també als membres del BTP-GO (especialment a en Toni, en Xavi i la Lledó pels nostres viatges a congressos). També vull agrair a la Pili, Manuel i Lorena l'ajuda per els laboratoris (i en algun moment de crisi). I no voldria deixar d'agrair a les secres, la Montse i la Rosa per ser-hi sempre, la Loli i la Míriam per l'ajuda al principi i als nous (que últimament hi ha hagut molt de moviment) per l'ajuda al final, especialment la Laura per l'ajuda amb l'estada.

Per sort a la universitat no tot ha sigut feina. Dono les gràcies a qui ha endolcit les setmanes des del primer dia amb els dimecres de pastís (Juliana, Caterina, Marina, Cesc, Patón, Andrea, Rebeca, Laura, Luís, Javi, Mabel, Nati, Tere, Patricio, Ottavia, Clara, Pedro, Natalia, Alba, Jose, María, Dani, Eva, Gaby...). També us dono les gràcies per les

moltes activitats que vam fer junts, que ens va unir com a pinya i que va fer que fos més fàcil sortir del llit cada matí. Gràcies també als Fans de Jose Luís (Dani, Oriol, Borja, Natalia i Eva) per haver aconseguit que els últims mesos d'escriptura fossin molt més entretinguts amb les estones de cafè mirant amb menyspreu als energúmens del bar. També agraeixo a la resta dels companys dels dinars. Aquests últims mesos he estat mig desaparegut, però agraeixo que continueu fent pinya pels dinars (special thanks to Xudong and Kaidi, you are awesome guys!).

També gràcies als companys de despatx (Kírian, Luismi, María, Javi, Javi (lip), Mabel, Dani, Arnau, Albert (ald), Tere, Eva (comp), Miquel, Francesco, Congcong...) per haver-me aguantat, especialment en els moments d'escriptura. Gràcies també als membres d'altres grups que han aconseguit que aquesta experiència fos inoblidable, ja sigui per la cerdo-experiencia, la taverna Xumi o les festes de la UAB. Kirian, Luismi, Edu, Irene, Javi (mabs), Gerard, Elena, Ponte, Miquel, Albert (lip), Josu, Sonia, Jordi, Javi (lip), Daniela, Natalia (ald)... Espero no deixar-me a ningú, si no, em sap greu, però moltes gràcies! I gràcies a tots els membres del departament en general!

I want to acknowledge the people that I met in Australia. Stefano and Pablo, thanks to accept me to your group and spend as much time teaching me and discussing about the topic of my thesis. I learnt a lot from you and I enjoyed so much working in your lab. Special thanks to Pablo, I annoyed you a lot of times with silly and stupid questions, but you were more than a mentor! Also thanks to the people of the lab (Juliette, Paula Andrea, Igor, Claudia, Maddalena, Rita, Dino…) for your help when I was lost. But Australia was not just work, It was one of the best experiences that I could wish. I met a lot of awesome people: Juliette, Rita, Igor, Sam, Felix, Josh, Katrin, Ludwika, Daniel, Mike… Thanks for so much! My office mates (Yarong, Weiwei, Natascha, Claudia and Tomás), thanks for sharing as good moments in the small OT office, I enjoyed a lot our weird conversations! Paula Andrea, gracias por apoyarme y divertirme tantas veces. Maca, gracias por integrarme desde el primer momento y haber sido mi gran apoyo. María, gracias por ser mi alma gemela, haberme entendido tanto y haber compartido tanto. Tomás, gracias por haber venido y haber-me invitado a tus planes! Sergi i Míriam, moltes gràcies per tots els moments que hem compartit i per integrar-me! Finally, Tim and Dasomm, thanks for allowing me to spend the last months with you and sharing your point of view about home and friendship. You are really special. I miss all of you so much!

Ahora quiero agradecer a la familia de Barcelona, los amigos de vida, por haber convertido esta gran ciudad en mi casa. Primero de todo quiero agradecer a Richi, mi primer mejor amigo en Barcelona, por escucharme, entenderme y compartir tantos buenos momentos. Luego quiero agradecer al Piso ISO (Clara, Luís y Pedro), ese pisito que se convirtió en el centro de una gran familia dónde nos apoyábamos en los peores momentos y disfrutábamos juntos de los mejores. Muchas gracias por compartir lo que creo que hicimos que fuera un poco nuestro hogar. También quiero agradecer a Alba, tantas veces que hablamos de ciencia y tantas que compartimos momentos geniales. Gracias por ofrecerme tu piso y haberme hecho sentir tan bien en él. A pesar de tener a Chechu a veces por en medio… jajaja con nuestras conversaciones absurdas que no iban a ningún lado. Gracias por esos momentos Chechu! Gracias también a Jose, por

nuestros momentos escuchando música top en los respirómetros y tantos momentos fuera de la uni. Gracias también a Javivi por demostrarnos que estamos viejos y no aguantar ni dos días de chirigotas! Aleli, gracias por ser un descubrimiento, tan tímidos que os creía al principio y que imprescindibles os habéis vuelto. Gracias por escuchar mis rayadas mentales. Los dos sois geniales! Gracias Víctor por haber conseguido tantas veces que consiguiera desconectar de la tesis con tus cenas y fiestas! Gracias Elena por explicarme tanto antes de irme a Australia y por escucharme en mis grandes momentos de dudas. Gracias Fung por poner un puntito de inteligencia de vez en cuando y haberme comprendido en los momentos más duros. Gracias Eva, la última incorporación pero no menos importante, por animarme y estar ahí siempre. Por último quiero agradecer el apoyo más importante en Barcelona. Gracias Natalia por transmitirme tanto, por haber confiado tanto en mí, por haberme ayudado, escuchado, abrazado… No sé qué habría sido de mí y de todo esto si no hubieras venido a Barcelona. Dile a tu padre que cuidaste más de mí que yo de ti.

Ara vull donar les gràcies a la primíssima. Gràcies per haver vingut a fer la tesi a la UAB. Ens hem conegut de manera diferent i ho agraeixo molt. Som més semblants del que podríem arribar a esperar i m'alegro de que ens haguem entès tant. Moltes gràcies per tot!

Gràcies als amics de l'Eeeep. Sou els amics que fa més temps que em coneixeu i sabeu per tot el que he passat. Us agraeixo que sempre m'hagueu fet costat, que m'hagueu fet sentir que per molt lluny que vagi, quan torni sempre que estigui amb vosaltres em senti a casa. Perdoneu si us he avorrit amb les meves histories de la "tesi", però heu sigut la meva principal vàlvula d'escapament. Gràcies Joan O., Joan C., Esther, Pau, Paula, Adrià, Rosa, Erika, Núria, Maria, Dolça, Marta, Guillem, Eric...

Per últim, vull agrair a la meva família. A l'avi Ramon perquè encara que no hi sigui, les seves ensenyances de quan era petit continuen ressonant dins meu. A la iaia Isabel per recordar-me sempre i perquè entre viatge i viatge dels seus, sempre troba històries per treure'm un somriure. A l'avi Franciscu (ho he escrit expressament així) per les forces i ganes que m'ha donat de veure'l emocionat d'orgull en cada pas endavant que he fet. A la iaia Lluïsa per sempre patir per tots i demostrar que l'amor que sent per tots és infinit. A la meva germana, la Laura, per demostrar-me que, tot i ser molt diferents l'un de l'altre i viure ben lluny, puc comptar sempre amb ella, i donar-me una empenta de força enorme amb un truc d'skype. I finalment als meus pares (Antoni i Adela). Gràcies per tot. Per haver-me donat suport, escoltat, ajudat, ensenyat... Sé que he sigut un fill reservat, que m'he guardat moltes preocupacions per mi. Però alhora m'he pogut alliberar d'elles quasi cada cop que us he vist en tornar a casa. De debò gràcies! No hagués arribat fins on he arribat sense vosaltres. Ah! I per últim gràcies a en Bruc, que ha sigut com un germanet de peluix.

Resum de la tesi

Les activitats industrials com són les industries papereres, farmacèutiques, minera, de processat d'aliments, etc. generen aigües residuals amb un alt contingut de sulfat. El sulfat com a tal no resulta altament perjudicial per a la salut, però si s'aboca en rius o sistemes de clavegueram, els microorganismes coneguts com bactèries reductores de sulfat (sulfate reducing bacteria, SRB) el poden transformar en sulfur d'hidrogen. El sulfur d'hidrogen és un compost que fa mala olor, és corrosiu i s'ha demostrat tòxic inclús a baixes concentracions. Per aquests motius el tractament d'efluents rics en sulfat és indispensable. A més a més, la recuperació de sofre elemental d'aquests efluents per poder ser reutilitzat com a fertilitzant o matèria primera a la indústria és una oportunitat de recuperació de recursos en el marc de l'economia circular.

Els sistemes bioelectroquímics (bioelectrochemical systems, BES) són una tecnologia innovadora basada en l'habilitat d'alguns bacteris d'intercanviar electrons amb un elèctrode sòlid. Últimament, l'estudi dels BES s'ha focalitzat en el tractament d'aigües residuals i en la recuperació de productes gràcies a l'activitat dels microorganismes que colonitzen els elèctrodes.

En aquesta tesi s'ha estudiat l'ús de BES per al tractament i recuperació de compostos de sofre, concretament, el tractament d'aquestes aigües residuals amb sulfat. El sistema permet la reducció de sulfat en un biocàtode mentre en l'ànode succeeix l'electròlisi d'aigua per generar el flux d'electrons necessari. Els microorganismes que colonitzen la superfície del càtode utilitzen l'hidrogen generat a partir dels electrons per transformar el sulfat en sulfur d'hidrogen. No obstant això, els resultats obtinguts han demostrat que gràcies a l'electròlisi de l'aigua que té lloc a l'ànode es produeix un flux d'oxigen cap al càtode que permet el creixement dels microorganismes capaços de produir sofre a partir del sulfur d'hidrogen, anomenats bacteris oxidants de sulfur (sulfide oxidising bacteria, SOB).

Per tal de millorar l'eliminació de sulfat i la producció de sofre es va estudiar com el pH del compartiment del càtode i el potencial de càtode podien influir en el procés. Es va observar que el pH neutre (pH = 7) era més beneficiós ja que un pH

àcid (pH = 5.5) podria inhibir l'activitat de les SRB i un pH bàsic (pH = 8.5) requeria de més energia per aconseguir resultats similars a causa de la limitació en la producció d'hidrogen a un pH elevat. En quant al potencial del càtode, es va poder observar que a menors potencials, major eliminació de sulfat, però a partir d'un potencial de -1.0 V vs. SHE, el sistema no podia augmentar la velocitat d'eliminació.

A més a més, també s'ha estudiat el tractament d'aigua residual real procedent d'un sistema de dessulfuració de gasos de combustió. S'ha observat que amb l'aigua real l'eliminació de sulfat es reduïa, però en canvi la producció de sofre elemental augmentava.

Finalment, com que el flux d'oxigen de l'ànode al càtode no es podia controlar amb els sistemes anteriors, s'han dissenyat dues noves configuracions per poder millorar la producció de sofre elemental. La primera ha consistit en l'addició d'una cel·la electroquímica per tal d'oxidar el sulfur d'hidrogen en l'ànode permetent el control del potencial i així poder-ne controlar la producció.

La segona configuració ha consistit en l'addició d'una cel·la de combustible amb un càtode exposat a l'aire aprofitant la capacitat del sulfur d'hidrogen a ser oxidat en un ànode espontàniament i així produir energia en comptes de requerir-la en el procés d'oxidació.

Resumen de la tesis

Las actividades industriales tales como las industrias papeleras, farmacéuticas, minera, de procesado de alimentos, etc. generan aguas residuales con un alto contenido en sulfato. El sulfato como tal no resulta muy perjudicial para la salud, pero si se vierte en ríos o sistemas de alcantarillado, los microorganismos conocidos como bacterias reductoras de sulfato (sulfate reducing bacteria, SRB) lo pueden transformar en sulfuro de hidrógeno. El sulfuro de hidrógeno es un compuesto que huele mal, es corrosivo y se ha demostrado tóxico incluso a bajas concentraciones. Por estos motivos, el tratamiento de efluentes ricos en sulfato es indispensable. Además, la recuperación de azufre elemental de estos efluentes para poder ser reutilizado como fertilizante o materia prima en la industria es una oportunidad de recuperación de recursos en el marco de la economía circular.

Los sistemas bioelectroquímicos (bioelectrochemical systems, BES) son una tecnología innovadora basada en la habilidad de algunas bacterias de intercambiar electrones con un electrodo sólido. Últimamente, el estudio de los BES se ha focalizado en el tratamiento de aguas residuales y en la recuperación de productos gracias a la actividad de los microorganismos que colonizan los electrodos.

En esta tesis se ha estudiado el uso de BES para el tratamiento y recuperación de compuestos de azufre, concretamente, el tratamiento de estas aguas residuales con sulfato. El sistema permite la reducción de sulfato en un biocátodo mientras en el ánodo se produce la electrólisis del agua para generar el flujo de electrones necesario. Los microorganismos que colonizan la superficie del cátodo utilizan el hidrógeno generado a partir de los electrones para transformar el sulfato en sulfuro de hidrógeno. Sin embargo, los resultados obtenidos han demostrado que gracias a la electrólisis del agua que tiene lugar en el ánodo se produce un flujo de oxígeno hacia el cátodo que permite el crecimiento de microorganismos capaces de producir azufre a partir del sulfuro de hidrógeno, llamados bacterias oxidantes de sulfuro (sulfide oxidizing baceria, SOB).

Para mejorar la eliminación de sulfato y la producción de azufre se estudió como el pH del compartimento del cátodo y el potencial de cátodo podían influir en el

proceso. Se observó que el pH neutro (pH = 7) era más beneficioso ya que un pH ácido (pH = 5.5) podría inhibir la actividad de las SRB y un pH básico (pH = 8.5) requería más energía para conseguir resultados similares debido a la limitación en la producción de hidrógeno a un pH elevado. En cuanto al potencial del cátodo, se pudo observar que a menores potenciales, mayor eliminación de sulfato, pero a partir de un potencial de -1.0 V vs. SHE, el sistema no podía aumentar la velocidad de eliminación.

Además, también se ha estudiado el tratamiento de agua residual real procedente de un sistema de desulfuración de gases de combustión. Se ha observado que con el agua real la eliminación de sulfato se reducía, pero en cambio la producción de azufre elemental aumentaba.

Finalmente, dado que el flujo de oxígeno del ánodo al cátodo no se podía controlar con los sistemas anteriores, se han diseñado dos configuraciones nuevas para mejorar la producción de azufre elemental. La primera ha consistido en la adición de una celda electroquímica para oxidar el sulfuro de hidrógeno en el ánodo permitiendo el control del potencial y así poder controlar la producción.

La segunda configuración ha consistido en la adición de una celda de combustible con un cátodo expuesto al aire aprovechando la capacidad del sulfuro de hidrógeno a ser oxidado en un ánodo espontáneamente y así producir energía en vez de requerirla en el proceso de oxidación.

Thesis abstract

Industrial activities such as paper, pharmaceutical, mining, food processing, etc. generate wastewater with high sulfate content. Sulfate as such is not very harmful to health, but if it is poured into rivers or sewage systems, the microorganisms known as sulfate reducing bacteria (SRB) can transform it into hydrogen sulfide. Hydrogen sulfide is a compound with bad odour, is corrosive and has been shown toxic at low concentrations. For these reasons, the treatment of sulfate-rich effluents is essential. In addition, the recovery of elemental sulfur from these effluents in order to be reused as fertilizer or raw material in the industry is an opportunity to recover resources in the framework of the circular economy.

Bioelectrochemical systems (BES) are a novel technology based on the ability of some bacteria to exchange electrons with a solid electrode. Lastly, the study of the BES has focused on the treatment of wastewater and the recovery of products thanks to the activity of the microorganisms that colonize the electrodes.

In this thesis, the use of BES for the treatment and recovery of sulfur compounds was studied, specifically, the treatment of these wastewaters with sulfate in a biocathode. The system allows the reduction of sulfate at a biocatode while at the anode electrolysis of water occurs to generate the necessary electron flow. The microorganisms that colonize the surface of the cathode use the hydrogen produced from the electrons to transform the sulfate into hydrogen sulfide. However, the results obtained showed that thanks to the water electrolysis that takes place at the anode an oxygen flow to the cathode is generated, allowing the growth of microorganisms capable of producing sulfur from hydrogen sulfide, called sulfide oxidizing bacteria (SOB).

The influence of pH of the cathode compartment and the cathode potential was studied in order to improve sulfate removal and sulfur production. It was observed that neutral pH (pH = 7) was more beneficial since an acidic pH (pH = 5.5) could inhibit the activity of the SRB and a basic pH (pH = 8.5) required more energy to achieve similar results due to the limitation in the production of hydrogen at a high pH. Regarding the potential of the cathode, it could be observed that lower

potentials led to greater sulfate removal rate, but from a potential of -1.0 V vs. SHE, the system could not increase the removal rate.

In addition, the impact of real wastewater coming from a flue gas desulphurization system in the system was also studied. It was observed that with real water the sulfate removal decreased, however, the production of elemental sulfur increased.

Finally, since the oxygen flow from the anode to the cathode could not be controlled with the previous systems, two new configurations were designed to improve the production of elemental sulfur. The first one consisted in the addition of an electrochemical cell to oxidize the hydrogen sulfide at the anode, allowing the control of the potential and thus controlling the production.

The second configuration consisted in the addition of a fuel cell with a cathode exposed to the air taking advantage of the capacity of the hydrogen sulfide to be oxidized at an anode spontaneously and thus produce energy instead of requiring it in the oxidation process.

List of abbreviations

AEM	Anionic exchange membrane
AMD	Acid mine drainage
ARB	Anode respiring bacteria
AutH2	Autotrophic and hydrogenotrophic
BES	Bioelectrochemical system
BES-EC	Bioelectrochemical system with electrochemical cell
BES-FC	Bioelectrochemical system with fuel cell
C-BES	Cube shape bioelectrochemical system
CEM	Cationic exchange membrane
COD	Chemical oxygen demand
CV	Cyclic voltammetry
DO	Dissolved oxygen
EC	Electrochemical cell
EDS	Energy dispersive spectrometry
FC	Fuel cell
FGD	Flue gas desulfurization
H-BES	H shape bioelectrochemical system
HPR	Hydrogen production rate
HRT	Hydraulic retention time
ICP-MS	Inductively coupled plasma mass spectrometry
IEM	Ionic exchange membrane
LSV	Linear sweep voltammetry
MA	Membrane adsorption
MEC	Microbial electrochemical cell
MFC	Microbial fuel cell
OCV	Open circuit voltage
PTFE	Polytetrafluoroethylene
SCE	Saturated calomel electrode
SD	Sulfate diffusion

SEM	Scanning electron microscope
SHE	Standard hydrogen electrode
SOB	Sulfide oxidizing bacteria
SPR	Sulfide production rate
SRB	Sulfate reducing bacteria
SRR	Sulfate removal rate
TDS	Total dissolved sulfide
TESPR	Theoretical elemental sulfur production rate
TIC	Total inorganic carbon
TOC	Total organic carbon
TSS	Total suspended solids

Table of content

Chapter 1

Introduction

1.1. Fundamentals of sulfur cycle

The total amount of sulfur annually extracted from the lithosphere is around 120 Tg S in fossil fuels and sulfur-containing raw material and it is used in the chemical industry. About 58% of it is emitted to the atmosphere. Half of the rest enters to the soil through fertilizers and the other part enters to rivers through wastewaters. These values suggest that the anthropogenic sulfur fluxes to the atmosphere and hydrosphere have reached similar levels than natural fluxes and they could increase notably all over the world by the end of this century (Loka Bharathi, 2008).

Sulfur is one of the most abundant elements on Earth, mainly present in rocks and sediments as pyrite (FeS_2) or gypsum ($CaSO_4$) and in seawater as sulfate. In the environment, sulfur is present in a broad range of oxidation states from -2 (completely reduced) to +6 (completely oxidized) (Figure 1.1) and it is used for energy transformation and growth of a large amount of microorganisms. Sulfate (SO_4^{2-}) is used as a nutrient and it is reduced to sulfide (S^{2-}) to be incorporated into sulfur-containing amino acids and enzymes.

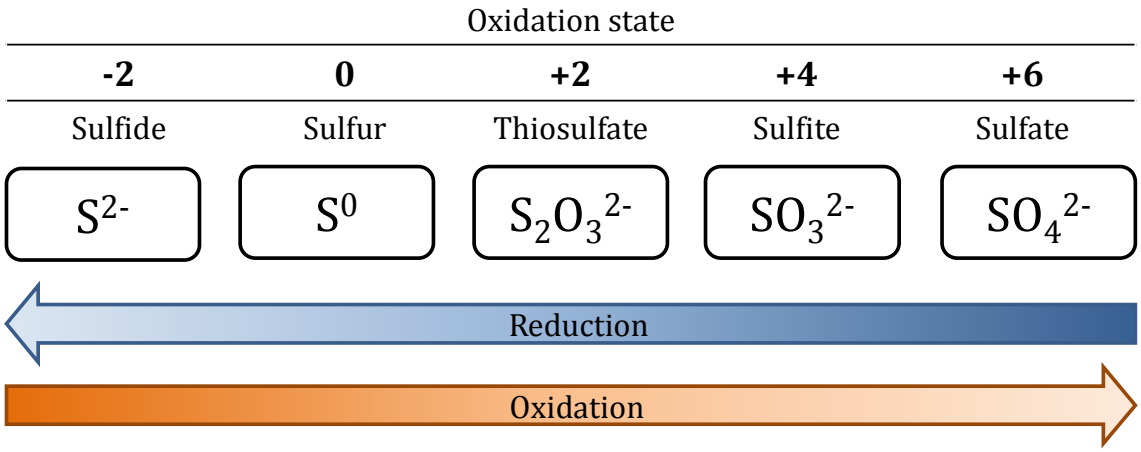

Figure 1.1. Main chemical species of sulfur with their corresponding oxidation states.

Microbes, especially bacteria, play an important role in oxidative and reductive cycle of sulfur (Figure 1.2). The reductive cycle is driven by sulfate reducing

bacteria (SRB), which use inorganic sulfate as electron acceptor in anaerobic respiration producing sulfide using hydrogen or organic matter as electron donor. The oxidative cycle is driven by photosynthetic or chemosynthetic sulfur oxidizing bacteria (SOB) oxidizing sulfide to sulfur or sulfate using oxygen or nitrate as electron acceptor (Reyes-Alvarado et al., 2018). Several intermediates such as thiosulfate and elemental sulfur can be formed by incomplete sulfide oxidation (Muyzer and Stams, 2008). Sulfur can also be disproportionate by SRB where sulfur or thiosulfate acts as both the electron donor and acceptor formatting sulfate and sulfide respectively (Tang et al., 2009).

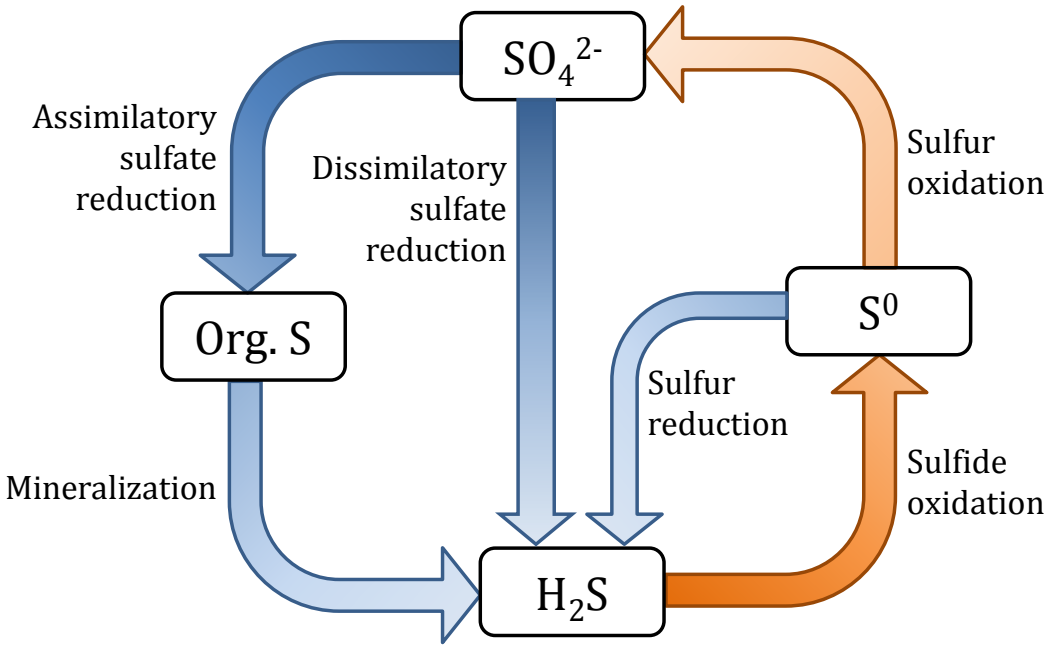

Figure 1.2. Contribution of microorganisms in sulfur cycle (adapted from Saha et al. (2018)).

1.2. High sulfate content wastewaters

1.2.1. Environmental impact

High sulfate content wastewaters are generated in many processes such as pulp and paper industry, food processing, animal husbandry, dye and detergent manufacture, etc. (Lens and Pol, 2015). High concentrations of sulfate are also found in acid mine drainage wastewaters, which also present high content of

metals (Kaksonen and Puhakka, 2007), and in flue gas desulfurization (FGD) systems which are used to control SO_2 emissions from industries (Srivastava and Jozewicz, 2001). Nowadays, the main anthropogenic source of sulfur in the environment is the combustion of high-sulfur coals. For this reason, FGD systems should be optimized in order to avoid problems such as urban air pollution and acid deposition. This acid deposition is estimated that can affect 10^7 km^2 of land in south and eastern Asia with sulfur deposition greater than 1 g S m^{-2} $year^{-1}$ by 2020 (Brimblecombe, 2015). Excessive discharge of sulfate may also affect public water supply and human health, consequently the World Health Organization recommended to keep the sulfate concentration in drinking water below 250 mg L^{-1} (Clair et al., 2003). However, several authorities have established the maximum levels recommended for its disposal (Table 1.1). For these reasons, the treatment of sulfate rich wastewaters prior to discharge into the environment is an essential step.

Table 1.1. Recommended maximum sulfate levels (adapted from Bowell (2004)).

Authority	**Sulfate concentration (mg L^{-1})**
USA	500
Canada	1000
European Union	1000
South Africa	600
Australia	1000
World Health Organization (drinking water)	250

Although sulfate is not a very harmful pollutant, discharging high concentrations may lead to several environmental issues due to sulfide formation such as corrosion, bad odors and toxicity (Pol et al., 1998a). This sulfide can be either precipitated with the potential metal-ions contained in the wastewater or biologically oxidized to elemental sulfur (Bijmans et al., 2008). The recovery of elemental sulfur from sulfate has a strong potential due to a stable worldwide

market demand about 70 million tons per year in the fertiliser market (Cope, 2012). Even though nowadays there is an excess of elemental sulfur generated from hydrodesulfurization in petroleum refining processes (Chung et al., 2013), elemental sulfur production has gained a lot of interest because it can be used in vulcanization, rechargeable batteries and thiol coupling reactions (Boyd, 2016).

1.2.2. Physicochemical treatment

Several physicochemical treatments have been implemented in order to decrease the sulfate content from wastewaters. The cheapest one consists of lime addition for insoluble gypsum (K_{sp} = $10^{-2.3}$) formation (Bowell, 2004). However, lime addition does not guarantee the complete removal of sulfate at high sulfate concentrations. Other process such as SAVMIN, CESR and Walhalla processes were implemented in order to improve the sulfate removal compared with lime precipitation. The improvement consisted of ettringite recovery ($Ca_6Al_2(SO_4)_3(OH)_{12}\cdot 26H_2O$) by the addition of aluminum hydroxide and lime, which allowed the almost complete sulfate removal (Janneck et al., 2012; Reinsel, 1999).

Barite formation ($BaSO_4$) by barium carbonate addition gave positive results as well as several problems such as the need the precipitation of other carbonate compounds and the high cost of $BaCO_3$ (Hlabela et al., 2007). BaS addition was added to decrease the amount of other precipitates but at expenses of a posterior H_2S stripping (Bosman et al., 1990). Finally, the use of $Ba(OH)_2$ was proposed in order to avoid the abovementioned problems of the other Ba salts (Adlem et al., 1991). However, a barium recovery plant to recycle barium salts was required due to the barium high cost and to its environmental toxicity.

Membrane processes such as reverse osmosis and nanofiltration have been also used to treat sulfate. Several modifications of reverse osmosis have been implemented but all of them required several pre-treatment steps in order to extend the life of membranes, which highly increase the costs (Runtti et al., 2018). Nanofiltration led to lower costs than reverse osmosis due to lower pressures

applied (Barr, 2001). However, nanofiltration requires several filtration steps to complete remove the sulfate from water (Preuß et al., 2012).

The best physicochemical processes for sulfate removal developed until now are GYP-CIX and Sulf-IX. GYP-CIX and Sulf-IX consist are based on ion exchange resins that use low cost chemicals (lime and sulfuric acid) for the removal of calcium sulfate (Brown et al., 2002; Doughty and Littlejohn, 2015).

No physicochemical treatment of sulfate allows elemental sulfur recovery. The main physicochemical process to obtain elemental sulfur consists of the modified Claus process (Mokhatab et al., 2018). In the original Claus process the partial sulfide oxidation (Eq. 1.1) took place in one step according to the following exothermic reaction:

$H_2S + 0.5O_2 \rightarrow 0.125S_8 + H_2O$ Eq. 1.1

However, the original Claus process was limited because the reaction temperature was hardly controllable since it is an extremely exothermic reaction (Mokhatab et al., 2018). The modified Claus process consists of a two-step process. In the first one more air is added in order to oxidize one-third of the H_2S to SO_2 (Eq. 1.2), which is highly exothermic:

$H_2S + 1.5O_2 \rightarrow SO_2 + H_2O$ Eq. 1.2

The second step consists of the reaction between H_2S and SO_2 (Eq. 1.3), which is endothermic but limited by equilibrium achieving the 60 – 70% of H_2S conversion to elemental sulfur.

$2H_2S + SO_2 \rightarrow 1.5S_2 + 2H_2O$ Eq. 1.3

Other technologies that adapt the modified Claus process are being implemented at smaller scale or for low gas quality streams such as Selectox, Clinsulf, Sulferox and Crystasulf processes (Goar and Fenderson, 1996; Mokhatab et al., 2018; von Gemmingen and Lahne, 1994).

1.2.3. Biological treatment

The biological treatment for sulfate rich wastewaters in bioreactors is based on biological sulfate reduction to sulfide and a subsequent sulfide oxidation (Table 1.2). In a first step, under anaerobic conditions, SRB use sulfate as electron acceptor and produce sulfide as final product (Pol et al., 1998a). This process can be performed autotrophically, i.e. using as electron donor H_2 (Eq. 1.4, Table 1.2), or heterotrophically, i.e. using organic matter as electron donor (Eq. 1.5, Table 1.2). Sulfide produced in the previous reduction requires further treatment to convert it into a sulfur compound not associated to harmful effects (Muyzer and Stams, 2008). For example, sulfide can be partially oxidized to elemental sulfur (Eq. 1.6, Table 1.2) by SOB. Oxygen limiting conditions are required in this step. If excess oxygen is provided then oxidation further proceeds to thiosulfate or sulfate (Eq. 1.7, Table 1.2).

Table 1.2. Gibbs energy change (ΔG^0_r) and equilibrium potential (E^0_r) of specific reactions with sulfur species.

Reaction	**ΔG^0_r (kJ mol^{-1})**	**E^0_r (V)**	
$SO_4^{2-} + 4\ H_2 + H^+ \leftrightarrows HS^- + 4\ H_2O$	-152	+0.197	Eq. 1.4
$SO_4^{2-} + CH_3COO^- \leftrightarrows HS^- + 2\ HCO_3^-$	-48	+0.062	Eq. 1.5
$HS^- + 0.5\ O_2 + H^+ \leftrightarrows S^0 + H_2O$	-209	+1.085	Eq. 1.6
$S^0 + 3/2\ O_2 + H_2O \leftrightarrows SO_4^{2-} + 2\ H^+$	-587	+1.014	Eq. 1.7

Calculated based on half reactions reported in Table 1.3, using the Growth Reference System (biochemical standard conditions: 1 atm, 298.15 K, 1 mol L^{-1}, pH=7).

Elemental sulfur can be easily recovered from sulfide because it can be biologically produced (Eq. 1.6, Table 1.2) either in aerobic (using O_2 as electron acceptor) and anoxic (using NO_3^-/ NO_2^- as electron acceptor) conditions. On the other hand, the elemental sulfur recovery from sulfate is more complicated because, considering that sulfate partial reduction to elemental sulfur has not been described, two

processes are needed: sulfate reduction to sulfide (Eq. 1.4 and 1.5, Table 1.2) and partial sulfide oxidation to elemental sulfur (Eq. 1.6, Table 1.2).

The traditional physicochemical treatments include high cost of the chemical reagents and production of sludge, which has to be treated or disposed (Tichý et al., 1998) and sometimes the removal of sulfate is inefficient (Kaksonen and Puhakka, 2007). For high-strength sulfate wastewaters, biological sulfate removal is a cost-effective alternative for the high-cost physicochemical treatments. In addition, there are reports of some applied biological processes for the treatment of high-sulfate wastewaters in view of resource recovery (Pol et al., 1998a).

In the biological treatment of sulfate, there are the passive treatment applications for the contaminated groundwater and surface waters, and the active bioreactors. Typical methods of groundwater treatment in AMD spills are placing or injecting substrates into the subsurface (Groudev et al., 1998) and using permeable reactive barriers (Gibert et al., 2011; Waybrant et al., 1998). These methods allow the increase of SRB activity thanks to the substrates addition and, as a consequence, the precipitation of metal sulfides, but the treatment time required is long.

On the other hand, there are several methodologies for the passive treatment of surface waters. Infiltration beds are similar to reactive barriers used for groundwater but they are constructed into the ditches of mining areas (Kaksonen and Puhakka, 2007). Anoxic ponds, i.e. water basins supplemented with organic substrates, are used in the upstream of anoxic limestone drains (Gazea et al., 1996). Finally, constructed wetlands have been considered the lowest-cost technology to improve the water quality for AMD. Constructed wetlands are artificial wetlands used for the treatment of municipal and industrial wastewaters used in AMD in order to reduce sulfate in their beds and precipitate metals. In general, constructed wetlands are highly complex ecosystems where physical, chemical and biological processes take place simultaneously (Sheridan et al., 2018). However, the required treatment area might be large with difficult resources recovery and with a poor control and predictability (Gazea et al., 1996).

The active bioreactors allow improving sulfate treatment because of SRB can be selectively enriched and their activity can be more controlled at expenses of higher costs. A lot of different configurations can be used such as continuously stirred

tank reactor, anaerobic contact process, anaerobic filter reactor, fluidized-bed reactor, gas lift reactor, up flow anaerobic sludge blanket reactor, anaerobic hybrid or baffled reactor and membrane bioreactor (Hulshoff et al., 2001; Johnson, 2000; Kaksonen and Puhakka, 2007; Speece, 1983).

The most used technologies are the SANI® process and the SULFATEQ® process. The SANI® process (sulfate reduction, autotrophic denitrification and nitrification integrated, Hong Kong) has been implemented at full-scale for the removal of sulfur and nitrogen from saline sewage at a ratio of > 0.5 mg SO_4^{2-}-S/mg COD (Wu et al., 2016). The SULFATEQ® process (Paques B. V., The Netherlands) is a biological treatment used in metallurgical and mining industries to treat wastewater streams that contain oxidized sulfur compounds and can use organic matter and H_2 as electron donor (Schröder-Wolthoorn et al., 2008). Nevertheless, a second reactor is needed to partially oxidize sulfide to elemental sulfur in the case of limited metal content to precipitate sulfide.

The best results on sulfate reduction obtained until now were reported in a gas lift reactor at lab scale, achieving sulfate removal rates of 10 g SO_4^{2-}-S L^{-1} d^{-1} (Houten et al., 1994). These high rates are explained because, according to thermodynamics, hydrogenotrophic sulfidogenensis is more favorable than methanogenesis (Weijma et al., 2002) since SRB are generally more efficient in hydrogen utilization than methanogenic bacteria (Davidova and Stams, 1996).

1.3. Bioelectrochemical systems

1.3.1. Fundamentals of bioelectrochemical systems

Bioelectrochemical systems (BES) are a novel technology based on the ability of some bacteria to exchange electrons with a solid electrode. Then, BESs combine the metabolism of these microorganisms with electrochemistry. The microorganisms placed at the anode responsible for organic matter oxidation are called anode respiring bacteria (ARB). As any electrochemical cell (Figure 1.3), the system consists of an anode, where an oxidation reaction takes place (loss of electrons), and a cathode, where a reduction reaction takes place (gain of electrons).

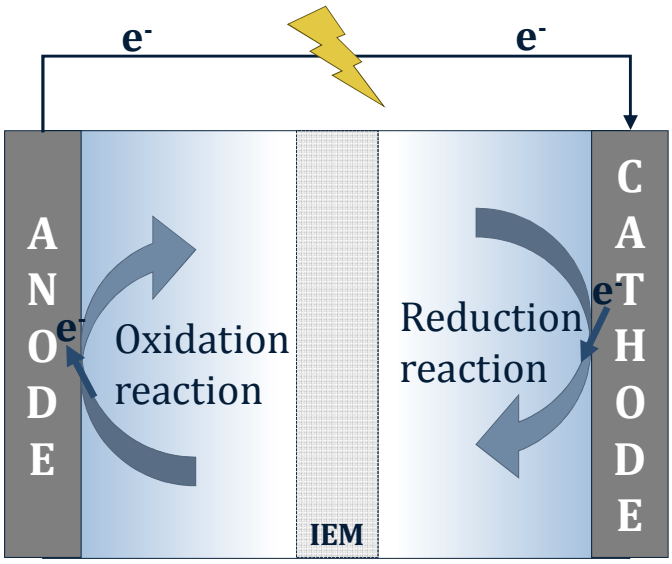

Figure 1.3. Schematic of an electrochemical cell.

Then, there is an electrode connection that allows the electron flow between both electrodes (from the anode to the cathode). An ionic exchange membrane (IEM) or separator can be placed between both electrodes in order to separate the electrolytes (conductive aqueous solution) but allowing the ionic diffusion between the chambers for charge balancing. In BES, one or both reactions are catalyzed by microorganisms. The first evidence of the existence of microorganisms that were able of extracellular electron transfer was in 1910 (Potter, 1910).

Depending on the oxidation and reduction reactions (Figure 1.4), the process can be spontaneous (negative Gibbs free energy) or it could require some energy input to drive it (positive Gibbs free energy). The thermodynamics of the overall reaction can be evaluated in terms of Gibbs free energy (ΔG_r), but it can also be evaluated in terms of overall cell electromotive force (E_{emf}), defined as the potential difference between the cathode and the anode (Eq. 1.8), which is positive for a thermodynamically favorable reaction. The flow of electrons is favored towards more positive reduction potentials.

$$E_{emf} = E_{cat} - E_{an} \qquad \text{Eq. 1.8}$$

Where the E_{cat} and E_{an} are the half-cell potentials of the cathode and anode respectively at specific conditions.

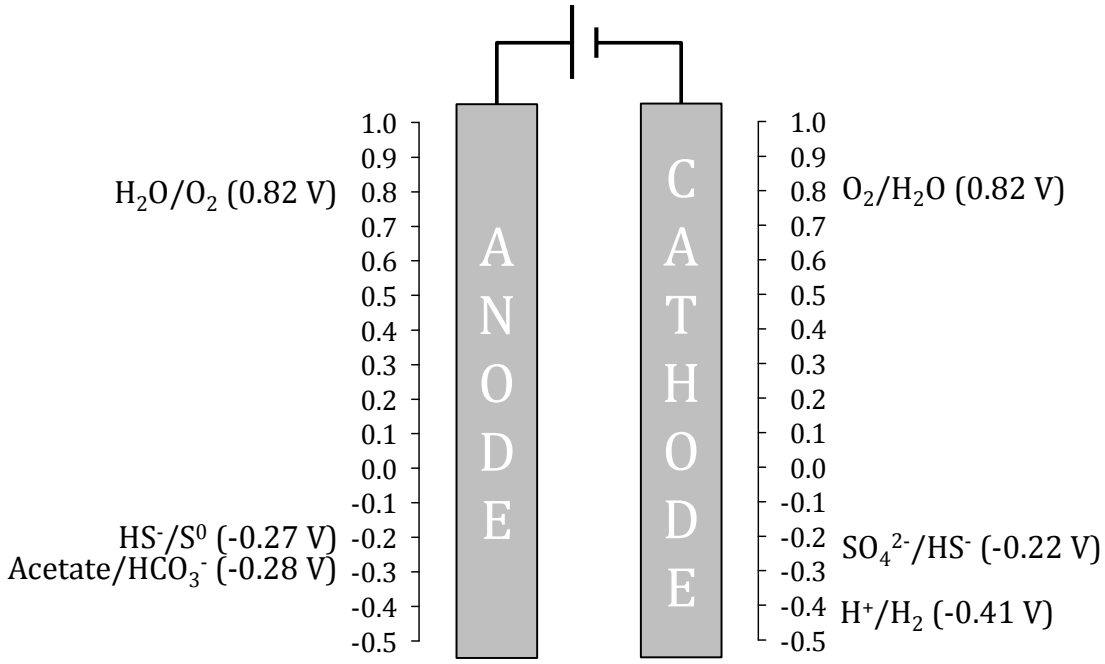

Figure 1.4. Scale of theoretical reduction potentials associated to redox processes at pH 7 and 298.15 K (shown against the standard hydrogen electrode).

1.3.2. Applications of BES

According to the energy requirement there are two major variants of BES: microbial fuel cell (MFC), when the E_{emf} is positive; and microbial electrochemical cell (MEC) when the E_{emf} is negative. In an MFC (Figure 1.5), the potential of the process occurring at the anode is lower than that occurring on the cathode and therefore the electrical connection of the anode with a cathode produces an electron flow that can be used elsewhere as electricity. The most studied process is the acetate anodic oxidation by ARB coupled with the cathodic reduction of oxygen:

$E_{emf} = E_{cat} - E_{an}$ → 0.82 V – (-0.28 V) = +1.10 V

As the E_{emf} is positive, the process will produce electricity.

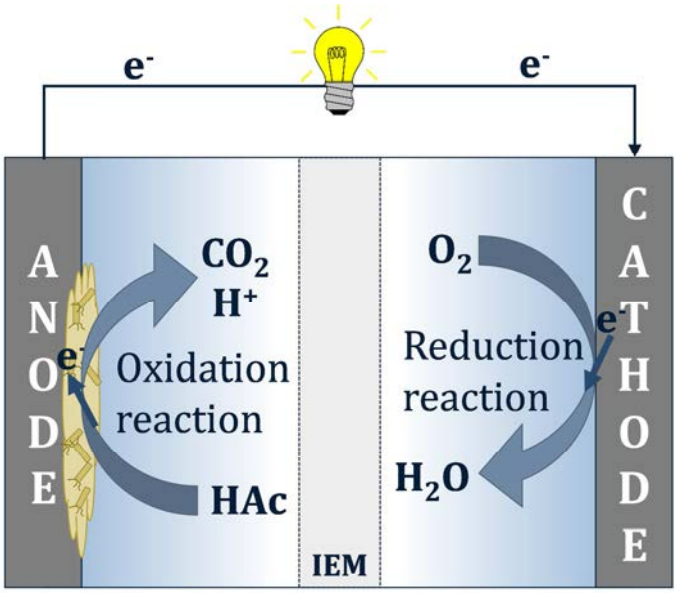

Figure 1.5. Schematics of an MFC where acetate oxidation takes place at the anode and oxygen reduction takes place at the cathode.

Finding alternatives to electricity generation in BES is very attractive from an economic point of view, since the economic value of hydrogen (or other added value products) is higher than that of electricity (Cusick et al., 2010; Harnisch et al., 2011). The reaction between protons and electrons can lead to formation of hydrogen in a MEC (Figure 1.6). However, this process is not spontaneous and requires the application of an external voltage to cathode. Therefore, to the contrary of an MFC, the potential of the reaction occurring at the cathode is lower than that at the anode and an energy input is required to drive the process and to obtain the product of interest. The most studied process is the acetate anodic oxidation by ARB coupled with the cathodic reduction of protons for hydrogen production:

$E_{emf} = E_{cat} - E_{an}$ → -0.41 V – (-0.28 V) = -0.13 V

As the E_{emf} is negative, the process will require electricity.

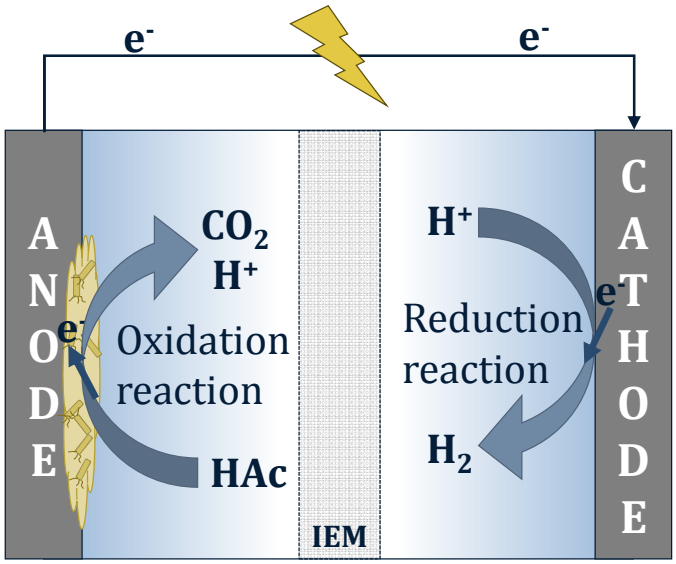

Figure 1.6. Schematic of a MEC where acetate oxidation takes place at the anode and proton reduction takes place at the cathode.

1.3.3. Biocathodes

The reductive reactions that take place at the cathode have led to a wide range of possibilities regarding the possibility of removing different contaminants and the production of targeted compounds (Zhang and Angelidaki, 2014). Recently, the research on BES has focused on by-products recovery such as heavy metals, nutrients and industrial chemicals from wastewater (Jadhav et al., 2017). Microorganisms present in the biocathode can theoretically interact with the electrode surface. This interaction allows the microorganisms taking the electrons or to use the hydrogen produced and to recover value added products (Figure 1.7) at expenses of electricity as MEC because the E_{emf} is negative.

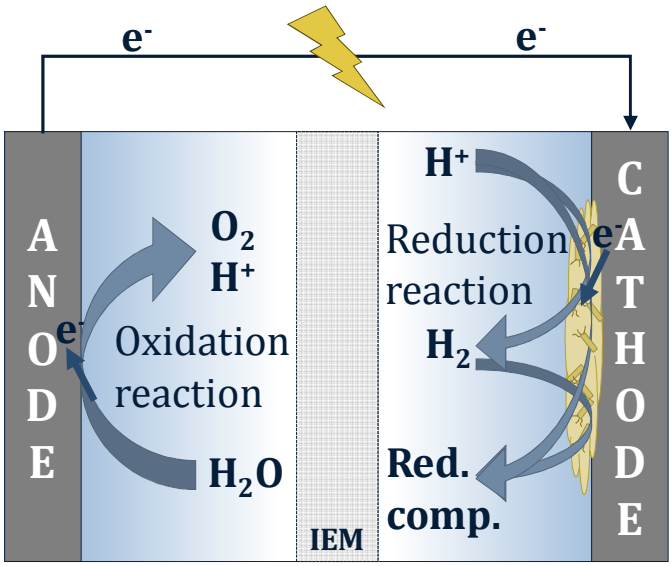

Figure 1.7. Schematic of an MEC where water oxidation takes place at the anode and reduced compounds (Red. comp.) are produced in the biocathode.

The first biocathode used in BES was to improve the oxygen reduction in an MFC in order to increase the electricity production (Clauwaert et al., 2007). After that, biocathodes have been used for hydrogen production enhancement (Cheng and Logan, 2007; R. a Rozendal et al., 2008), synthesis of organic compounds such as VFA (Nevin et al., 2011; Rabaey and Rozendal, 2010), methane production (Cheng et al., 2009), heavy metals recovery (Dominguez-Benetton et al., 2018), nitrate removal (Pous et al., 2015) or sulfate removal (Coma et al., 2013). The electron transfer in biocathodes for the processes abovementioned is still a knowledge gap, but several mechanisms have been proposed for the electron transfer in bioanodes (Kondaveeti et al., 2018). So, it is thought that the electron transfer in biocathodes is similar than the ones in bioanodes (Rosenbaum et al., 2011) and are shown in Figure 1.8. Direct electron transfer (Figure 1.8A) refers to the ability of microorganisms to transport electrons through their membrane directly with a solid electrode or using the so-called bacterial nanowire (Figure 1.8E). However, the electron transport can also be mediated by soluble redox compounds produced on the electrode surface (Figure 1.8C) or secreted by other microorganisms (Figure 1.8D). In addition, direct interspecies syntrophy can also be stablished between two microorganisms (Figure 1.8B).

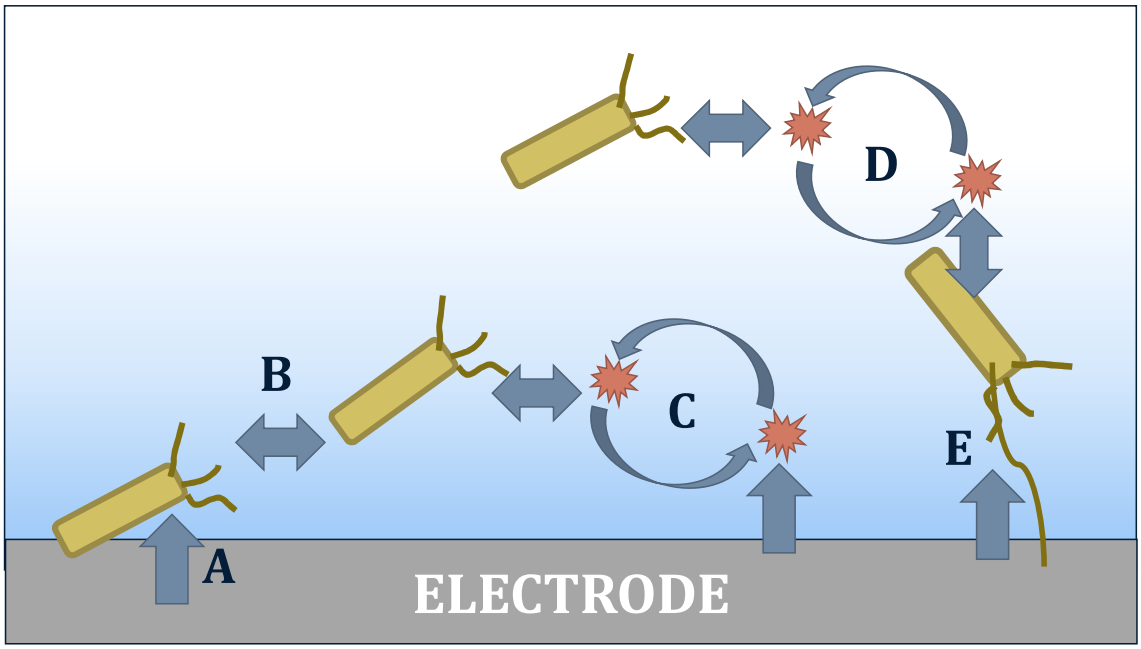

Figure 1.8. Electron transfer mechanisms established between the electrode surface and the microorganisms. A: direct electrons transfer, B: direct inter species electron transfer, C: mediated electron transfer, D: mediated interspecies electron transfer and E: direct electron transfer through nanowires (adapted from Harnisch and Rabaey (2012)).

1.4. Use of BES for sulfate removal and sulfur recovery

The appearance of BES is opening up the possibility of creating new processes related to the sulfur cycle. The link between the sulfur cycle and BES has recently gained the attention of many researchers according to the number of publications in the topic (Figure 1.9). Anodic hydrogen sulfide oxidation to elemental sulfur or sulfate and cathodic sulfate reduction to hydrogen sulfide are the main processes studied nowadays. However, the versatility of BES is allowing the implementation of other processes such as removal of thiosulfate, treatment of acid mine drainage or elemental sulfur recovery.

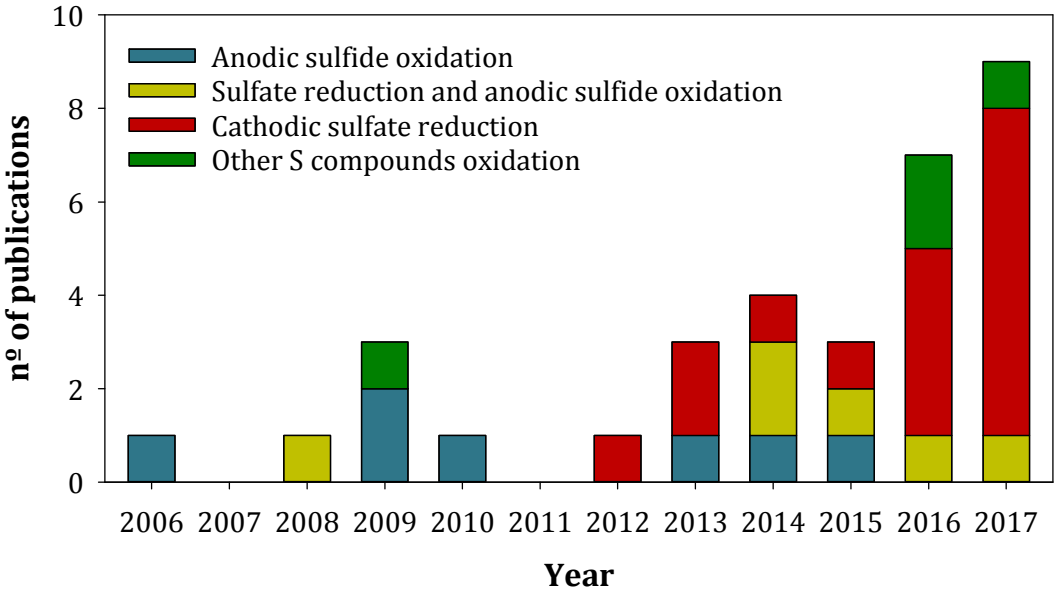

Figure 1.9. Number of publications of the application of bioelectrochemical systems for the treatment of wastewaters with different S compounds (adapted from Blázquez et al. (2019b)).

Due to the shortage of electron donor typically found in sulfate-rich wastewaters (Liamleam and Annachhatre, 2007), the sulfate reduction step usually requires the addition of organic compounds or hydrogen, resulting in high operational expenses. BESs aim at reducing the costs of treating such wastewaters and, when possible, at recovering sulfur with CO_2 as carbon source and electricity as reducing agent. If this electricity is produced from renewable sources (e.g. with solar panels), sulfur recovery could be economically viable and sustainable when compared to current physical-chemical systems or to current biological processes. In this sense, BESs would enable sulfur recovery from liquid effluents from a wide range of industries abovementioned. BESs provide oxidative and reductive environments where a large list of processes related to the S-cycle can occur. Potentially, all half reduction reactions described in Table 1.3, together with its inverse oxidation reactions, could take place in BES.

Table 1.3. Gibbs energy change (ΔG^0_r) and equilibrium potential (E^0_r) of specific half reactions with sulfur species, protons, oxygen and bicarbonate as electron acceptors.

Half reaction	**ΔG^0_r (kJ mol^{-1})**	**E^0_r (V)**	
$SO_4^{2-} + 2\ H^+ + 2\ e^- \leftrightarrows SO_3^{2-} + H_2O$	101	-0.521	Eq. 1.9
$4\ SO_4^{2-} + 20H^+ + 14\ e^- \leftrightarrows S_4O_6^{2-} + 10\ H_2O$	393	-0.291	Eq. 1.10
$2\ SO_4^{2-} + 10\ H^+ + 8\ e^- \leftrightarrows S_2O_3^{2-} + 5\ H_2O$	189	-0.244	Eq. 1.11
$SO_4^{2-} + 8\ H^+ + 6\ e^- \leftrightarrows S^0 + 4\ H_2O$	115	-0.198	Eq. 1.12
$SO_4^{2-} + 9\ H^+ + 8\ e^- \leftrightarrows HS^- + 4\ H_2O$	167	-0.216	Eq. 1.13
$2\ SO_3^{2-} + 6\ H^+ + 4e^- \leftrightarrows S_2O_3^{2-} + 3\ H_2O$	-13	+0.032	Eq. 1.14
$SO_3^{2-} + 7\ H^+ + 6\ e^- \leftrightarrows HS^- + 3\ H_2O$	66	-0.114	Eq. 1.15
$S_4O_6^{2-} + 2\ e^- \leftrightarrows 2\ S_2O_3^{2-}$	-15	+0.080	Eq. 1.16
$S_2O_3^{2-} + 6\ H^+ + 4e^- \leftrightarrows 2\ S^0 + 3\ H_2O$	230	-0.595	Eq. 1.17
$½\ S_2O_3^{2-} + 4\ H^+ + 4\ e^- \leftrightarrows HS^- + 1.5\ H_2O$	72	-0.188	Eq. 1.18
$5\ S^0 + 2\ e^- \leftrightarrows S_5^{2-}$	66	-0.341	Eq. 1.19
$S^0 + H^+ + 2\ e^- \leftrightarrows HS^-$	52	-0.269	Eq. 1.20
$S_5^{2-} + 5\ H^+ + 8\ e^- \leftrightarrows 5\ HS^-$	194	-0.251	Eq. 1.21
$2\ H^+ + 2\ e^- \leftrightarrows H_2$	80	-0.413	Eq. 1.22
$O_2 + 4\ H^+ + 4\ e^- \leftrightarrows 2\ H_2O$	-315	+0.816	Eq. 1.23
$2\ HCO_3^- + 9\ H^+ + 8\ e^- \leftrightarrows CH_3COO^- + 4\ H_2O$	214	-0.278	Eq. 1.24

Calculated using the Growth Reference System (biochemical standard conditions: 1 atm, 298.15 K, 1 mol L^{-1}, pH=7) following the procedure reported by Gildemyn et al. (2017) and based on data from Heijnen (1999).

Figure 1.10 shows the main anodic and cathodic processes associated to the sulfur cycle already implemented in BES (Blázquez et al., 2019b) and detailed in tables 1.2 and 1.3. In the case of the sulfur cycle, many compounds can be oxidized at an

anode: hydrogen sulfide (H_2S or TDS, total dissolved sulfide), polysulfide (S_n^{2-}), elemental sulfur (S^0) or thiosulfate ($S_2O_3^{2-}$). Purely electrochemical reactions can also occur depending on the anode potential in parallel to the biocatalyzed anodic processes. On the other hand, the cathode can act as electron donor driving reductive reactions of organic and inorganic compounds catalyzed by different microorganisms. A typical reaction studied in this case is the sulfate reduction to hydrogen sulfide (Eq. 1.13, Table 1.3). Electrochemical hydrogen production may also drive other reductive biological processes by microorganisms growing as biofilm or in planktonic form. All these interactions complete a complex scenario which can be driven towards selected final products of interest by deciding on well-designed operational conditions.

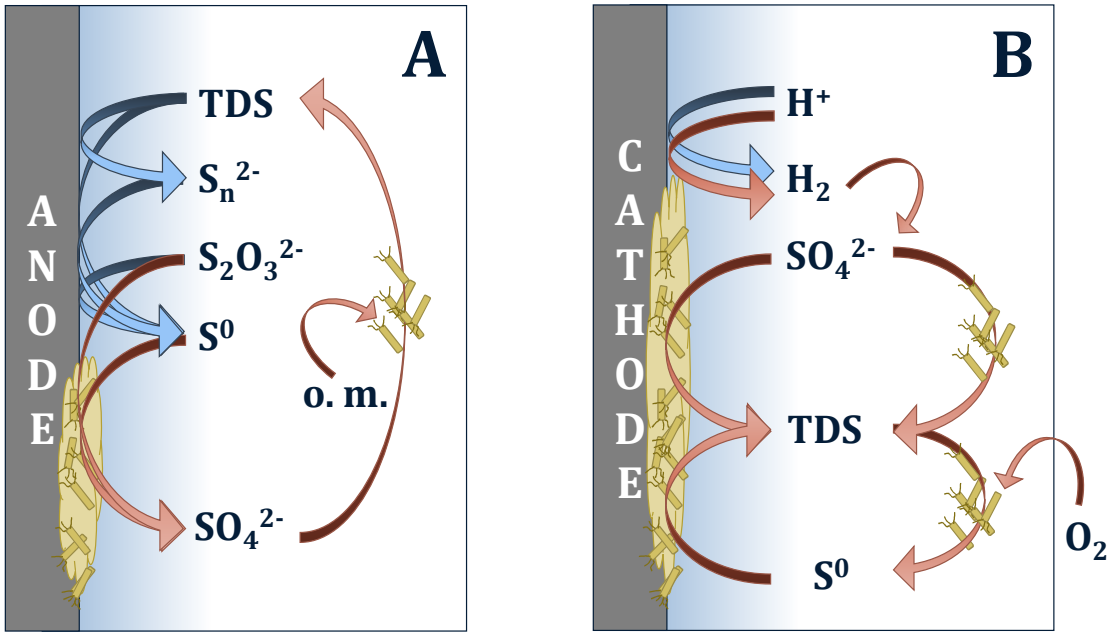

Figure 1.10. Sulfur-related oxidation and reduction processes occurring at the anode (A) and at the cathode (B) of bioelectrochemical systems. Blue arrow, abiotic reaction; red arrow, biotic reaction; o. m., organic matter (adapted from Blázquez et al. (2019b)).

1.4.1. Sulfate removal

A MEC with cathodic bioelectrochemical H_2 production (Eq. 1.22, Table 1.3) can be a solution for the treatment of sulfate-rich wastewaters: autotrophic SRB may use the H_2 produced *in situ* on the cathode surface avoiding the use of external electron donor supply. However, Su et al. (2012) reported for the first time the microbially catalyzed sulfate reduction to sulfide in a cathode acting as electron donor with no hydrogen production and was supported by other authors (Coma et al., 2013; Luo et al., 2014). The sulfate reduction directly driven by the electrons of the cathode was assumed because the cathode potentials used were around -0.2 V vs. SHE and the theoretical H_2 production at pH 7 takes place at -0.41 V vs. SHE (Eq. 1.22, Table 1.3) and experimentally has been observed to take place at -0.61 V vs. SHE catalyzed by *Desulfovibrio caledoniensis* (Yu et al., 2011). The hydrogen production catalyzed by *Desulfovibrio caledoniensis* can be explained because several strains of *Desulfovibrio* sp. have been reported to have capability to directly exchange electrons with the cathode (Cordas et al., 2008) because of the high amount of hydrogenase observed on electrode surfaces of reactors with high abundance of *Desulfovibrio* sp. (Marshall et al., 2017), which increases the electroactivity of the biocathode (Aulenta et al., 2012). However, really low sulfate removal rates have been observed with high cathode potentials (Coma et al., 2013; Gacitúa et al., 2018; Guan et al., 2016; Luo et al., 2014; Su et al., 2012) demonstrating that lower cathode potentials are required to improve the sulfate treatment of wastewaters.

Subsequently, many studies on BES optimization for sulfate reduction have been focused on (i) the effect of cathode potential (Gacitúa et al., 2018; Guan et al., 2016; Luo et al., 2014), (ii) initial pH (Liang et al., 2013; Luo et al., 2017), (iii) cathodic materials (Pozo et al., 2017a; Wang et al., 2017a), (iv) biofilm (Gacitúa et al., 2018; Pozo et al., 2016, 2015), (v) the use of organic matter (Wang et al., 2017b, 2017c), (vi) the presence of heavy metals (Teng et al., 2016). Therefore, some studies were conducted in order to improve the sulfate removal with BES, but no studies were conducted on elemental sulfur recovery in biocathodes, causing an effluent with high concentration of TDS.

1.4.2. Elemental sulfur recovery

The utilization of BES for the treatment of wastewater with high sulfur compounds content opens up the possibility to implement configurations aiming at its recovery as elemental sulfur. The bioelectrochemical conversion of sulfur compounds was not investigated until 2006 when Rabaey et al. (2006) studied the biological role in the anodic sulfide oxidation and it was followed by other authors (Gong et al., 2013; Pham et al., 2008; Sun et al., 2009), but without clear results on the biological effect on sulfide oxidation. The ambiguous biologic contribution was due to spontaneous sulfide oxidation in an anode (Dutta et al., 2008). The oxidation mechanism is described in Eq. 1.20 (Table 1.3) showing that such half reaction has the lower Gibbs energy required among the non-spontaneous processes. Other researchers aimed to reduce sulfate to sulfide and to oxidize sulfide to elemental sulfur in an anode (Chatterjee et al., 2017; Lee et al., 2014; Zhao et al., 2008) but at expenses of external organic matter supply.

The main problem observed by most authors was the electrode deactivation by the electrodeposited solid sulfur on the anode surface decreasing the efficiency and the power generation of the systems. Some methodologies have been investigated to continuously remove the elemental sulfur produced and, as a result, to regenerate the electrode. Shih and Lee (Shih and Lee, 1986) already proposed the use of organic solvents such as toluene or benzene to the agitated anodic compartment to remove the elemental sulfur electrochemically deposited. Later, Mao et al. (1991) avoided the electrode deactivation induced by elemental sulfur by adding alkali at high temperature. However, these processes were not sustainable due to the addition of toxic organic solvents, the application of extreme conditions, the high-energy requirements and its limited applications.

1.5. Research motivation and thesis overview

1.5.1. Research motivations

This thesis has been conducted in the Department of Chemical, Biological and Environmental Engineering of the UAB, in the Research Group on Biological Treatment and Valorisation of Liquid and Gas Effluents (GENOCOV) (www.genocov.com) within the project "Recuperación bioelectroquímica de azufre elemental de aguas con elevada carga de sulfates" (REBECA) ref. CTM2014-62179-EXP funded by the Ministerio de Economía of Spanish government. This thesis started on 2015 with the initial goal of treating high-sulfate content wastewaters using bioelectrochemical systems in view of elemental sulfur recovery.

The project proposed the use of BES for sulfate treatment with elemental sulfur recovery in a biocathode in a single step. However, the partial reduction of sulfate to elemental sulfur has not been described yet and this causes the need of a two-step process with hydrogen sulfide as intermediate through the sulfate reduction. Thus, as BESs consist of a very versatile technology and the treatment of high content sulfate wastewaters was not widely studied, there is a wide variety of possibilities for improvement.

1.5.2. Thesis overview

This document is divided into nine chapters.

Chapter 1 comprises a general introduction to the topic with a literature review and the state of the art.

Chapter 2 comprises the main objectives of this thesis.

Chapter 3 described the general materials and methods used to accomplish the thesis objectives.

Chapter 4 consists of the proof of concept that the elemental sulfur can be produced in a biocathode using the oxygen diffused from the anodic chamber to the cathodic chamber allowing the growth of sulfide oxidation bacteria.

Chapter 5 discusses some key parameters that can affect the sulfate removal and the elemental sulfur recovery such as the membrane, the cathode potential and the pH.

Chapter 6 includes the application of the previous studied system with real wastewater from a flue desulfurization system effluent.

The experimental parts of **Chapters 7 and 8** were performed in the Advanced water of management center of the University of Queensland, Australia. These chapters study different configurations in order to improve the elemental sulfur recovery, which consist of the use of an electrochemical cell and a fuel cell with air-cathode respectively.

Chapter 9 presents a general discussion and the conclusions of the thesis.

Finally, **Chapter 10** presents the references used along the thesis.

Chapter 2

Objectives

The general objective of this thesis is the treatment of wastewater with high sulfate content in the biocathode of bioelectrochemical systems towards the recovery of elemental sulfur.

Bioelectrochemical systems have already demonstrated to be a really versatile technology for treating different types of wastewater and for recovering energy or other valuable products. However, the treatment of sulfate in biocathodes has not been widely studied before this thesis, thus presenting several challenges and knowledge gaps to fulfill. The following specific objectives were proposed in order to gain knowledge about this process and improve the treatment of sulfate and the recovery of elemental sulfur through this novel technology:

- Demonstration of the technical feasibility of the treatment of wastewater with high sulfate content without the supply of external electron donor at high removal rates and recovery of elemental sulfur under oxygen limiting conditions.
- Evaluation of the most influencing parameters for efficient sulfate removal and elemental sulfur recovery such as the characteristics of the membrane used, pH and cathodic potential and how these factors influence microbial populations.
- Demonstration of the feasibility of bioelectrochemical systems for the treatment of real wastewater and to study how this real wastewater influences the recovery of elemental sulfur and the different microbial populations of the system.
- Integration of an electrochemical cell to improve the recovery of elemental sulfur in the anode using a new bioelectrochemical system configuration.
- Evaluation of an air-cathode fuel cell to improve elemental sulfur recovery in the new configuration of the integrated bioelectrochemical system.

Chapter 3

Materials and methods

This chapter summarizes the methodologies used along the thesis. Several reactors (with different volumes and configurations) were used to study and improve the treatment of high-strength sulfate wastewater in view of elemental sulfur recovery. Also, different techniques/parameters/indices were used in order to evaluate the efficiency of the processes. Some experiments were performed at the facilities of the Advanced Water Management Center (AWMC) at the University of Queensland, Australia (UQ) in the frame of collaboration between the two research groups and this is why different materials and methods for each lab are described in this chapter.

3.1. Reactors design

The inoculum reactor and bioelectrochemical systems at laboratory scale used for the sulfate reduction and elemental sulfur production in this thesis are detailed in the following sections. Reactors detailed in sections 3.1.1., 3.1.2, and 3.1.3. were located in the GENOCOV facilities (UAB, Catalonia, Spain) laboratories and reactors detailed in sections 3.1.4. and 3.1.5. were from AWMC (UQ, Queensland, Australia) laboratories.

3.1.1. Inoculum reactor

The inoculum for our BES systems needed to be highly enriched in hydrogenotrophic autotrophic SRB (AutH_2-SRB). AutH_2-SRB were selected in a reactor of 1.0 L and a headspace of 0.6 L (Figure 3.1) operated in batch mode and connected to a 1.0 L gas sampling bag with a twist-type valve (Cali-5-Bond, Ritter).

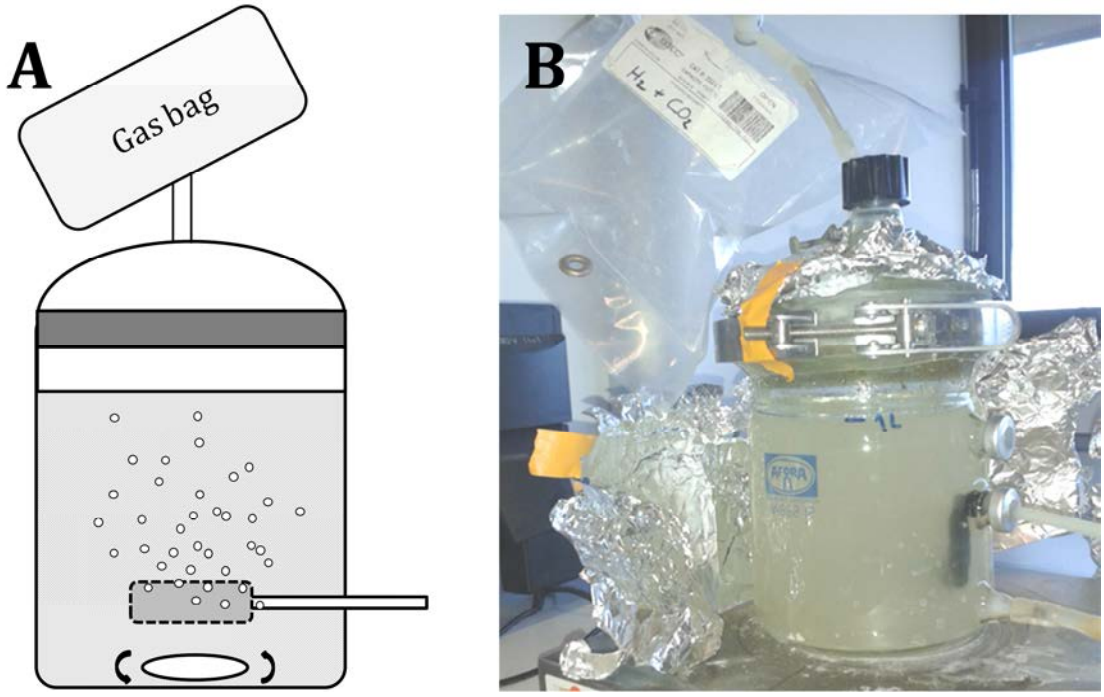

Figure 3.1. Scheme (A) and picture (B) of the inoculum reactor.

3.1.2. Cube-shape reactor (C-BES)

The C-BES (Figure 3.2) consisted of a two-chamber system. Two 28 mL methacrylate vessels were separated by the membrane inserted in a lateral aperture of 3.8 cm in diameter. An anionic exchange membrane (AEM, AMI-7001, Membranes International INC) was used in *Chapter 4* and a cationic exchange membrane (CEM, CMI-7000, Membranes International INC) in *Chapter 5*. The cathode compartment had a glass cylinder on top (with 40 mL of total volume and 35 mL of working volume in the cathodic compartment), tightly sealed with PTFE rubber cap that enabled gas diffusion to the catholyte using a gas-tight bag (0.1 L, Cali-5-bond, Ritter) connected through the rubber cap to the glass cylinder. The cathode consisted of a titanium wire connected to a graphite fiber brush (20 mm diameter x 30 mm length) made with fibers of 7.2 μm in diameter (type PANEX33 160K, ZOLTEK). The anodes were a titanium sheet (Ti plus 50 g m^{-2} Pt, Magneto, The Netherlands).

The graphite brushes of the cathodes were thermally treated at 450 ºC for 30 min to enhance biomass adhesion. Membranes were pretreated to allow membrane hydration and expansion by soaking them overnight in a 5 wt% sodium chloride solution at 37 ºC according to the supplier indications.

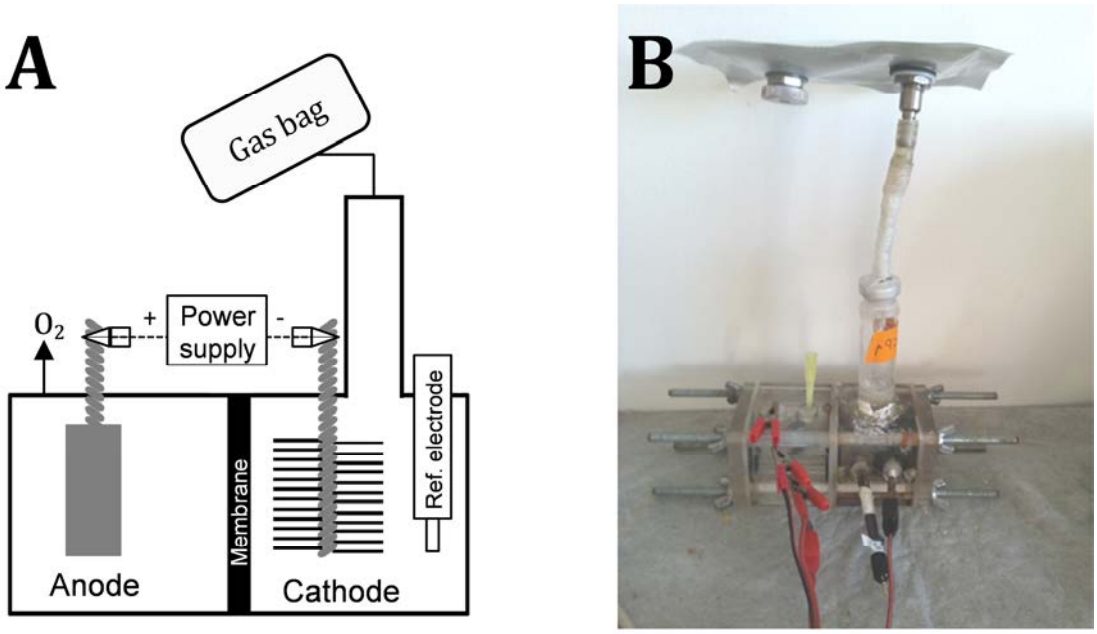

Figure 3.2. Scheme (A) and picture (B) of the C-BES.

3.1.3. H-shape reactor (H-BES)

The H-BES (Figure 3.3) consisted of a two-chamber system separated by a membrane and comprised two 400 mL glass vessels (350 mL of working volume) separated by a membrane with a lateral 7 cm diameter aperture. An AEM (AMI-7001, Membranes International INC) was used in *Chapter 4* and a CEM (CMI-7000, Membranes International INC) in *Chapter 5* and *6*. The cathode consisted of a graphite fiber brush (70 mm diameter x 70 mm length) made with the same fibers of 7.2 μm in diameter as in *3.1.2. Cube-shape reactor (C-BES)*. The cathode compartment was stirred and connected to a gas bag (0.5 L, Cali-5-bond, Ritter). The anodes were a titanium sheet (Ti plus 50 g m^{-2} Pt, Magneto, The Netherlands). The graphite brushes and membranes were pretreated as explained in *3.1.2. Cube-shape reactor (C-BES)*. The pH in the cathode was monitored with a pH probe (Hach pH electrode Crison 5233) connected to a pH meter (Hach MultiMeter Crison 44), and was automatically controlled at 7.0 through the addition of HCl (1 M) with a dispensing burette (Multi-Burette 2S-D, Crison Instruments).

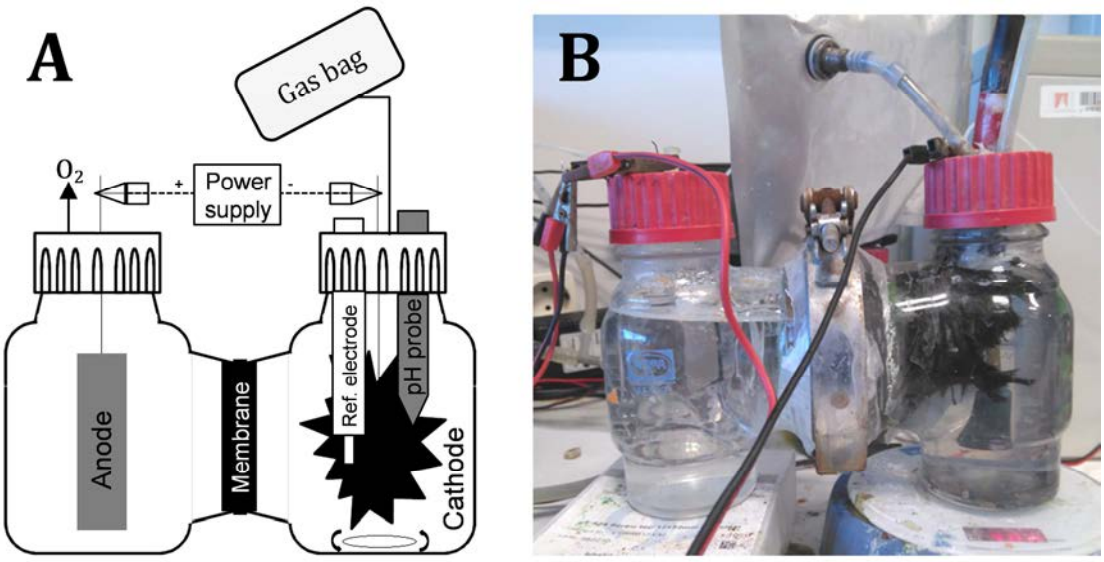

Figure 3.3. Scheme (A) and picture (B) of the H-BES.

3.1.4. Flat plate reactor + electrochemical cell (BES-EC)

The BES-EC reactor (Figure 3.4) consisted of four parallel acrylic frames (internal dimensions of 20 x 5 x 2 cm). The first and second frames were separated by a CEM (CMI-7000, Membranes International, USA). The second and third frames were separated by a plastic mesh (with 5 x 5 mm of grid and 1 mm of thickness) in order to avoid contact between the electrodes of each frame. The second and third frames consisted of a single middle chamber because they were not completely separated and shared the same electrolyte. The third and the fourth frames were separated by an AEM (AMI-7001; Membranes International, USA). The BES consisted of an abiotic anode made of platinum wire (purity 99.95%, 0.50 mm diameter x 50 mm long; Advent Research Materials, UK) located in the first frame and a biocathode made of unmodified graphite granules with a diameter of 6 mm or higher (El Carb 100; Graphite Sales, USA) in the second frame. Prior to inoculation, the graphite granules were washed in acid/base as previously described (Dutta et al., 2010) to remove impurities. Furthermore, three graphite rods (Ø5 mm, 8 cm long; element14, Australia) were embedded in the graphite granule bed and used as current collectors. The coupled electrochemical cell (EC) consisted of an anode located in the third frame made of reticulated vitreous carbon (RVC) of 19 x 4 x 1 cm (45 ppi pore size, Duocel RVC foam; ERG, USA) and a cathode located in the fourth frame which was a mixed metal oxide (MMO) $Ti/Ru_{0.7}Ir_{0.3}O_2$ electrode with 12 g m^{-2} coating on Ti mesh (dimensions: 4.8 x 5 cm; thickness: 1 mm; Magneto Special Anodes, Netherlands). One saturated calomel reference electrode (SCE; RE-2BP KCl sat., equiv. +0.244 V vs. SHE at 25 °C; BASi, USA) was embedded in the second frame in order to measure/control the biocathode potential of the BES, and another one in the third frame in order to measure/control the anode potential of the EC. Current density for BES and EC was defined as the average current in Ampere per square meter of membrane surface area.

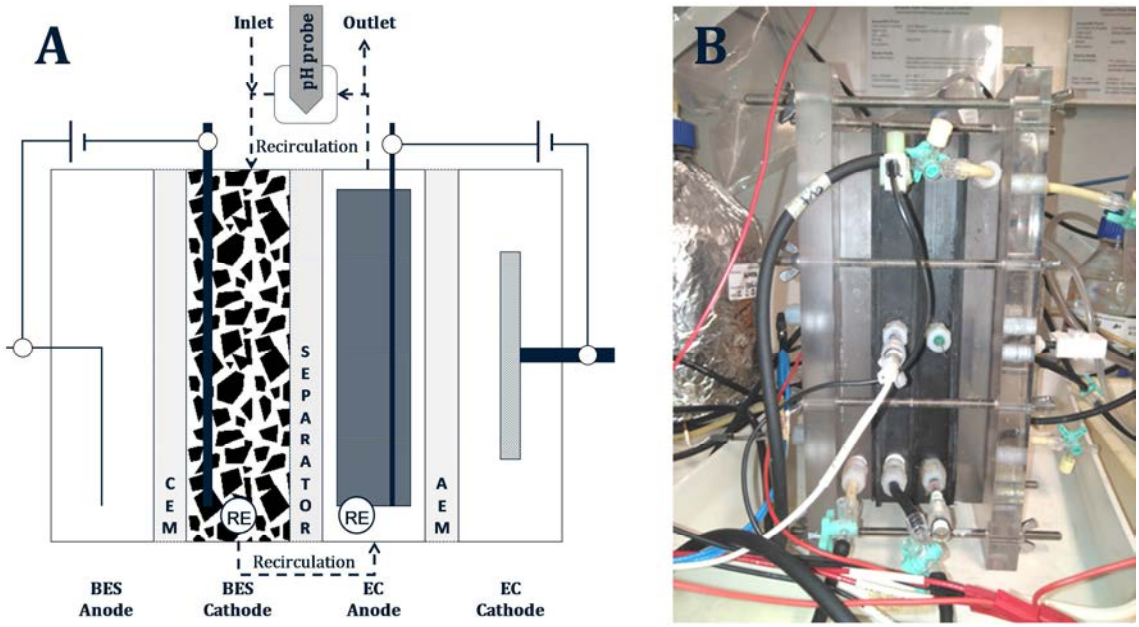

Figure 3.4. Scheme (A) and picture (B) of the BES-EC.

3.1.5. Flat plate reactor + fuel cell (BES-FC)

The BES-FC reactor (Figure 3.5) consisted of a modification of the reactor explained in *3.1.4. Flat plate reactor + electrochemical cell (BES-EC)*. In this case, the reactor consisted of three parallel acrylic frames (internal dimensions of 20 x 5 x 2 cm) instead of four. The BES consisted of an abiotic anode made of platinum wire (purity 99.95%, 0.50 mm diameter x 50 mm long; Advent Research Materials, UK) located in the first frame and a biocathode made of unmodified graphite granules with a diameter of 6 mm or higher (El Carb 100; Graphite Sales, USA) in the second frame. These frames were separated by a CEM (CMI-7000; Membranes International, USA). The third frame contained the coupled fuel cell (FC) that consisted of an anode made of RVC of 19 x 4 x 1 cm (45 ppi pore size, Duocel RVC foam; ERG, USA) and an air-cathode that consisted of carbon cloth coated with carbon powder and platinum suspension on the inner side (0.125 mg cm^{-2}, Platinum nominally 40% on high surface area advanced carbon support HiSPEC 4100™ powder, Alfa Aesar), whereas the outer side was coated with a polytetrafluoroethylene (PTFE) solution, which permitted oxygen diffusion into the cell while preventing water leakage (Cheng et al., 2006a, 2006b). Between the RVC and the air-cathode there was another plastic mesh in order to avoid the

contact between both electrodes and possible short circuit. One saturated calomel reference electrode (SCE; RE-2BP KCl sat., equiv. +0.244 V vs. SHE at 25 °C; BASi, USA) was embedded in the second frame in order to measure/control the biocathode potential of the BES. Current density for BES and FC was defined as the average current in Ampere per square meter of membrane surface area.

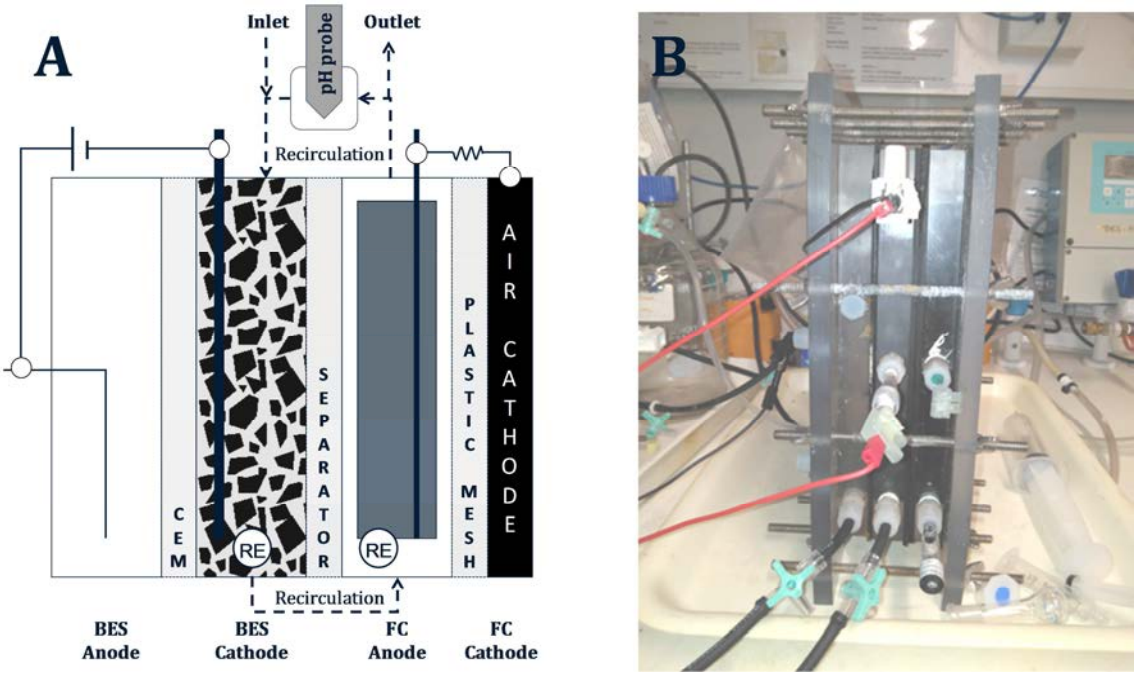

Figure 3.5. Scheme (A) and picture (B) of the BES-FC.

3.2. Analytical methods

3.2.1. Analytical methods Chapters 4, 5 and 6

All samples were filtered at 0.22 µm with disposable 0.22 µm syringe filter driven units (Millipore, USA) in order to remove any biomass or impurity present in the sample. Liquid samples were diluted with Mili-Q Water (18 MΩ cm^{-1}). Sulfate and thiosulfate concentrations were analyzed by ion chromatography with conductivity detection using a Dionex ICS-2000 equipment with an Ultimate 3000 Autosampler Column Compartment, an IonPac AS18 column and an IonPac AG18 pre-column (ThermoScientific, USA) with a detection range from 1 to 100 mg S L^{-1}.

Total dissolved sulfide concentration was measured with a sulfide selective electrode (VWR International Eurolab, S.L, USA). This electrode has its own internal reference electrode and presents a high sensitivity to S^{2-}. Thus, the samples must be buffered above pH 12 with an anoxidant buffer solution preciously to the analysius to convert HS^- and H_2S to S^{2-}. So, the samples were previously diluted with sulfide anti-oxidant buffer solution in order to minimize oxidation and stripping of sulfide as in Dutta et al. (2010). The buffer contained ascorbic acid (acts as sulfide antioxidant) and EDTA (avoids interferences with metallic compounds) dissolved in NaOH (2M).

The total suspended solids (TSS) where analyzed according to Standard Methods (American Public Health Association, 2005). By this way, an aliquot of liquid sample was firstly filtered through a pre-weighed standard glass microfiber of 0.7 μm (GF/F grade, Whatman, USA) and dried at constant temperature of 105 ºC. The increase of weight represents the organic and inorganic matter in suspension in the sample. The relation between weight increase and the sample volume is the concentration of TSS.

For the real wastewater characterization, the sample was homogenized and also filtered at 0.22 μm. Sulfate and thiosulfate (range from 1 mg S L^{-1} to 100 mg S L^{-1}), chloride (range from 1 mg Cl L^{-1} to 100 mg Cl L^{-1}), nitrite and nitrate (range from 1 mg N L^{-1} to 100 mg N L^{-1}) were analyzed by the ion chromatography. Ammonium nitrogen was analyzed by an ammonium analyzer (AMTAXsc, Hach Lange, range from 1 mg N L^{-1} to 100 mg N L^{-1}), which is based on the potentiometric determination of ammonia after basification of the sample. Phosphate was measured by a phosphate analyzer (PHOSPHAXsc, Hach Lange, (range from 1 mg P L^{-1} to 10 mg P L^{-1}), which is based on the vanadomolybdate yellow method. TIC and TOC were analyzed by the high temperature combustion device multi N/C® 2100S (Analytik Jena, Germany). Calcium and Magnesium were analyzed by spectrophotometry using an automatic analyzer (Y15, Biosystems, Spain). The conductivity was measured by COND 8 (XS instruments, Italy).

H_2 production was analyzed by gas chromatography (7820-A, Agilent Technologies, USA) using a thermal conductivity detector and a HP-mole sieve column with argon as carrier gas to ensure a good response in the H_2 peak. H_2S

production was analyzed by gas chromatography (Hewlett-Packard HP 5890 A, Agilent Technologies, USA) using a thermal conductivity detector and a Porapak Q column with helium as carrier gas. Gas production was evaluated as in Ambler and Logan (2011). In this methodology, the sample is analyzed in a first run, then a known volume of nitrogen is added as a reference compound and the resulting mixture is again analyzed. Mass balances calculations including the change in sample composition and the volume added allow the calculation of the initial gas volume as presented by Eq 3.1.

$$V_{total,initial} = \frac{V_{added,N_2}(1-x_{run2,N_2})+V_{run1}(x_{run2,N_2}-x_{run1,N_2})}{x_{run2,N_2}-x_{run1,N_2}} \quad \text{(Eq. 3.1)}$$

Where $V_{total,initial}$ is the initial total gas volume in the bag, V_{added,N_2} is the known volume of nitrogen added, V_{run1} is the volume injected in the GC in the first analysis, and x_{run1,N_2} and x_{run2,N_2} are the molar fraction of nitrogen in the first and second analyses respectively.

3.2.2. Analytical methods Chapters 7 and 8

Sulfate (range from 0.1 mg S L^{-1} to 150 mg S L^{-1}), sulfite (range from 0.1 mg S L^{-1} to 40 mg S L^{-1}), sulfide (range from 0.1 mg S L^{-1} to 40 mg S L^{-1}) and thiosulfate (range from 0.1 mg S L^{-1} to 150 mg S L^{-1}) were measured using an ion chromatograph (IC) with UV and conductivity detector (Dionex ICS-2000, Sunnyvale, USA). The samples were filtered at 0.22 μm with filters (Millipore, USA) and were diluted using a sulfide anti-oxidant buffer (SAOB) solution in order to minimize oxidation of sulfide (Keller-Lehmann et al., 2006). The difference between the sulfate after H_2O_2 oxidation and other species measured before H_2O_2 oxidation was regarded as polysulfide (Dutta et al., 2009b). Elemental sulfur was assumed to be the difference between all measured sulfur-species of the inlet and all measured sulfur-species of the outlet as explained elsewhere (Pozo et al., 2017b).

3.3. Solid phase characterization

The solid phase, accumulated from reactor purges, was characterized following the procedure developed by Montebello et al. (2014). Solid samples were centrifuged

at 7000 rpm during 10 minutes to separate the liquid phase and graphite leftovers from elemental sulfur and metal sulfides. Graphite fibers were easily removed from the solid centrifuged because of the density differences. Samples were lyophilized and homogenized. A thermogravimetric analysis (simultaneous differential scanning calorimetry and differential thermal analysis system, NETZSCH -STA 449 F1 Jupiter) was carried out with pure oxygen atmosphere to determine if the temperature of volatilization of solid samples corresponded to the oxidation of elemental sulfur to sulfur dioxide. In addition, 50 mg of the solid were combusted in an adiabatic bomb calorimeter at 1200 °C with pure oxygen (CHNS analyzer, Thermo Scientific Flash 2000) to quantify the total sulfur concentration. After SO_2 absorption, the sulfate formed was analyzed with a high-performance liquid chromatograph (HPLC Alliance, Waters 2695, Waters) and a conductivity detector (Waters 432, Waters). The total sulfur concentration was quantified from the sulfate concentration. Finally, analysis of metals was performed from 100 mg of solid samples previously digested with aqua regia ($HCl:HNO_3$ – 3:1 (v/v)) in a microwave at 190 °C (Ethos Plus, Milestone Laboratory System) during 25 min. Then, the digested solution was filtered through a free-ash filter and the volume was made up to 100 mL. Metals analysis was conducted by inductively coupled plasma mass spectrometry (ICP-MS, 7500ce, Agilent).

3.4. Scanning electron microscopy

Samples of graphite fiber brush (cathode) were collected, fixed with a solution of 3% glutaraldehyde, and processed according to conventional electron microscopy methods as previously described (Julián et al., 2010). Samples were treated with osmium tetraoxide, dehydrated with ethanol and dried at critical point with carbon dioxide (BAL-TEC CPD030; BalTec). Then, the samples were coated with few nanometers of Au-C (E5000 Sputter Coater) to increase signal detection and visualized on a Scanning Electron Microscope (SEM, Zeiss EVO ® MA 10). Elemental sulfur deposition over the biocathode was further determined by an energy dispersive spectrometer (EDS, Oxford INCA) connected to the SEM.

3.5. DNA extraction

Sample of the inoculum and samples from the biomass on the cathode, on the membrane surface and also in suspension were taken in *Chapter 6* before and after real wastewater treatment and in *Chapters 4* and *5* just samples from cathodic biofilm. The samples were collected in a sterile Eppendorf from the graphite brush and membrane with a sterile spatula. All samples were centrifuged at 10,000 g (Thermo Scientific Hareus Pico17, USA). The supernatant was eliminated to remove residues from the growth medium. DNA was extracted using a PowerSoil DNA Isolation Kit (MoBio Laboratories, Inc., Carlsbad, CA) according to the manufacturer instructions. The quality and quantity of the DNA was measured using a NanoDrop® spectrophotometer (ThermoScientific, USA). Paired-end sequencing of the extracted DNA was performed on an Illumina MiSeq platform based upon RTL protocols from a cathode DNA sample (20 ng μL^{-1}, quality ratio of 1.8) by Research and Testing Laboratory (Lubbock, TX) in *Chapter 4* and *5* and by Scsie UV (Valencia, Spain) in *Chapter 6*. Bacterial 16S rRNA variable region V1-V2 was targeted using the primer pair 28F-388R.

3.6. Microbial diversity analysis

The sequences of *Chapters 4* and *5* were checked using Dechipher (Database Enabled Code for ideal Probe Hybridization Employing R) with Decipher's Find Chimeras web tool to uncover short-length sequence (less than 1000 nucleotides) chimeras (http://decipher.cee.wisc.edu/FindChimeras.html, Wright et al., 2012). Sorting and trimming were performed using the Pipeline Initial Process at the Ribosomal Database Project (RDP) Pyrosequencing Pipeline (http://rdp.cme.msu.edu/index.jsp) (Cole et al., 2009) with default settings. The RDP Classifier was used to assign 16S rRNA gene sequences to a taxonomical hierarchy with a confidence threshold of 95%, since DNA sequences were < 250 bp (Claesson et al., 2009). The relative abundance of each phylogenetic group was calculated as the number of sequences associated with that group divided by the total number of sequences per sample. In the case of *Chapter 6* the results from Scsie UV (Valencia, Spain) were not treated afterwards.

3.7. Calculations

The observed sulfate reduction rate (SRR_o, Eq. 3.2) and sulfide production rate (SPR_o, Eq. 3.3) in the cathode were calculated keeping in mind the number of days of each cycle, as follows:

$$SRR_o = \frac{C^{Cat}_{SO_4^{2-}-S,i} - C^{Cat}_{SO_4^{2-}-S,f}}{t} \quad \text{(Eq. 3.2)}$$

$$SPR_o = \frac{C^{Cat}_{TDS-S,f} - C^{Cat}_{TDS-S,i}}{t} \quad \text{(Eq. 3.3)}$$

Where $C^{Cat}_{SO_4^{2-}-S,i}$ and $C_{SO_4^{2-}-S,f}$ are the concentrations of sulfate in the cathode at the beginning and at the end of cycle, $C^{Cat}_{TDS-S,f}$ and $C^{Cat}_{TDS-S,i}$ are the concentration of total dissolved sulfide (TDS) in the cathode at the end and at the beginning of the cycle and t is the number of days of the cycle. The SRR_o and SPR_o calculations did not consider the possible sulfate diffusion through the membrane.

The sulfate reduction rate (SRR, Eq. 3.4) and sulfide production rate (SPR, Eq. 3.5) of the BES were calculated as:

$$SRR = \frac{V^{Cat}\left(C^{Cat}_{SO_4^{2-}-S,i} - C^{Cat}_{SO_4^{2-}-S,f}\right) - V^{An}\left(C^{An}_{SO_4^{2-}-S,f} - C^{An}_{SO_4^{2-}-S,i}\right)}{t \cdot V^{Cat}} \quad \text{(Eq. 3.4)}$$

$$SPR = \frac{V^{Cat}\left(C^{Cat}_{TDS-S,f} - C^{Cat}_{TDS-S,i}\right) + V^{An}\left(C^{An}_{TDS-S,f} - C^{An}_{TDS-S,i}\right)}{t \cdot V^{Cat}} \quad \text{(Eq. 3.5)}$$

Where $C^{An}_{SO_4^{2-}-S,f}$ and $C^{An}_{SO_4^{2-}-S,i}$ are the concentrations of sulfate in the anode at the beginning and at the end of cycle, $C^{An}_{TDS-S,i}$ and $C^{An}_{TDS-S,f}$ are the final and initial TDS concentration in the anode. V^{Cat} and V^{An} are the volumes of the cathode and anode respectively.

The sulfur balance (Eq. 3.6) of the BES were calculated as follows:

$$S\ Balance = 100\,\frac{V^{Cat}\sum_{k=1}^{3} C^{Cat}_{k,f} + V^{An}\sum_{k=1}^{3} C^{An}_{S,f}}{V^{Cat}\sum_{k=1}^{3} C^{Cat}_{k,i} + V^{An}\sum_{k=1}^{3} C^{An}_{S,i}} \quad \text{(Eq. 3.6)}$$

Where $C^{Cat}_{k,f}$ and $C^{Cat}_{k,i}$ are the final and initial concentration of sulfate, thiosulfate and TDS in the cathode, respectively, and $C^{An}_{k,f}$ and $C^{An}_{k,i}$ are the same measurements in the anode.

The concentration of theoretical elemental sulfur produced in one cycle (${S^0}_t$) (Eq. 3.7) and theoretical elemental sulfur production rate (TESPR, Eq. 3.8) were calculated as follows:

$${S^0}_t = C^{Cat}_{SO_4^{2-}-S,i} * \left(\frac{100-S\ balance}{100}\right) \quad \text{(Eq. 3.7)}$$

$$TESPR = \frac{{S^0}_t}{t} \quad \text{(Eq. 3.8)}$$

The recovered elemental sulfur in suspension (S^0) (Eq. 3.9) was calculated as follows:

$$S^0 = TSS * \frac{\%\ of\ S}{100} \quad \text{(Eq. 3.9)}$$

Where *TSS* is the total suspended solids and *% of S* is the percentage of sulfur in the TSS as measured with the CHNS analyzer. The elemental sulfur fraction attached to the walls of the reactor was not included as recovered elemental sulfur, but was estimated as the difference between S^0_t and S^0.

In the case of *Chapters 7* and *8*, where the reactors operated at continuous mode, the rates and balances were calculated differently. The observed sulfate removal rate (SRR, Eq. 3.10) and sulfide production rate (SPR, Eq. 3.11) in the cathode were calculated as follows:

$$SRR = \frac{C_{SO_4^{2-}-S,in} - C_{SO_4^{2-}-S,out}}{HRT} \quad \text{(Eq. 3.10)}$$

$$SPR = \frac{C_{TDS-S,out}}{HRT} \quad \text{(Eq. 3.11)}$$

Where $C_{SO_4^{2-}-S,in}$ and $C_{SO_4^{2-}-S,out}$ are the concentrations of sulfate at the inlet and at the outlet effluents, $C_{TDS-S,out}$ is the concentration of total dissolved sulfide at the outlet effluent and *HRT* is the hydraulic retention time of the medium in the middle chamber.

The concentration of theoretical elemental sulfur produced (${S^0}_t$, Eq. 3.12), theoretical elemental sulfur production rate (TESPR, Eq. 3.13) and the elemental sulfur proportion (Eq. 3.14) were calculated as follows:

$${S^0}_t = C_{SO_4^{2-}-S,in} - C_{S\ species-S,out} \quad \text{(Eq. 3.12)}$$

$$TESPR = \frac{{S^0}_t}{HRT} \quad \text{(Eq. 3.13)}$$

$$Elemental\ sulfur\ percentage = \frac{TESPR}{SRR} \cdot 100 \quad \text{(Eq. 3.14)}$$

Where $C_{S\ species-S,out}$ is the sum of all the concentrations of S-species measured at the outlet effluent.

The electron recovery for reducing sulfate (Eq. 3.15) and producing hydrogen (Eq. 3.16) were calculated as follows:

$$S\text{-}electron\ recovery\ = 100\frac{n_S \cdot SRR \cdot V^{Cat} \cdot F}{I \cdot PM_S} \quad \text{(Eq. 3.15)}$$

$$H\text{-}electron\ recovery = 100\frac{n_H \cdot HPR \cdot V^{Cat} \cdot F}{I \cdot PM_H} \quad \text{(Eq. 3.16)}$$

Where n_S is the number of moles of electrons needed to reduce one mole of sulfate (8 mole of electrons), n_H is the number of moles of electrons needed to produce one mole of hydrogen (2 mole of electrons), *SRR* is the sulfate reduction rate, *HPR* is the hydrogen production rate (calculated as in Ambler and Logan (2011)), *F* is Faraday's constant (96485 C mole of electrons^{-1}), *I* is the intensity, PM_S is the molar weight of sulfur (32 g mole^{-1}) and PM_H is the molar weight of hydrogen (2 g mole^{-1}).

Chapter 4

Treatment of high-strength sulfate wastewater using an autotrophic biocathode in view of elemental sulfur recovery

The main motivation of this chapter was to demonstrate for the first time the feasibility of elemental sulfur recovery from high-strength sulfate wastewater using an autotrophic biocathode. This work proposes a novel single stage process for recovering elemental sulfur, based on the coexistence of sulfate-reducing and sulfide-oxidizing bacteria (SRB and SOB) in a biocathode of a bioelectrochemical system (BES) without external addition of electron donor or acceptor. We observed high-rate autotrophic sulfate reduction by SRB with H_2 as the sole electron donor and hydrogen sulfide oxidation by SOB with DO diffused from the anode.

Abstract

This work is the first to demonstrate that, in addition to an efficient sulfate-rich wastewater treatment, elemental sulfur could be recovered in a biocathode of a BES under oxygen limiting conditions. The key of the process is the biological oxidation of sulfide to elemental sulfur simultaneously to the sulfate reduction in the cathode using the oxygen produced in the anode that diffuses through the membrane. High sulfate reduction rates (up to 388 mg SO_4^{2-}-S L^{-1} d^{-1}) were observed linked to a low production of sulfide. Accumulation of elemental sulfur over graphite fibers of the biocathode was demonstrated by energy dispersive spectrometry, discarding the presence of metal sulfides. Microbial community analysis of the cathode biofilm demonstrated the presence of sulfate-reducing bacteria (mainly *Desulfovibrio* sp.) and sulfide-oxidizing bacteria (mainly *Sulfuricurvum* sp.). Hence, this biocathode allows simultaneous biological sulfate reduction and biological sulfide oxidation to elemental sulfur, opening up a novel process for recovering sulfur from sulfate-rich wastewaters.

4.1. Introduction

The biological treatment of high-strength sulfate wastewater is restricted to anaerobic reactors where biological sulfate reduction is demonstrated as an efficient process for removing sulfate from wastewaters with either H_2 (Eq. 4.1) or organic matter (Eq. 4.2) as electron donor. Sulfate-reducing bacteria (SRB) are anaerobic microorganisms that use sulfate as a terminal electron acceptor resulting in the production of sulfide (Muyzer and Stams, 2008), that may lead to significant issues such as corrosion, bad odors and toxic issues on human health (Pol et al., 1998b). Under microaerophilic conditions, sulfide can be partially oxidized (Eq. 4.3) by sulfide-oxidizing bacteria (SOB) to elemental sulfur. Therefore, oxygen limiting conditions are needed to avoid thiosulfate and sulfate production.

$SO_4^{2-} + 4H_2 + H^+ \rightarrow HS^- + 4H_2O$ $\Delta G^º = -151.9$ KJ mol^{-1} (Eq. 4.1)

$SO_4^{2-} + CH_3COO^- \rightarrow HS^- + 2HCO_3^-$ $\Delta G^º = -47.6$ KJ mol^{-1} (Eq. 4.2)

$HS^- + 0.5O_2 \rightarrow S^0 + OH^-$ $\Delta G^º = -169$ KJ mol^{-1} (Eq. 4.3)

Sulfate-rich wastewaters are usually deficient in electron donors and hence an external supply is necessary (Liamleam and Annachhatre, 2007). Hydrogen is commonly used as electron donor for sulfate reduction because, according to thermodynamics, hydrogenotrophic sulfidogenensis is more favorable than methanogenesis (Weijma et al., 2002) since SRB are generally more efficient in hydrogen utilization than methanogenic bacteria (Davidova and Stams, 1996).

Recent studies have suggested that biological sulfate reduction can also be driven by electricity as the sole electron source by using bioelectrochemical systems (BESs). Sulfate reduction to hydrogen sulfide in a biologically catalyzed cathode has been reported by several authors (Coma et al., 2013; Luo et al., 2014; Pozo et al., 2015; Su et al., 2012; Teng et al., 2016). These works operated a two-chamber BES to study the sulfate removal efficiency in the biocathodic compartment and to evaluate both the current output and electron recovery efficiency. Even so, these studies are based on the sulfate reductive process and, as such, they have not studied the possibility to recover sulfur in the same device.

Hence, we propose a novel process for elemental sulfur recovery from high-strength sulfate wastewaters using a BES which integrates both the sulfate reduction to sulfide and a sequential partial oxidation of sulfide to elemental sulfur in the same reactor. Sulfate is biologically reduced to sulfide in the biocathode (using hydrogen as intermediary rather than direct electron transfer) while sulfide is partially oxidized to elemental sulfur using part of the oxygen produced in the anodic water electrolysis. Consequently, elemental sulfur is produced in the cathode. Hydrogen would be bioelectrochemically generated without the need of external organic fermentable compounds or external hydrogen gas supply. Therefore, we need a reductive process to drive sulfate reduction to sulfide and an oxidative process to obtain elemental sulfur from sulfide. The difficulty of the system lays in providing these two scenarios in the same single-chamber.

Thus, the aim of this work is to show the technical feasibility of this novel process for the treatment of high-strength sulfate wastewaters without external donor dosage and i) to obtain high-rate autotrophic sulfate reduction by SRB with hydrogen as the sole electron donor, ii) to recover elemental sulfur in the same compartment under oxygen limiting conditions and iii) to study the microbial communities of the system.

4.2. Experimental

4.2.1. Hydrogenotrophic and autotrophic SRB enrichment

This reactor was inoculated with biomass from a lab-scale sewer system (Auguet et al., 2015). The reactor was periodically sparged with CO_2 that served as: i) carbon source, ii) pH buffer, and iii) agent for sulfide stripping, thus preventing possible inhibitions. After CO_2 sparging with the reactor open, the reactor was closed and a gas sampling bag was filled with a mixture of H_2 and CO_2 and connected to the reactor so that both were continuously absorbed in the liquid phase following gas-liquid equilibrium. Hydrogen was the sole electron donor available. The gas phase consisted of approximately 60% of H_2 and 40% of CO_2. Every 3-4 days, 125 mL of sludge were purged and the volume was replaced with new mineral medium. Sulfate content was ensured by periodically adding 10 mL of

a concentrated pulse of $MgSO_4$ to reach a concentration of 500 mg SO_4^{2-}-S L^{-1}. The reactor was operated at room temperature (T= 24 ± 2 ºC) and pH was in the range 6.5 – 7.

The mineral medium used for the AutH_2-SRB growth was a modification of that used in Coma et al. (2013). The medium was prepared with tap water and contained (mg L^{-1}) 2311 $MgSO_4 \cdot 7H_2O$, 146.6 $NaHCO_3$, 9.2 NH_4Cl, 327 $Na_2HPO_4 \cdot 2H_2O$, 144 $KH_2PO_4 \cdot 2H_2O$, 1.7 $CaCl_2 \cdot 2H_2O$, 1.6 KCl and 1 mL of microelements solution. The microelements solution was described by Montpart et al. (2014) and contained (mg L^{-1}): 1000 EDTA, 164 $CoCl_2 \cdot 6H_2O$, 228 $CaCl_2 \cdot 2H_2O$, 20 H_3BO_3, 40 $Na_2MoO_4 \cdot 2H_2O$, 2 Na_2SeO_3, 20 $Na_2WO_4 \cdot 2H_2O$, 40 $NiCl_2 \cdot 6H_2O$, 2320 $MgCl_2$, 1180 $MnCl_2 \cdot 4H_2O$, 100 $ZnCl_2$, 20 $CuSO_4 \cdot 5H_2O$ and 20 $AlK(SO_4)_2$.

4.2.2. Experimental procedure

The BES for elemental sulfur recovery consisted of two-chamber systems with anode and cathode separated by an anion-exchange membrane (AEM). Two configurations at different scale were used: i) two parent cube-shaped BES (C-BES, Figure 3.2) and ii) H shaped BES (H-BES, Figure 3.3). The results presented under the C-BES configuration come from both parent cells.

Cathodes of both BESs were inoculated with the AutH_2-SRB-enriched sludge. After the inoculation, cycles of 3-7 days were completed using fresh mineral medium in order to acclimate biomass. The fresh medium was prepared with distilled water and contained (mg L^{-1}) 444 - 4438 Na_2SO_4, 1000 $NaHCO_3$, 300 NH_4Cl, 3484 $K_2HPO_4 \cdot 2H_2O$, 2722 $KH_2PO_4 \cdot 2H_2O$, 85 $MgCl_2 \cdot 2H_2O$, 100 KCl and 1 mL of microelements solution. The anodic medium contained 2 g NaCl L^{-1} dissolved in distilled water. The whole experimental operation was divided into three different periods according to the initial sulfate concentrations of the batch experiments (Table 4.1). A first period to enrich the microbial community (period I), a second period to study the activity at a moderate initial substrate concentration (period II, 500 mg SO_4^{2-}-S L^{-1}) and a third period of high initial sulfate concentration (period III, 1000 mg SO_4^{2-}-S L^{-1}) to increase the biological activity. Moreover, in order to determine the sulfate diffusion through the membrane in the worst-case scenario,

the anolyte was replaced for a fresh one in the last five cycles of period III in the H-BES and the sulfate concentration of both compartments was measured.

Table 4.1. Operational conditions of both BES for each experimental period.

Period	Days	Initial sulfate concentration (mg SO_4^{2-}-S L^{-1})	Duration of cycles (days)
I	0-178	100-500	3-7
II	178-230	500	3-4
III	230-330	1000	3-4

During the operation of the H-BES, the pH in the cathode was monitored with a pH probe (Hach pH electrode Crison 5233) connected to a pH meter (Hach MultiMeter Crison 44), and was automatically controlled at 7.0 through the addition of HCl (1 M) with a dispensing burette (Multi-Burette 2S-D, Crison Instruments). The pH of the C-BES was also measured but not automatically controlled. Both BESs were operated at room temperature (T= 24 ± 2 ºC).

An abiotic experiment was also carried out using another H-BES to characterize the oxygen transfer from the anode to the cathode through the membrane with a dissolved oxygen (DO) probe (CellOx 325, WTW) in the cathode. Cathodic DO evolution was monitored in two scenarios: i) with a cathode potential set at -0.8 V vs. SHE and ii) without potential applied and pure oxygen sparged into the anodic compartment.

4.3. Results and discussion

4.3.1. Autotrophic sulfate removal

Two BESs (C-BES and H-BES) were inoculated with an enriched $AutH_2$-SRB community in the cathode, which was set at -0.8 V vs. SHE. Both BESs were operated in batch mode during 330 days showing promising results. Figure 4.1

shows the results obtained during the whole experimental period, which was divided into three different periods (Table 4.1).

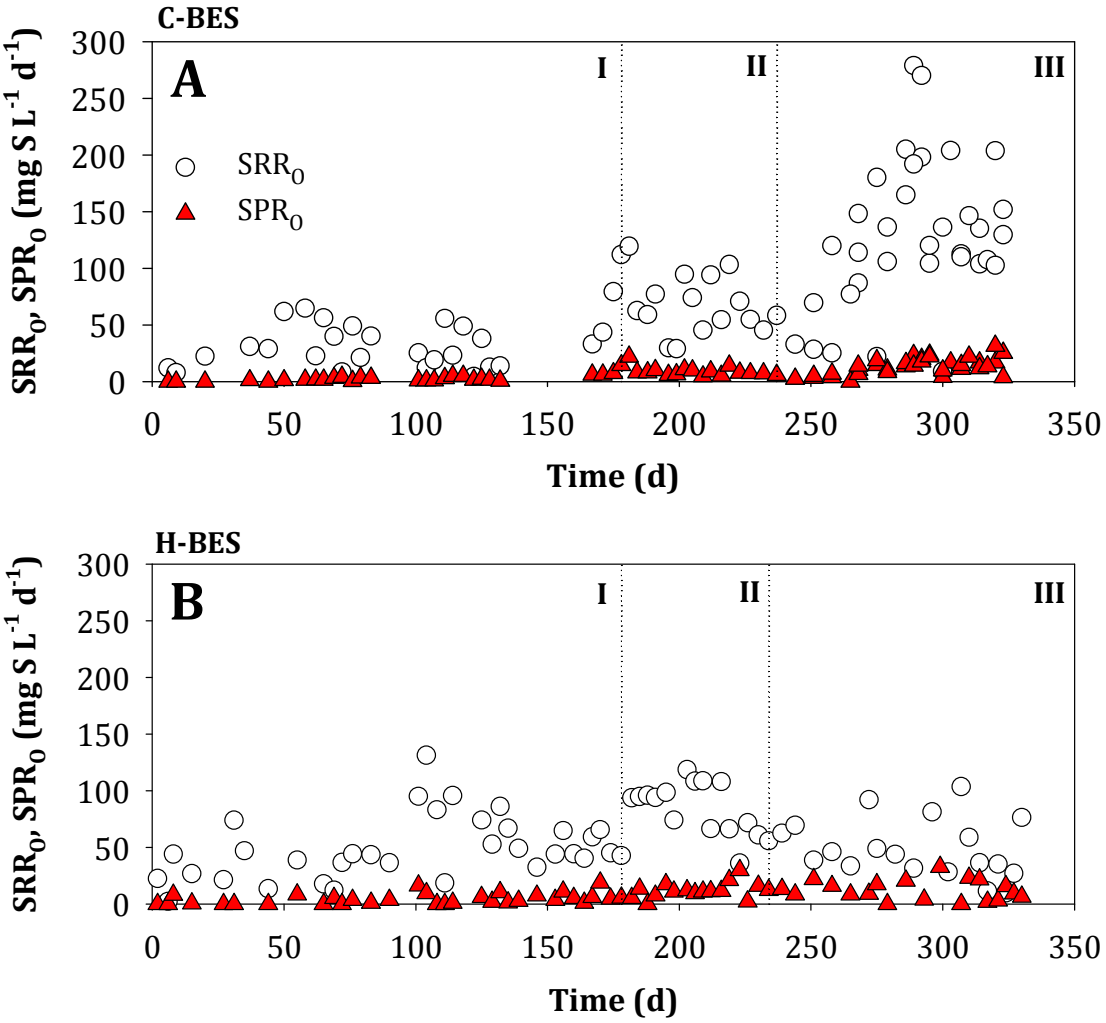

Figure 4.1. Observed sulfate removal rate (SRR_0) and observed sulfide production rate (SPR_0) observed during the long-term operation of A: the C-BES and B: the H-BES.

In the first period, the H-BES showed higher observed SRR and observed SPR than the C-BES. Note that we use the term observed SRR and observed SPR since, as discussed below, part of these ions could be transferred through the AEM. During period II, the observed SRR increased and finally, in period III, the C-BES showed an observed SRR up to 280 mg SO_4^{2-}-S L^{-1} d^{-1}. The SRR in the H-BES for period III were similar to those in period II showing a maximum SRR up to

150 mg SO_4^{2-}-S L^{-1} d^{-1}. On the other hand, SPR was always much lower than SRR and hence the amount of sulfate removed did not match the sulfide produced, indicating that other S species should be playing an important role.

Table 4.2 shows the average SRR and SPR per cell and per period. The lowest SRR and SPR were found in the start-up period. In period II, the H-BES showed higher SRR and SPR than the C-BES. However, in period III, the SRR of the C-BES increased due to a higher initial sulfate concentration while the SRR of H-BES decreased because of a H_2 limitation due to a decrease of current density from 1.87 A m^{-2} to 0.91 A m^{-2}. Table 4.2 also reflects the important unbalance between SRR and SPR previously observed in Figure 4.1. Considering all the experimental results, SRR was 10 times higher than SPR.

Table 4.2. Average of observed sulfate removal rate (SRR_0) and observed sulfide production rate (SPR_0) in both BES configurations during the three periods of operation.

Period	C-BES SRR_0 (mg SO_4^{2-}-S L^{-1} d^{-1})	H-BES SRR_0 (mg SO_4^{2-}-S L^{-1} d^{-1})	C-BES SPR_0 (mg TDS-S L^{-1} d^{-1})	H-BES SPR_0 (mg TDS-S L^{-1} d^{-1})
I	32 ± 19	64 ± 32	2.4 ± 2.1	4.1 ± 4.8
II	73 ± 29	112 ± 22	9.8 ± 4.6	12.0 ± 7.4
III	121 ± 66	97 ± 25	12.9 ± 7.4	12.3 ± 8.8

Six different cycles of three days each from periods II and III for each BES configuration were daily monitored. Figure 4.2 shows the average results of sulfate, sulfide and thiosulfate evolution along the cycles. The maximum rates observed were 266 mg SO_4^{2-}-S L^{-1} d^{-1} in the C-BES (Figure 4.2A) and 231 mg SO_4^{2-}-S L^{-1} d^{-1} in the H-BES (Figure 4.2B) and both corresponded to the first day of the cycle. Thiosulfate concentrations were mainly below 5 mg $S_2O_3^{2-}$-S L^{-1} d^{-1} in both configurations and sulfite was not detected. Thus, TPR was considered negligible. The average sulfide concentration measured at the end of the cycles was 37 ± 9 mg TDS-S L^{-1} for the C-BES and 37 ± 14 mg TDS-S L^{-1} for the H-BES, much

lower than the initial sulfate concentration. Thus, such sulfur unbalance was hypothesized to indicate elemental sulfur production or sulfate/sulfide losses as discussed below.

The maximum rates observed the first day of cycle in selected cycles of period III were 388 mg SO_4^{2-}-S L^{-1} d^{-1} in the C-BES (Figure 4.2C) and 256 mg SO_4^{2-}-S L^{-1} d^{-1} in the H-BES (Figure 4.2D), which corresponded to a 45% and 11% increase, respectively, compared to these in period II. Similarly, thiosulfate concentrations were also mainly below 5 mg $S_2O_3^{2-}$-S L^{-1} d^{-1} and sulfite was not detected in both configurations. The average sulfide concentration measured at the end of the selected cycles was 36 ± 13 mg TDS-S L^{-1} for the C-BES and 25 ± 15 mg TDS-S L^{-1} for the H-BES, which indicated, again, a large sulfur unbalance, explained in section 3.2.

pH plays an important role on sulfate reduction and higher SRR are reported at acidic pHs. Liang et al. (2013) measured the SRR in a range of pHs (2.5, 4.5, 6.5 and 8.5), obtaining the highest SRR at pH=4.5 using ethanol as electron donor instead of H_2. In batch experiments, the cathodic pH increases due to the protons used in both hydrogen production (Eq. 4.4) and sulfate reduction (Eq. 4.1). Thus, alkaline pH conditions are expected to occur, which may lead to a reduction of SRB activity (Coma et al., 2013). pH was not controlled in the C-BES and reached values up to 8.3, which may have decreased microbial activity. However, the pH at the start of the cycle in C-BES was around 6.3 (lower than in H-BES that was controlled at 7). Thus, we observed higher maximum SRR and SPR along the first day in C-BES (Figure 4.2A) than in H-BES (Figure 4.2B). However, the SRR was progressively reduced as pH increased thereafter. On the other hand, the pH-controlled H-BES showed more constant SRR. In this way, the maximum rates observed the first day were always higher in C-BES than in H-BES.

$$2H^+ + 2e^- \rightarrow H_2 \qquad \Delta G^º = 0 \text{ KJ mol}^{-1} \qquad \text{(Eq. 4.4)}$$

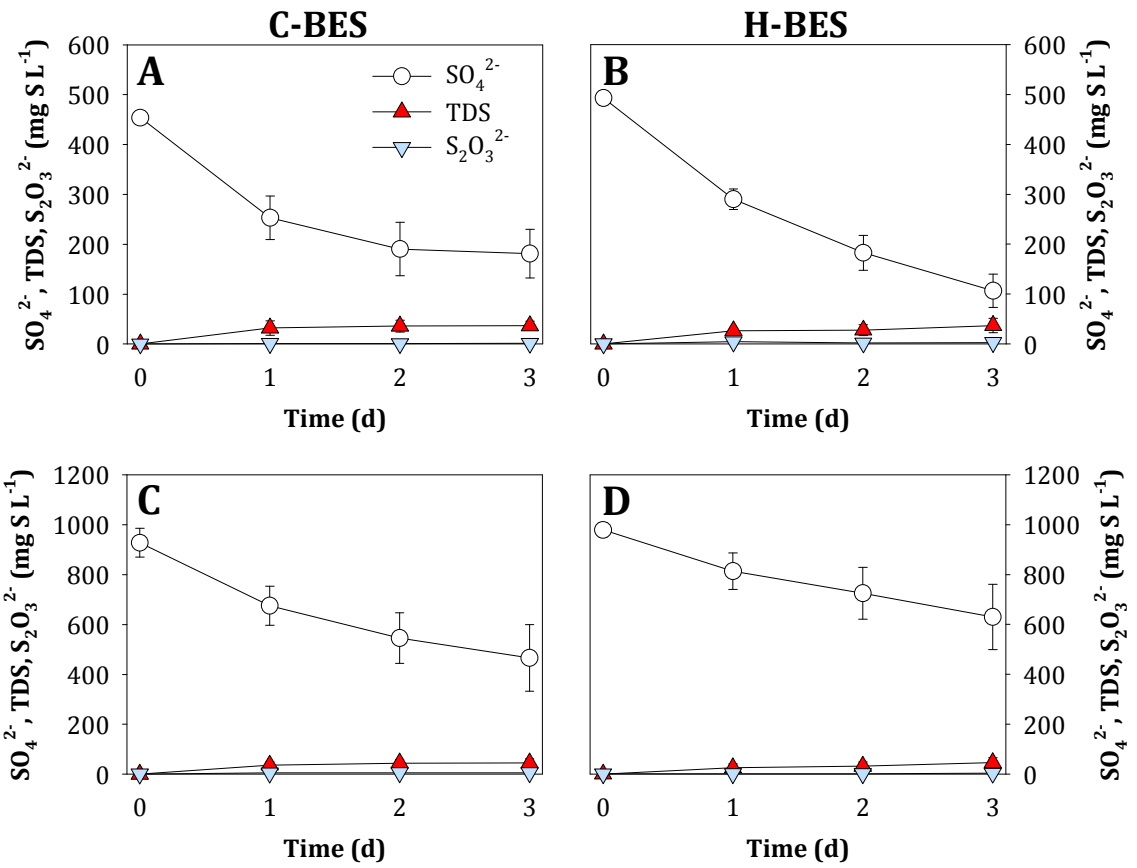

Figure 4.2. Sulfate, sulfide and thiosulfate concentrations averaged of six cycles at 500 mg SO_4^{2-}-S L^{-1} of initial concentration: A: C-MEC and B: H-MEC and in six cycles at 1000 mg SO_4^{2-}-S L^{-1} of initial concentration: C: C-MEC and D: H-MEC.

The SRR obtained in this work are one order of magnitude higher than most found in bioelectrochemical systems in literature. Su et al. (2012) and Coma et al. (2013) operated continuous-flow systems and achieved, respectively, SRR of 14.6 mg SO_4^{2-}-S L^{-1} d^{-1} (at -0.2 V vs. SHE) and around 60 mg SO_4^{2-}-S L^{-1} d^{-1} (at -0.26 V vs. SHE). Moreover, no sulfur unbalance was detailed. Luo et al. (2014) attained a maximum SRR of 16.3 mg SO_4^{2-}-S L^{-1} d^{-1} in fed-batch operation at 0.8 V of fixed cell voltage, obtaining a cathode potential of -0.76 V vs. SHE. Interestingly, they recovered only 5% of sulfate as sulfide. Teng et al. (2016) worked in fed-batch experiments obtaining SRR of 32 mg SO_4^{2-}-S L^{-1} d^{-1} under acidophilic conditions (pH=3) and at 0.7 V of fixed cell voltage. In this case authors assumed that all sulfate was reduced to sulfide and then precipitated as ZnS because of the supply of Zn^{2+}. Pozo et al. (2015) obtained the maximum SRR reported until now in a BES

biocathode, which corresponds to a SRR of 188 mg SO_4^{2-}-S L^{-1} d^{-1} at a fixed cathode potential of -0.9 V vs. SHE. In spite of a higher cathodic potential and, thus, a lower hydrogen production, our system provided higher SRR of 388 mg SO_4^{2-}-S L^{-1} d^{-1} at -0.8 V vs. SHE. These are outstanding results in terms of sulfate reduction capacity considering that the BES presented herein has not been optimized and further improvements may lead to increased SRRs. These SRRs obtained are far from those reported in high-rate expanded granular sludge blanket reactors using H_2 (10 g SO42--S L-1 d-1, van Houten et al., 1994). However, BES offer important advantages in terms of H_2 production, gas-liquid transfer, efficiency and H_2 supply costs to make BES a competitive technology for treatment of high-strength sulfate wastewaters.

4.3.2. Sulfur imbalance: elemental sulfur formation

Regarding the sulfur unbalance, 13.8 ± 4.1% of the SO_4^{2-}-S removed was accounted for as TDS-S in the C-BES and 11.4 ± 7.9% in the H-BES in period II. Despite the higher initial sulfate concentrations in period III, very similar percentages were obtained compared with period II. Only 13.3 ± 12.1% of the SO_4^{2-}-S removed was accounted for as TDS-S in the C-BES and 12.0 ± 7.5% in the H-BES. We verified that such sulfur unbalance was caused by elemental sulfur production rather than to sulfate/sulfide losses (i.e. through the membrane or precipitation). Sulfate, thiosulfate and total dissolved sulfide were also analyzed in the anodic compartment of the H-BES during several experiments of period III to quantify the possible sulfate/sulfide losses through the membrane (Table 4.3). A fresh anolyte was used to observe the possible diffusion through the membrane in the worst-case scenario.

The average diffusion obtained was of 4.7 ± 2.3% per day of sulfate. Neither sulfide nor thiosulfate were detected in the anodic compartment. Thus, almost 5% of the sulfate present in the cathode was transferred to the anode every day the first cycles with fresh anolyte. Otherwise, after some cycles, the diffusion was reduced because the anolyte increased its sulfate concentration, decreasing the gradient of concentration between both compartments, which is the driving force for the diffusion. Also, the gas bag was analyzed in order to assess the concentration of

H_2S in the gas phase, which was found negligible. However, such sulfate migration through the membrane cannot explain the observed sulfur unbalance. Thus, elemental sulfur formation was identified as the reason for most of this sulfur unbalance.

Table 4.3. Sulfate measurements in the cathodic and anodic compartments in the last cycles in order to calculate the diffusion through the membrane and the balance of sulfur.

	Time	**Sulfate concentration**		**Sulfate mass**		**Diffusion**	
	Day	**Cathode**	**Anode**	**Cathode**	**Anode**		
	d	*mg S L^{-1}*	*mg S L^{-1}*	*mg S*	*mg S*	*mg S d^{-1}*	*%*
	0	996	0	349	0		
Cycle 1	1	867	91	303	37	23	6.6
	2	810	123	283	49		
	3	737	174	258	69		
Cycle 2	3	983	174	344	69	18	5.2
	7	741	354	259	141		
Cycle 3	7	998	354	349	141	16	4.5
	8	884	403	310	161		
	9	828	389	290	156		
Cycle 4	10	743	471	260	189	3	0.9
	10	983	471	344	189		
	13	807	496	282	198		
Cycle 5	13	985	496	345	198	22	6.4
	14	879	586	308	235		
	15	814	643	285	257		
	16	756	661	265	264		

4.3.3. Oxygen limiting conditions

An electron acceptor is needed to drive sulfide oxidation to elemental sulfur. This work proposes a limited supply of oxygen so that sulfide oxidation ends up in elemental sulfur as final product. Providing oxygen through an aeration device directly to the cathode would add complexity and increased costs to the process. The oxygen produced in the anode due to water hydrolysis that partially diffused through the membrane to the cathode was used instead. Hence, controlled oxygen diffusion was required. The extent of dissolved oxygen (DO) diffusion through the membrane was assessed using an abiotic cathode. Figure 4.3 shows the DO concentration in the cathodic compartment when the anodic compartment was saturated in oxygen (sparging pure O_2 in order to obtain a similar DO in the anodic compartment as when some potential is applied) in two different scenarios: i) without applied potential (Figure 4.3A) and ii) when the cathode was set at -0.8 V vs. SHE (Figure 4.3B). A DO increase at a slow rate of 0.84 mg O_2 L^{-1} h^{-1} was observed without applied potential due to DO transport through the membrane in agreement with Mariam et al. (2015), who showed the low oxygen permeability of the membrane used (AMI-7001). In contrast, DO was consumed in the cathode at an applied potential of -0.8 V vs. SHE and no oxygen was observed. However, DO concentrations about 20 mg O_2 L^{-1} or higher (reached in the anode during the experiments due to oxygen production as a result of water electrolysis) increased the DO gradient and, concomitantly, the oxygen diffusion through the membrane. It should also be noted that poising the cathode triggers off the competition between SOB and the cathode, which is able to reduce DO to water (Eq. 4.5) likewise for a microbial fuel cell (Rabaey and Verstraete, 2005). Such DO scavenging also helps to obtain the limiting oxygen conditions required for partial sulfide oxidation.

$$O_2 + 2H_2 \rightarrow 2H_2O \qquad \Delta G^º = -237.1 \text{ KJ mol}^{-1} \qquad \text{(Eq. 4.5)}$$

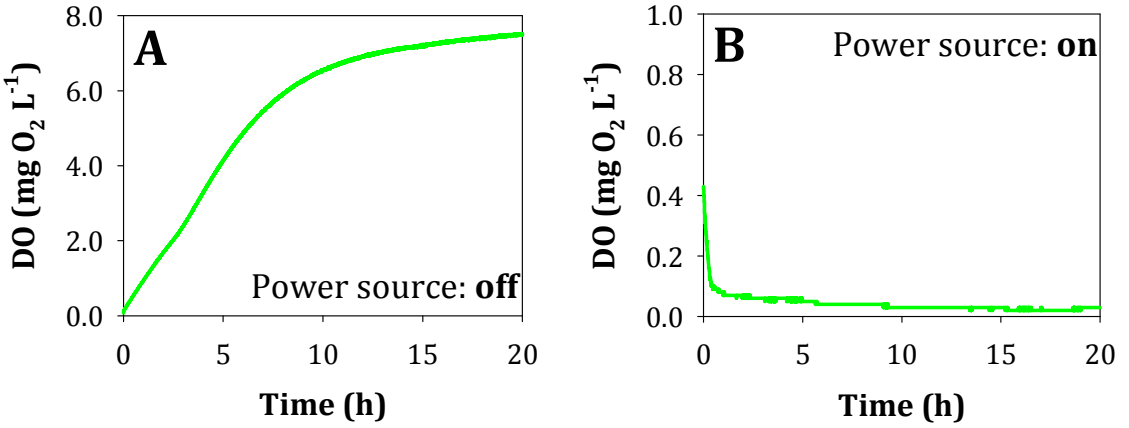

Figure 4.3. DO concentration in the cathode compartment with a DO-saturated anode (due to pure O_2 sparging) A: without applied potential and B: with a cathode potential of -0.8V vs. SHE.

4.3.4. Uncovering elemental sulfur

Elemental sulfur production in the cathode was assessed after approximately 200 days of operation. Samples of graphite fiber brush were collected from the biocathode for SEM analysis (Figure 4.4). The growth of biofilm and a solid deposition over the cathode surface can be observed. The circled part of the solid deposition was analyzed by EDS (Figure 4.5) and the spectra obtained indicated that the main element found in this solid was S. Also C and O could be observed, probably because of the presence of graphite and the biofilm, but at a lower level. No metals were detected by EDS, discarding sulfide precipitation and indicating that the main component of the solid depositions on the surface of biocathode was elemental sulfur. Other solid depositions were randomly analyzed by EDS and no metals were detected in none of them, being sulfur almost the sole component. These results confirmed that the sulfur imbalance produced during the experiments was due to elemental sulfur production. Even then, precipitates of salts of Mg, P and O were also detected in some few cases. Probably, $Mg_3(PO_4)_2$ was formed due to the abundance of magnesium and phosphate in the mineral medium.

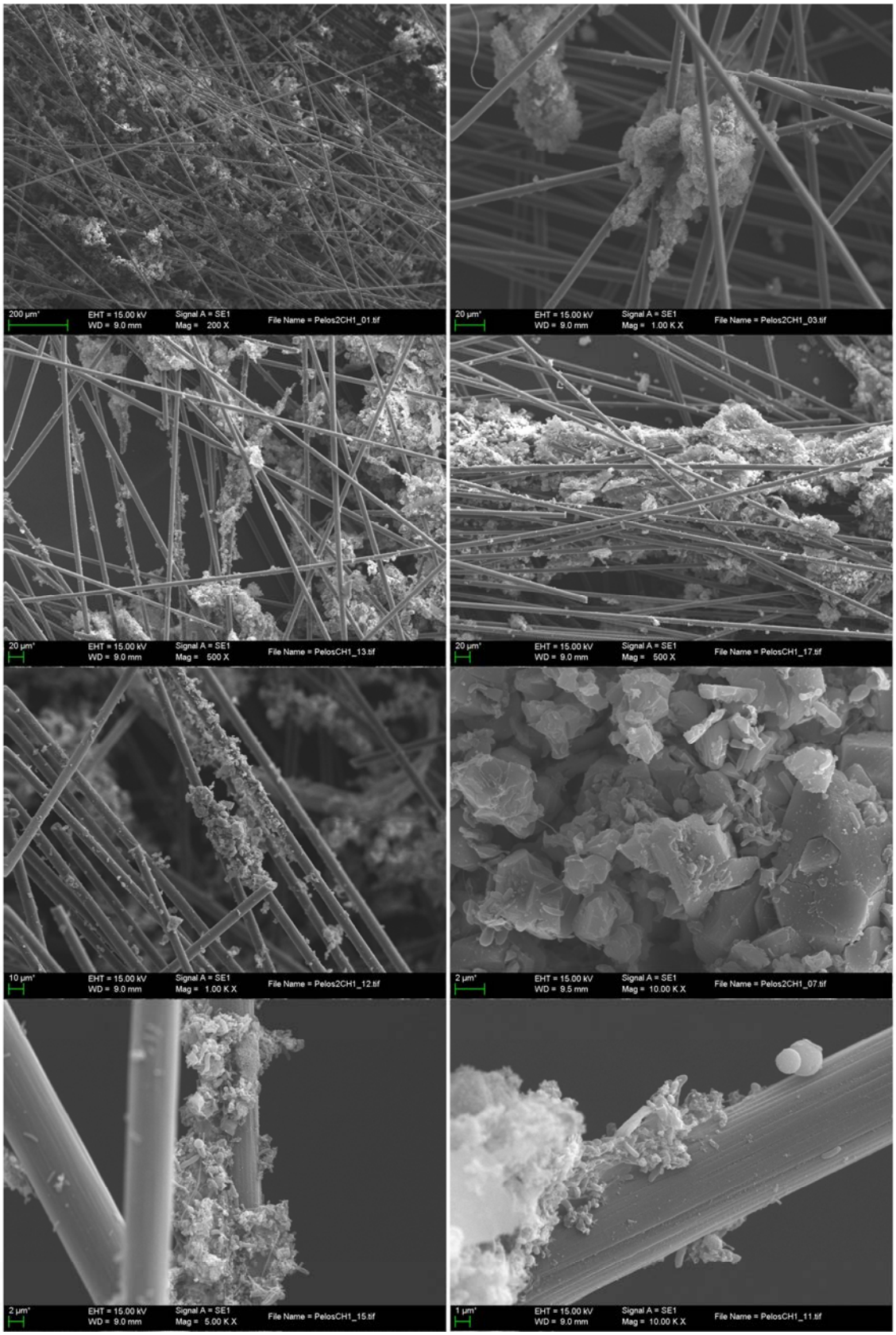

Figure 4.4. SEM pictures of the fibers of the biocathode with biofilm and salts precipitates.

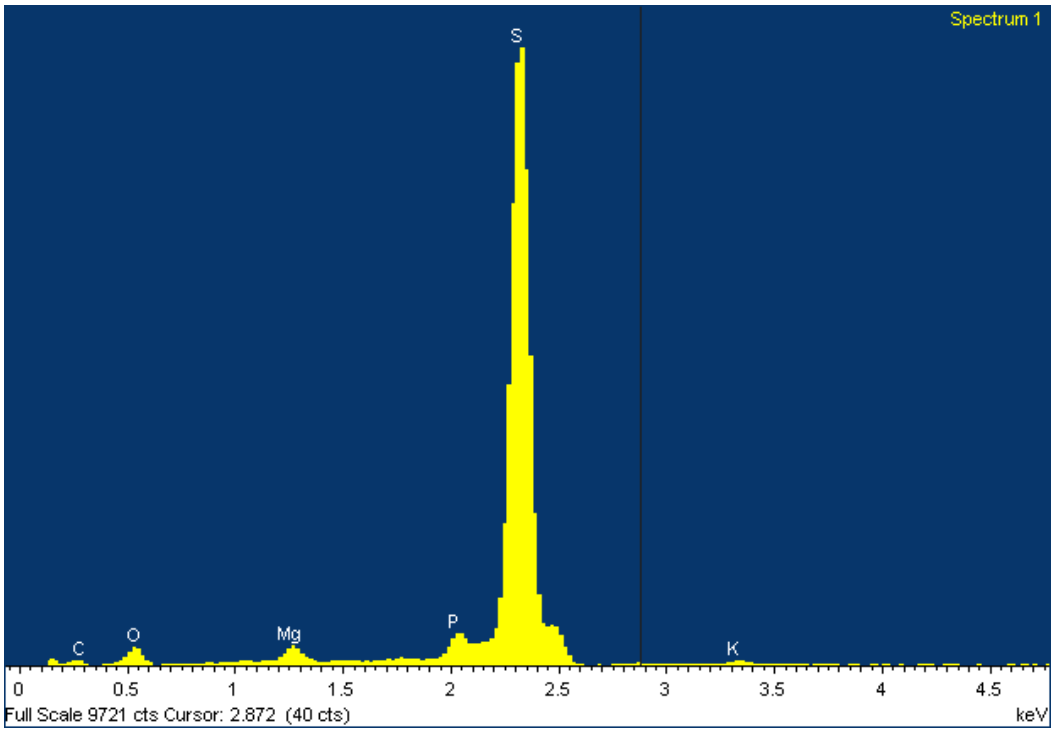

Figure 4.5. EDS of the depositions on the biocathode.

The solid phase accumulated from the purges of batch experiments were collected and characterized by thermogravimetry (Figure 4.6), CHNS analysis and ICP-MS (Table 4.4). Thermogravimetry measures the mass loss through the increase of temperature and the release of enthalpy. The curve of the solid sample analyzed shows a high mass loss and a peak of enthalpy release at 232 ºC, that corresponds to the autoignition temperature of sulfur (Pohanish, 2008). Since thermogravimetry was performed in the presence of O_2, the peak detected corresponded to the oxidation of elemental sulfur to sulfur dioxide.

Almost 50% of the solid recovered from the cell was elemental sulfur according to the results of the CHNS analysis (Table 4.4). Carbon had also a high predominance due to the graphite fibers of the cathode. However, a large difference was found between sulfur results of the CHNS analysis and that of ICP-MS, which was attributed to a partial digestion of the solid during the pre-treatment of the sample for the ICP-MS analysis. Even so, at least 14.2 ± 0.5% of the solid recovered, detected by ICP-MS, corresponded to sulfur, and no metals were detected. In this analysis, also Mg and P were detected, corroborating the precipitation of magnesium and phosphate salts.

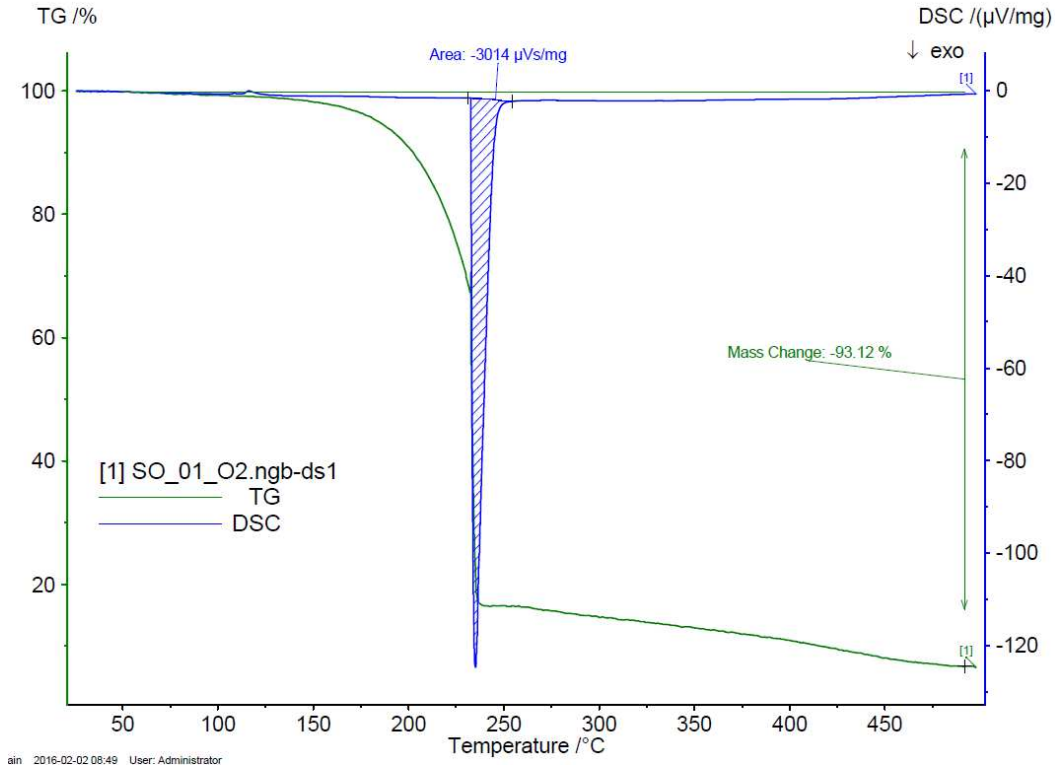

Figure 4.6. Profile of mass loss and release of enthalpy of solid sample from purges of batch experiments in a pure oxygen atmosphere. The main mass loss of the solid sample occurs at 230 ºC due to sulfur combustion.

Table 4.4. Main compounds detected from the solid phase accumulated from the purges of batch experiments by CHNS analysis and ICP-MS.

	C (mg g^{-1})	**S (mg g^{-1})**	**P (mg g^{-1})**	**Mg (mg g^{-1})**	**Me (mg g^{-1})[a]**
CHNS analysis	104 ± 28	446 ± 39	-	-	-
ICP-MS[b]	-	142 ± 5	77 ± 27	43 ± 10	< 10

[a] Amount of all metal ions detected.

[b] After the digestion of all samples a solid fraction remained that was not possible to be analyzed.

4.3.5. Microbial community analysis

The microbial community of the H-BES biocathode was analyzed after 2 months of operation (Figure 4.7). Results obtained were in close agreement with experimental observations since the biocathode community was mainly composed of SRB (17.2%) and SOB (18.9%). Results showed a large percentage (47%) of *unclassified* species at different levels. Quality check data (data not shown) demonstrated the complexity to assign identity probably due to the large diversity of the community, to the limited coverage of the sequence database and to the amplicons length (360 bp on average).

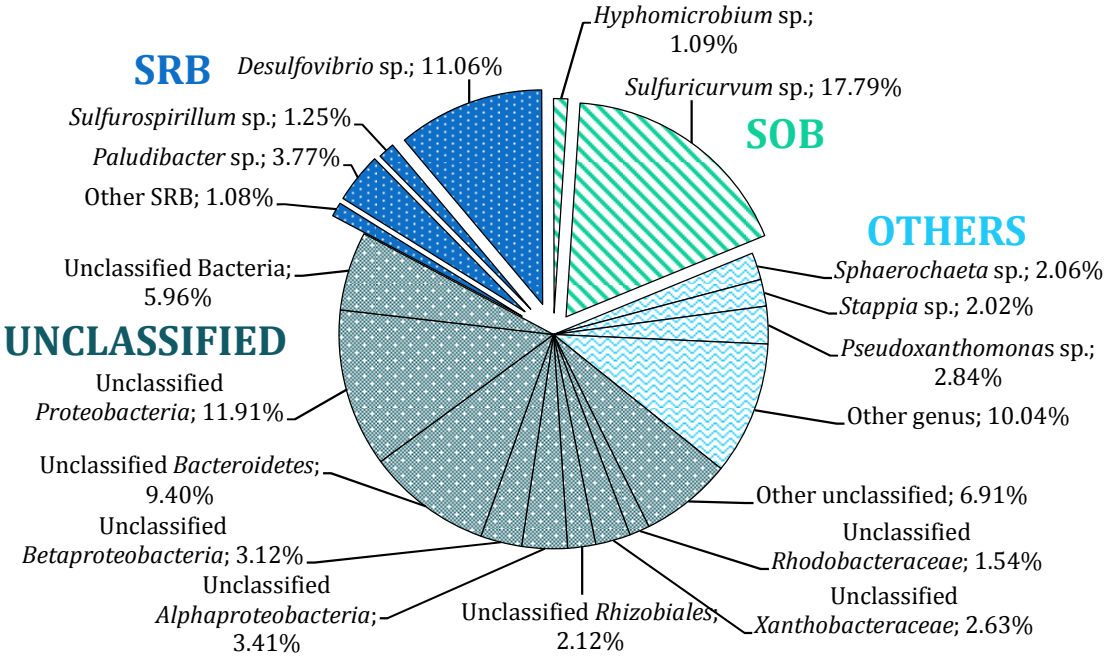

Figure 4.7. Microbial community distribution of the H-BES biocathode.

Desulfovibrio sp. was the main SRB genus detected, which is also the most studied genus of SRB. *Desulfovibrio* sp. has one of the highest affinities for hydrogen among SRB (Laanbroek et al., 1984) and has been also detected in bioelectrochemical systems (Rago et al., 2015) as an electroactive *Deltaproteobacteria* for sulfate reduction (Cordas et al., 2008; Teng et al., 2016; Yu et al., 2011). Moreover, *Desulfovibrio* sp. is generally considered strictly anaerobic, even if some species of this genus are aerotolerant at the expense of having a limited growth (Sigalevich et

al., 2000). Also *Paludibacter* sp. has been found to have a good removal capacity of sulfate under acidic conditions (Liang et al., 2013). A small fraction of *Sulfurospirillum* sp., a SRB able to reduce sulfur under microaerophilic conditions (Finster et al., 1997), was also detected. Other SRB included *Desulfomicrobium* sp., *Desulfobulbus* sp., *Desulforhopalus* sp. and *Geobacter* sp., which belong to *Deltaproteobacteria* class. Despite the low percentage of some species in the microbial community, results evidenced the large diversity of SRB in the biocathode.

Regarding SOB, *Sulfuricurvum* sp. was the main genus detected, which is capable of growing under microaerophilic and anaerobic conditions (Kodama and Watanabe, 2004). Moreover, *Sulfuricurvum* sp. has been described as an autotrophic genus capable to oxidize sulfide, elemental sulfur, polysulfide, sulfite, thiosulfate and also hydrogen and to accumulate elemental sulfur extracellularly (Handley et al., 2014). Also, *Hyphomicrobium* sp., which was found in a small percentage, has also been described to be able to oxidize hydrogen sulfide (Zhang et al., 1991).

Moreover, homoacetogenic bacteria were not observed in the analysis of the biocathode community, indicating that, in the presence of sulfate and hydrogen as sole electron donor, homoacetogens were outcompeted by SRB. This fact is a key aspect to further scale-up by ensuring an effective, high-throughput use of the electron donor (H_2) for sulfate reduction purposes only.

According to bTEFAP results, SRB and SOB, dominated basically by *Desulfovibrio* sp. and *Sulfuricurvum* sp., played a key role in the sulfate reduction and elemental sulfur recovery (Eq. 4.1 and Eq. 4.3) in this system.

4.4. Conclusions

This study shows for the first time the treatment of high-strength sulfate wastewater using bioelectrochemical systems with the possibility to recover elemental sulfur and without any external electron donor dosage. The process is characterized by microaerophilic conditions in the biocathode compartment due to oxygen diffusion through the membrane during water electrolysis in the anode. A mixture of SRB (17%, mainly *Desulfovibrio* sp.) and SOB (19%, mainly

Sulfuricurvum sp.) able to reduce sulfate to sulfide and partially oxidize sulfide to elemental sulfur in an autotrophic biocathode was detected. In addition, homoacetogenic bacteria, a potential hydrogen scavenger, were not detected in our system.

The autotrophic biofilm grown in the BES was able to remove sulfate with hydrogen as the sole electron donor at a much higher SRR (up to 388 mg SO_4^{2-}-S L^{-1} d^{-1}) than those previously reported, even under at a low applied potential for hydrogen production (-0.8 V vs. SHE). Moreover, the sulfur unbalance detected in our BES, in spite of sulfate diffusion through the membrane (up to 5% per day in the worst-case scenario), was due to the production of elemental sulfur over the cathode surface as was detected by energy dispersive spectrometry and CHNS and ICP-MS analyses.

Chapter 5

Evaluation of key parameters on simultaneous sulfate reduction and sulfide oxidation in an autotrophic biocathode

The motivation of this chapter was to gain knowledge about which parameters could improve the sulfate reduction and the elemental sulfur production. So, this chapter describes new advances in the use of bioelectrochemical systems for the recovery of elemental sulfur from sulfate-rich wastewaters. This work presents long-term evaluation of the most significant parameters influencing simultaneous sulfate reduction and sulfide oxidation in an autotrophic biocathode: effect of type of membrane (AEM or CEM), cathode potential and operational pH, including its effect on the microbial community.

Abstract

This study evaluates different parameters that influence the simultaneous sulfate reduction and sulfide oxidation in an autotrophic biocathode: ion-exchange membrane (IEM), cathodic pH and cathode potential. Two different membranes were studied to evaluate sulfate and sulfide adsorption and diffusion from the cathode to the anode, observing that a cation-exchange membrane (CEM) widely decreased these effects. Three different cathode pH (5.5, 7 and 8.5) were studied in a long-term operation observing that pH = 7 was the optimal for sulfate removal, achieving reduction rates around 150 mg SO_4^{2-}-S L^{-1} d^{-1}. Microbial community analysis of the cathode biofilm demonstrated a high abundance of sulfate-reducing bacteria (SRB, 67% at pH 7, 60% at pH 8.5 and 42% at pH 5.5), mainly *Desulfovibrio* sp. at pH 5.5 and 7 and *Desulfonatronum* sp. at pH 8.5. The cathode potential also was studied from -0.7 to -1.2 V vs. SHE achieving sulfate removal rates higher than 700 mg SO_4^{2-}-S L^{-1} d^{-1} at cathode potentials from -1.0 to -1.2 V vs. SHE. Also, the highest cathodic recovery and the highest sulfur species imbalance were observed at a cathode potential of -1.0 V vs. SHE, which indicated a higher elemental sulfur production.

5.1. Introduction

BESs require the presence of an ion-exchange membrane (IEM), which can affect the oxygen diffusion required for this partial sulfide oxidation. The IEM allows separating the anodic oxidation reaction of the cathodic reduction reaction at expenses of higher costs (i.e. higher applied voltage), since membranes increase the internal resistance of the BES and generate pH gradients (Rozendal et al., 2007). IEMs consist of polymeric structures containing charge and carrying functional groups that facilitate transport of oppositely charged ions. IEMs are classified as cation exchange membranes (CEM) or anion exchange membranes (AEM). Since CEM allow a high protons transport (Mariam et al., 2015), AEMs have not been as widely used as CEM. However, AEMs have different characteristics such as higher ion diffusion, lower ion transport resistance and less membrane fouling (Piao et al., 2013).

The presence of an IEM also leads to the appearance of pH gradients, which can be deleterious for the SRB activity and increase the energy requirements according to the Nernst equation. The accumulation of protons and hydroxyls leads to a pH drop in the anodic compartment and a pH increase in the cathodic chamber, respectively (Gil et al., 2003; Rozendal et al., 2006). The preferred range of pH for SRB activity is between 6 and 8 (Hao et al., 1996) while SRB growth is severely affected at pH < 5.5 (Fortin et al., 1996) and inactivated at pH < 5 (Johnson et al., 2009). Since SOB can grow in a pH range between 1 and 10 (Islander et al., 1991) SOB are less affected by pH.

Gildemyn et al. (2017) showed that most studies on microbial electrosynthesis rely on indirect electron transfer via hydrogen rather than a direct utilization of electrons from the cathode. Hence, efficient cathodic hydrogen production is fundamental for the sulfate reduction process. The cathode potential has a strong influence on the hydrogen production rate, which also can affect the cathodic biofilm growth and the cathode properties (Liang et al., 2009). Some authors studied the effect of cathode potential (from -0.6 to -1.0 V vs. SCE) on SRB in order to obtain highly efficient sulfate reduction (Luo et al., 2014) or at a cathode potential of -0.2 V vs. SHE to avoid the H_2 production for sulfate reduction with

electrons directly derived from the electrode (Su et al., 2012). However, these results present low sulfate reduction rates due to their higher cathode potentials.

The aim of this work was to systematically evaluate the most influencing parameters for an efficient sulfate removal to sulfide and simultaneous partial sulfide oxidation to elemental sulfur in the cathode of a two-chamber BES in view of its scaling-up. The final goal of this process is to provide a feasible solution for the treatment of high-strength sulfate wastewaters without external electron donor dosage and under autotrophic conditions and, if possible, to recover most of the influent sulfate as elemental sulfur. Thus, this work studied i) the absorption and diffusion of sulfur species through different membranes, ii) the effect of cathodic pH, iii) the effect of cathodic potential, and iv) the microbial communities in each case.

5.2. Experimental

5.2.1. Membrane characterization

Two different IEMs were investigated to evaluate sulfate diffusion and sulfate and sulfide adsorption: a CEM (CMI-7000, Membranes International INC, USA) and an AEM (AMI-7001, Membranes International INC, USA). The main characteristics of the membrane separators are summarized in Table 5.1. Both membrane separators were pretreated to allow membrane hydration and expansion by soaking them overnight in a 5 wt% NaCl solution at 40ºC according to supplier instructions.

Four abiotic C-BESs (Figure 3.2) were used for diffusion experiments (two for each membrane). The same mineral medium used in biotic experiments was added for cathode and anode compartments. The electrodes of all C-BESs were connected to a power source (HQ Power, PS-23023, Belgium) with an applied potential of 2.6 V in order to maintain a cathode potential of -0.8 V vs. SHE in the C-BES.

Table 5.1. Main characteristics of the two studied ion-exchange membranes (IEMs).

Technical Specification	CMI-7000	AMI-7001
Functionality	Strong acid cation exchange membrane	Strong base anion exchange membrane
Polymer structure	Gel polystyrene cross-linked with divinylbenzene	Gel polystyrene cross-linked with divinylbenzene
Functional group	Sulphonic acid	Quaternary ammonium
Ionic form as shipped	Sodium	Chloride
Standard thickness (mm)	0.45	0.45
Electrical resistance (Ohm cm^2) 0.5 mol NaCl L^{-1}	<30	<40

Eight glass bottles of 100 mL were used for adsorption experiments, four for sulfate adsorption and the other four to evaluate sulfide adsorption. The cathodic mineral medium (explained in *4.2. Experimental*) was used for sulfate experiments, which was amended with sodium sulfide for sulfide experiments in order to obtain 100 mg TDS-S L^{-1}. One of each four bottles was used as control, i.e. without membrane. A piece of 20 cm^2 of the membranes was submerged in the corresponding medium. The studied IEMs were a new AMI, a long-term used AMI and a new CMI.

The percentage of sulfate diffused through the membrane in abiotic experiments (SD, Eq. 5.1) was calculated as follows:

$$SD = 100\left(\frac{V^{An}(C_f^{An}-C_i^{An})}{V^{Cat}C_i^{Cat}}\right) \quad \text{(Eq. 5.1)}$$

Where V^{An} and V^{Cat} are the volumes of anode and cathode compartments, respectively, C_f^{An} and C_i^{An} are the final and initial sulfate concentration in the anode, respectively, and C_i^{Cat} is the initial sulfate concentration in the cathode.

The membrane adsorption (MA, Eq. 5.2) was calculated as follows:

$$MA = \frac{V(C_i - C_f) - V^C(C_i^C - C_f^C)}{A} \quad \text{(Eq. 5.2)}$$

Where V and V^C are the volumes of the bottle with a piece of membrane and the control test, respectively, C_i and C_f are the initial and final concentrations of sulfate or TDS in the bottle, respectively, C_i^C and C_f^C are the same measurements in the control test and A is the membrane surface.

5.2.2. Cathodic pH experiments

The effect of cathodic pH was studied at three different H-BESs (Figure 3.3) operated at pH 5.5, 7.0 and 8.5 with each anode and cathode separated by a CEM. The initial inoculum of the H-BES at pH=7.0 was a sludge enriched in autotrophic SRB. The enrichment procedure can be found elsewhere (Blázquez et al., 2016). Such BES had been working for one year with an AEM. The purges from this reactor were used to inoculate the H-BESs at pH=5.5 and 8.5 and these two BESs were operated during two months with an AEM before the experiments presented in order to develop the biofilm over the cathode. Both electrodes were connected to a power source applying a potential of 3.6 V to obtain a cathode potential of -0.8 V vs SHE. The potential applied was increased up to 5 V in the H-BES at pH 5.5 and 8.5 in order to increase the intensity and hydrogen production from day 45 to 87.

The cathodic pH was monitored with pH probes (Hach pH electrode Crison 5233) connected to a pH meter (Hach MultiMeter Crison 44), and was automatically controlled at 5.5, 7.0 and 8.5 through the addition of HCl (3 M) with a dispensing burette (Multi-Burette 2S-D, Crison Instruments).

At the end of the operation, cyclic voltammetry (CV) experiments were conducted using the BES set at pH 7. Prior to each experiment, mineral medium was renewed and 3M HCl or NaOH was used to set the pH at 5.5, 7.0 and 8.5. After each experiment, one cycle of three days was conducted at pH 7. CVs were conducted by using a Multi Autolab system (Ecochenie, Utrecht, Netherlands). CVs were recorded at a scan rate of 1.0 mV/s from 0.28 V to -1.10 V vs. SHE of cathode potential in three-electrode mode, where cathode was the working electrode, the

anode the auxiliary electrode and a Ag/AgCl NaCl 3M (model RE-1B, BAS Inc.) as reference electrode.

5.2.3. Experiments with different cathode potentials

Three replicated C-BESs (Figure 3.2) with each anode and cathode separated by a CEM were used for these experiments. The inoculum was the same than that of H-BESs. The cathode potentials of C-BES studied were -0.7, -0.8, -0.9, -1.0, -1.1 and -1.2 V vs. SHE. Cathode potentials were changed every 5-6 cycles. In order to avoid any possible effect between consecutive experiments due to the previous cathode potential used, at least two cycles were carried out at cathodic potential -0.8 V vs. SHE between each experiment. A Multi Autolab System (Ecochenie, Utrecht, Netherlands) was used to poise the cathode potential.

The cycle duration varied depending on the potential applied. At potentials of -0.7, -0.8 and -0.9 V vs. SHE, the duration of the cycle lasted three days, while at potentials of -1.0, -1.1 and -1.2 V vs. SHE the cycle lasted just one day due to the high SRR observed removing almost all the sulfate after one day. After 60 days of operation, one of these C-BESs was sacrificed in order to analyze the microbial community.

5.3. Results and discussion

5.3.1. Role of membrane type

The membrane plays a very important role in this system since the diffusion of oxygen from the anode to the cathode is required, whereas the diffusion of sulfate from the cathode to the anode is undesirable. An AMI and a CMI were studied in four abiotic C-BESs (two C-BESs for each membrane) in order to evaluate the sulfate diffusion through the membrane separators (Figure 5.1A). The potential applied in all C-BESs was 2.6 V. This potential was chosen to obtain a cathodic potential of -0.8V vs SHE in the BES with CMI.

The sulfate diffusion from the cathode (with an initial concentration of 1000 mg SO_4^{2-}-S L^{-1}) to the anode with the AMI was 33.6 ± 2.6% in the first day meanwhile

the diffusion with the CMI was 0.16 ± 0.02%. After a cycle experiment of 3 days, the final diffusion with the AMI was 39.4 ± 4.2% and with the CMI was 0.54 ± 0.06%. Even so, in the second day, the C-BESs with AMI showed a similar sulfate concentration in the anode than the third day. Then, when the sulfate concentration in both compartments is similar, the sulfate diffusion decreases due to the drop in the gradient of concentration, which is the driving force for the mass transfer. As expected, the CMI prevents the diffusion of sulfate better than the AMI due to its capacity to avoid anions transport.

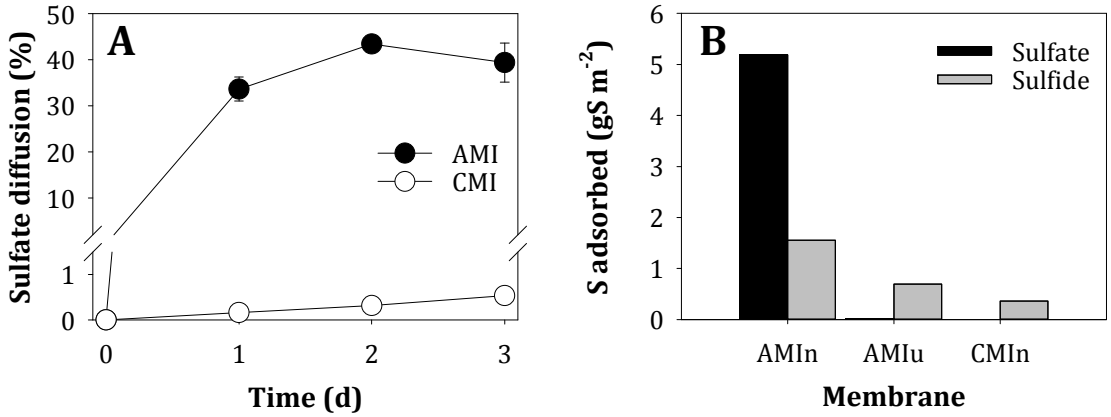

Figure 5.1. Effect of the ionic exchange membrane on sulfur species in a BES in terms of A: diffusion and B: adsorption. AMIn: new AEM, AMIu: used AEM and CMIn: new CEM.

Another abiotic experiment was conducted in order to evaluate the potential sulfate and sulfide adsorption of both IEMs (Figure 5.1B). The adsorption of S-compounds in the AMI was studied with both a brand-new piece of membrane (AMIn) that had never been in contact with sulfate and sulfide before and with another piece that was used in a BES experiment for sulfate-reduction during some weeks (AMIu). A new piece of membrane (CMIn) was used in the case of CMI. Sulfate adsorption was only observed using AMIn while the maximum adsorption was about 5.2 g SO_4^{2-}-S m^{-2} (8.3 mg SO_4^{2-}-S g^{-1} of membrane). In the case of sulfide, lower adsorption values were found in comparison with sulfate. The highest adsorption (1.5 g TDS-S m^{-2}, 2.4 mg TDS-S g^{-1} of membrane) was found with the

AMIn, being four times higher than that with the CMIn (0.4 g TDS-S m^{-2}, 0.6 mg TDS-S g^{-1} of membrane). Then, a new CMI provided the lowest S mass losses. The AMI adsorption capacity decreased with a used membrane, although it was always higher than the CMI.

The oxygen diffusion through the membrane was determined by Blázquez et al. (2016) using an AMI membrane observing an oxygen transfer rate of 2.82 mmole O_2 m^{-2} h^{-1}. The same test (explained in 4.3.3. *Oxygen limiting conditions*) was performed with CMI observing a similar diffusion of the oxygen (3.30 mmole O_2 m^{-2} h^{-1}). Overall, when using a CMI membrane the oxygen diffusion is similar to an AMI, but the sulfate diffusion through the membrane and its adsorption is mostly prevented. Thus, CMI would provide better characteristics for the bioelectrochemical treatment of sulfate.

5.3.2. Effect of cathodic pH

Three inoculated H-BES were operated using a CEM in cycles during 115 days at a cathode potential of -0.8 V vs. SHE and different pH to evaluate the effect of pH on sulfur recovery. The cathodic pH of these BES was set at 5.5, 7 and 8.5 during all the operation. Figure 5.2 shows the results obtained during the whole experimental period. The BES at pH 7 showed a higher SRR during all operation (Figure 5.2A) obtaining removal rates around 150 mg SO_4^{2-}-S L^{-1} d^{-1} 50 days after the start-up with cycles of 3-4 days. The BESs at pH 5.5 and 8.5 showed smaller SRRs of 18 ± 9 mg SO_4^{2-}-S L^{-1} d^{-1} and 25 ± 14 mg SO_4^{2-}-S L^{-1} d^{-1} respectively at the cathode potential of -0.8 V vs. SHE. In this first period, the intensity in the BES at pH 7 increased probably due to its higher activity (Figure 5.2E). A higher potential was applied from day 45 to 87 to the cells at pH 5.5 and 8.5 to increase its intensity up to similar values to the cell at pH 7, which involves a higher hydrogen production. When the applied potential was increased, the BES at pH 5.5 increased its removal rate up to 77 mg SO_4^{2-}-S L^{-1} d^{-1} and the BES at pH 8.5 up to 122 mg SO_4^{2-}-S L^{-1} d^{-1}. However, these SRRs decreased again when the cathodic potential was returned at -0.8 V vs. SHE at day 87.

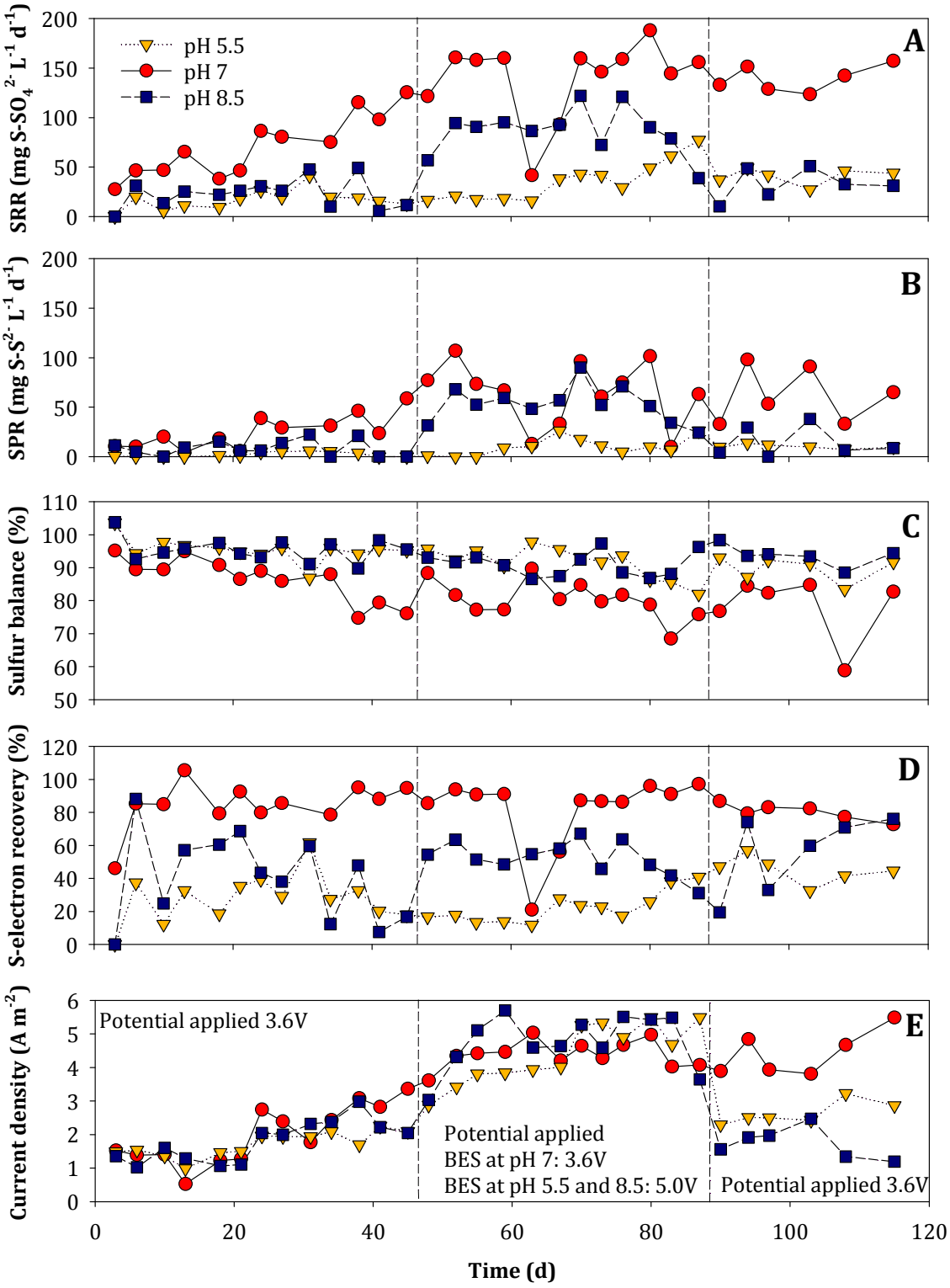

Figure 5.2. Effect of pH on long-term operation of three BESs at pH 5.5, 7.0 and 8.5 on A: sulfate removal rate (SRR), B: sulfide production rate (SPR), C: Sulfur balance, D: electron recovery and E: current density. Vertical bars indicate the period (days 47 – 87) when the applied potential was increased in BESs at pH 5.5 and 8.5.

Figure 5.2A also shows a high decrease of SRR on day 63 of operation in the cell at pH 7 due to a pH shock sharply decreasing to pH 1. Surprisingly, the system recovered after only two cycles, and 7 days later the SRR was again around 150 mg SO_4^{2-}-S L^{-1} d^{-1}. The fact that biomass grows as a biofilm and the outer layers of biofilm protected those on the inner side was probably the reason of the great resilience of the system.

The low SRR obtained at pH 5.5 could be due to the inhibition caused by the higher concentration of H_2S, since the protonated form of H_2S is favored at smaller pH (Moosa and Harrison, 2006) being almost all the TDS (97%) in the undissociated form at pH 5.5. This effect is decreased at pH 7 where the undissociated H_2S concentration decreased down to around 50% of TDS, and at pH 8.5 almost all TDS (97%) exists as HS^-.

The BES at pH 7 also showed higher SPR than the BES at pH 5.5 and 8.5 (Figure 5.2B), obtaining SPRs up to 107 mg TDS-S L^{-1} d^{-1}. However, when the applied potential of BESs at pH 8.5 was increased, the SPR was similar to the BES at pH 7, obtaining SPRs up to 90 mg TDS-S L^{-1} d^{-1}, thus indicating that smaller hydrogen production rather than operation at higher pH was the main cause for smaller SPR. In the case of the BES at pH 5.5, a maximum SPR of 26 mg TDS-S L^{-1} d^{-1} was obtained, indicating that the increase of the applied potential did not have an important improvement in SPR.

Figure 5.2C shows the sulfur balance during all operation of the three BESs. The higher imbalance occurred at pH 7, where higher SRR and SPR were observed. Around 75% of the initial sulfate was recovered as TDS, thiosulfate and sulfate after the cycles. According to Blázquez et al. (2016), such imbalance can be attributed to the partial sulfide oxidation to elemental sulfur thanks to the oxygen diffusion through the membrane. The sulfur imbalance at pH 5.5 was similar to that at pH 8.5; around 90% of the initial sulfate was recovered as sulfate, TDS and thiosulfate. Then, around 25% of the initial sulfate at pH 7 was probably converted to elemental sulfur after each cycle (around 250 mg S L^{-1}) and around 10% (around 100 mg S L^{-1}) at pH 5.5 and 8.5. An efficient recovery of all the elemental sulfur produced is not a straightforward issue. This elemental sulfur can be found either in the liquid phase or in the biomass (it could even be attached to the

electrode, to the membrane and to the reactor walls) and further research is needed in this particular aspect.

The electron selectivity for sulfate (i.e. ratio of electrons used for sulfate reduction versus the electrons arriving at the cathode) at each pH is shown in Figure 5.2D. The sulfate selectivity was also higher in BESs at pH 7 (between 80 and 100%), compared to that at pH 8.5 (between 40 and 60%) and to that at pH 5.5 (between 20 and 40%). This observation is in agreement with the fact that the SRR at pH 7 was higher despite the similar intensities in all BESs. In addition, this scenario indicates a probable limitation of the electron donor in the cathode, as all the hydrogen produced is being used for sulfate reduction. In case of achieving higher intensities, higher SRR at pH 7 could probably be observed.

After these long-term experiments, CVs were conducted at the three pHs using the BES operated at pH 7 (Figure 5.3). As can be observed, the smaller the pH was, the higher the intensity at a certain cathodic potential, which is in agreement with Nernst law. Then, if a cathodic potential is fixed, there would be more hydrogen production at acidic pH. This observation corroborates the fact that the observed decrease of performance at pH 5.5 was not due to the electron donor limitation. In addition, the CV at pH 7 showed a higher increase between cathodic potentials of -0.6 and -0.8 V vs. SHE, which could be due to a higher electroactivity of the biofilm at this pH because of its higher activity of SRB during the long-term operation.

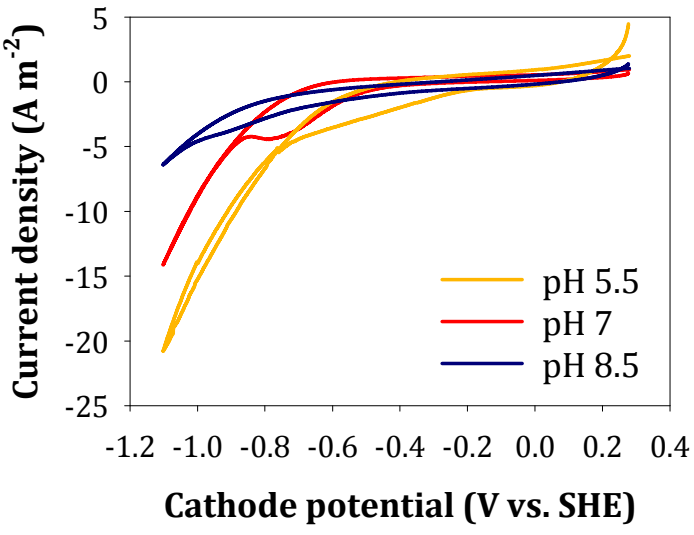

Figure 5.3. Cyclic voltammetry at different pHs at a scan rate of 1.0 mV s^{-1}.

Then, pH 7 was the optimal tested operational cathodic pH for SRB in BES. These results are in contradiction with the single study on the effect of pH in BES aiming at sulfate reduction (Liang et al., 2013) in which higher SRR was obtained at pH 4.5 than at pH 6.5. In that study, they used a single chamber BES where organic matter and sulfate coexisted and pH was not controlled but measured at the start and the end of the cycle. In fact, the experiment starting at pH 4.5 reached a final pH of 6.2, which are favorable conditions for SRB growth. On the other hand, our results were obtained at controlled pH setpoint during all the cycle, and hence the operational conditions were more stable.

5.3.3. Effect of cathode potential

Three replicated C-BES were operated in cycles during 126 days to evaluate the effect of cathode potential on a BES for sulfate reduction (Figure 5.4). The cathode potentials studied were -0.7, -0.8, -0.9, -1.0, -1.1 and -1.2 V vs. SHE. The pHs of these cathodes were monitored showing values in the range of 6 to 9 depending on the cathode potential.

Results obtained at different cathode potentials during the long-term operation are summarized in Figure 5.5. Both the SRR and SPR (Figure 5.5A) increased as cathode potential decreased. The lowest rates were observed at a cathode potential of -0.7 V vs. SHE obtaining a SRR of 13 ± 16 mg SO_4^{2-}-S L^{-1} d^{-1} and a SPR of 23 ± 2 mg TDS-S L^{-1} d^{-1}. These low rates can be attributed to the thermodynamics limitation of hydrogen production at this cathode potential. The highest average SRR and SPR, 785 ± 104 mg SO_4^{2-}-S L^{-1} d^{-1} and 409 ± 78 mg TDS-S L^{-1} d^{-1} respectively, were observed at a cathode potential of -1.1 V vs. SHE with a maximum punctual SRR of 973 mg SO_4^{2-}-S L^{-1} d^{-1}. The results observed in this system are quite higher than the maximum SRR of around 500 mg SO_4^{2-}-S L^{-1} d^{-1} at -1.1 V vs. SHE of cathode potential reported so far (Pozo et al., 2016). At cathode potentials of -1.0 and -1.2 V vs. SHE, the SRR was quite similar showing rates higher than 700 mg SO_4^{2-}-S L^{-1} d^{-1}. However, the sulfide production rate in the liquid phase (SPR_l) were smaller, 224 ± 32 and 266 ± 40 mg TDS-S L^{-1} d^{-1}, respectively. Thus, despite the fact that the SRR was similar, sulfide production

was smaller. In addition, at cathode potentials of -1.0, -1.1 and -1.2 V vs. SHE, some hydrogen sulfide was detected in the gas phase due to stripping caused by hydrogen (e.g. at -1.2 V, the concentration was $1.3 \cdot 10^4 \pm 1.6 \cdot 10^4$ ppm_v). In any case, emission rates were very low (e.g. at -1.2 V, the sulfide production rate in the gas phase (SPR_g) was 11 ± 13 mg TDS-S L^{-1} d^{-1}).

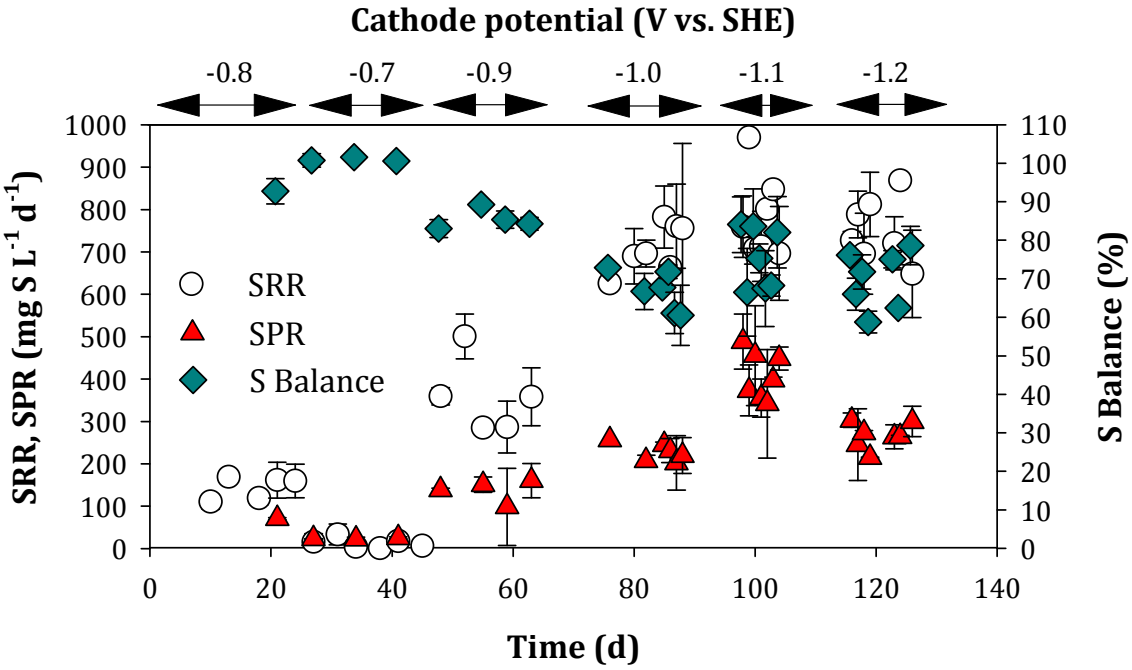

Figure 5.4. Long-term operation of two C-BES at different potential along the time. Between each cathode potential experiment, the cathode potential was set at -0.8 V vs. SHE during some days in order to avoid possible effects of the previous cathode potential.

SRR and SPR results showed a high imbalance between sulfate removed and sulfide produced (Figure 5.5B). As can be observed, the balance was better fulfilled at higher cathode potentials, obtaining a 100% at cathode potential of -0.7V vs. SHE. A high imbalance in these systems means a higher production of elemental sulfur due to oxygen diffusion through the membrane (Blázquez et al., 2016). Thus, the highest imbalance was observed at a cathode potential of -1.0 V vs. SHE, obtaining a sulfur balance of 66 ± 6% and a possible elemental sulfur recovery of 34% of the initial sulfate. The smaller imbalance in the case of cathode potentials

of -1.1 and -1.2 V vs. SHE could be due to a higher reduction capacity and a resulting higher TDS production or due to insufficient oxygen diffused for sulfide partial oxidation.

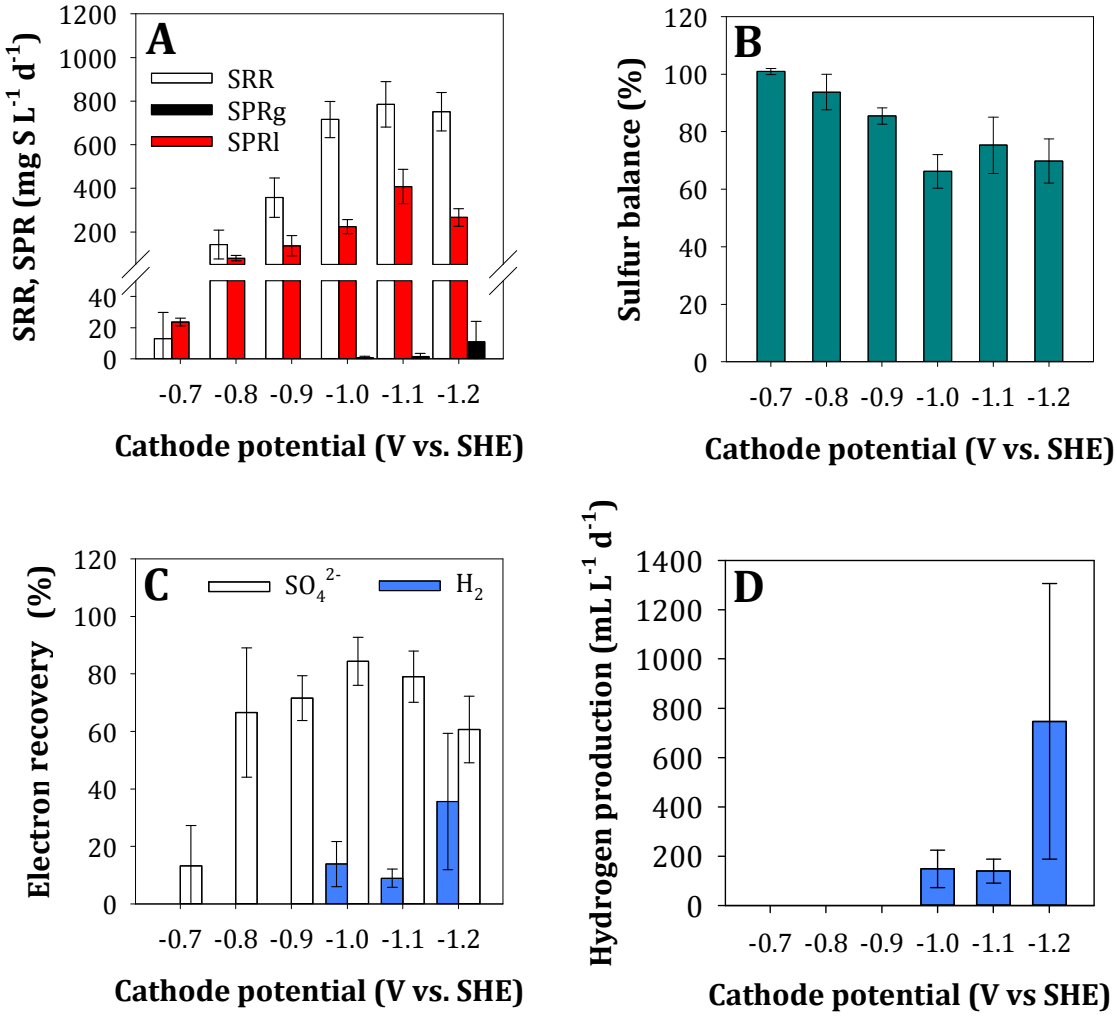

Figure 5.5. Average plots of the effect of cathodic potential to BES on A: sulfate reduction rate (SRR) and sulfide production rate in the liquid phase (SPR_l) and in the gas phase (SPR_g), B: sulfur balance, C: electron recoveries for sulfate reduction and hydrogen production and D: hydrogen production.

Figure 5.5C shows the electron recoveries for sulfate reduction and hydrogen production. As can be observed, at a cathode potential of -0.7 V vs. SHE, just a 13 ± 14% of the electrons were driven to reduce sulfate. At this cathode potential, hydrogen production is decreased and the few electrons reaching the cathode are

used to reduce the oxygen diffused from the anode. At cathode potentials of -0.8 and -0.9 V vs. SHE the electron recovery for sulfate was of 67 ± 23% and 72 ± 8% respectively, in spite of having higher electron recovery for sulfate than at -0.7 V vs. SHE, the rest of the electrons could be also used to reduce the oxygen diffused from the anode. On the other hand, at cathode potentials of -1.0, -1.1 and -1.2 V vs. SHE an excess of hydrogen was produced and even detected in the gas phase (Figure 5.5D) resulting in an unnecessary loss of electrons as hydrogen. Thus, the best electron recovery for sulfate reduction was detected at a cathode potential of -1.0 V vs. SHE showing an 84 ± 8% of electron recovery for sulfate reduction and a 14 ± 8% of electron recovery for hydrogen production.

Figure 5.6 shows the average results obtained along the cycle tests at different cathode potentials. At higher cathode potentials (i.e. -0.9 V vs. SHE) SRR was higher the first day than at the end of the cycle (Figure 5.6A). On the contrary, SRR was constant at lower cathode potentials. In the case of TDS concentration (Figure 5.6B), at higher cathode potentials, the larger SRR increase was observed in the first day for cathode potentials of -0.8 and -0.9 V vs. SHE and then it was maintained. Nevertheless, at lower cathode potentials, the increase of TDS concentrations was more linear and larger at a cathode potential of -1.1 V vs. SHE. At higher cathode potentials (from -0.7 to -0.9 V vs. SHE), the increase of pH along the cycle could decrease hydrogen production and, thus, SRR. However, at lower cathode potentials (from -1.0 to -1.2 V vs. SHE), due to a larger hydrogen production in spite of pH, an excess of hydrogen along all the cycle covered up the less hydrogen production at higher pH and for this reason the SRR was not affected. Thus, TDS production presents a similar behavior.

The sulfur balance is shown in Figure 5.6C. After one day of operation, the highest imbalances were observed at lower cathode potentials. However, the highest imbalance observed at the end of the cycle of 3 days (53 ± 5%) was at a cathode potential of -0.9 V vs. SHE, showing that with longer operation, higher amount of elemental sulfur could be produced. Sulfate reduction during the first days was higher than TDS production detected along the cycles, probably because of TDS oxidation after the first day. Thiosulfate production was less than 1% of reduced

sulfate. Thus, a higher imbalance of sulfur species was observed and, for this reason, more elemental sulfur was obtained the last days of the test.

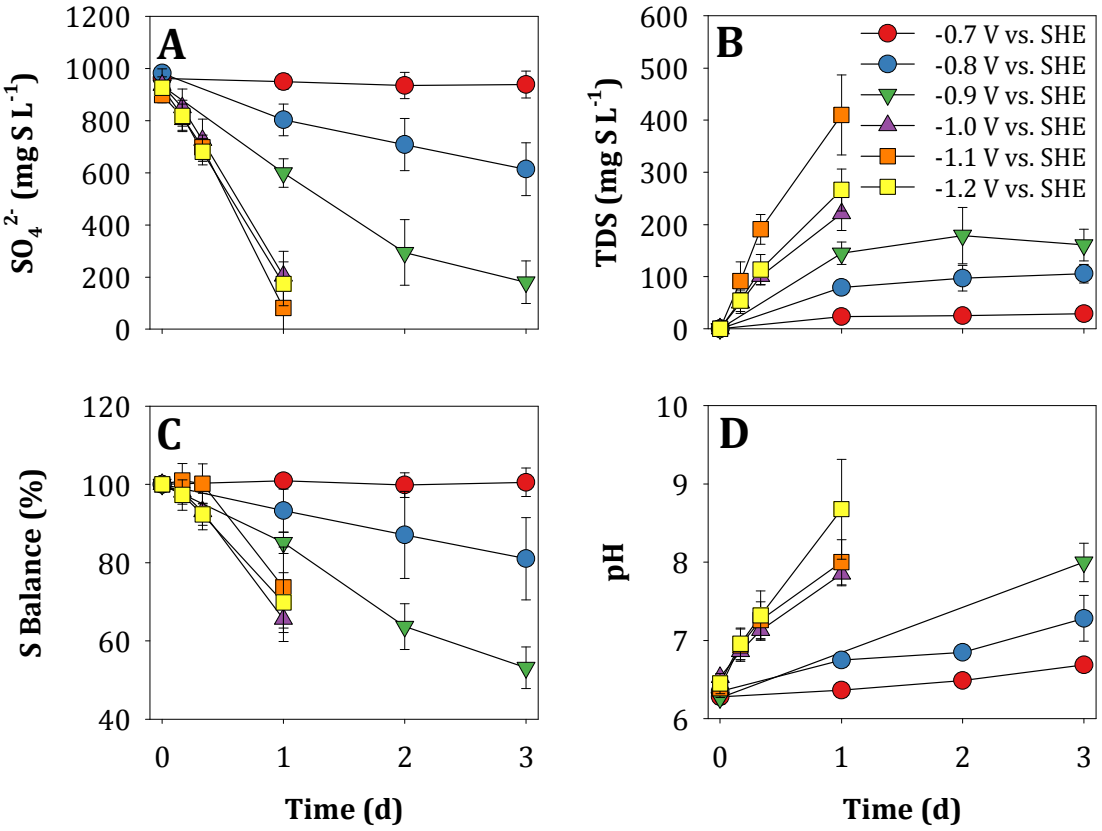

Figure 5.6. Effect of different cathodic potential along the cycle on A: sulfate concentration, B: TDS concentration, C: sulfur balance and D: pH.

The cathode potential affected the extent of catholyte basification (Figure 5.6D). Higher SRR were obtained at neutral pH than at acidic or alkaline pHs. At higher cathode potentials (-0.7 and -0.8 V vs. SHE), the pH was maintained around 7 during the three days. At a cathode potential of -0.9 V vs. SHE, the pH increased up to 8.0 (Figure 5.6D) leading to a SRR decrease. At lower potential values, the pH increased fast to 8.0 after just one day and reached pH 9.0 at the lowest cathodic potentials. The effect of the faster pH increase at lower potential was compensated by the higher H_2 availability.

Some authors investigated the sulfate removal using BESs with high cathode potentials. Su et al. (2012) operated a continuous-flow system and achieved a SRR

of 14.6 mg SO_4^{2-}-S L^{-1} d^{-1} at a cathode potential of -0.2 V vs. SHE, quite similar than the obtained in this study at -0.7 V vs. SHE. Coma et al. (2013) also operated a continuous-flow system and achieved a SRR of 60 mg SO_4^{2-}-S L^{-1} d^{-1} at a cathode potential of -0.26 V vs. SHE, much higher than the obtained in this study at -0.7 V vs. SHE. The continuous-flow operation could improve the efficiency of the system as was seen in the case of methane production (Batlle-Vilanova et al., 2015). Luo et al. (2014) attained a maximum SRR of 16.3 mg SO_4^{2-}-S L^{-1} d^{-1} at a cathode potential of around -0.76 V vs. SHE in a fed-batch operation, similar SRR than that obtained in this study at -0.7 V vs. SHE, but much lower compared with that obtained at -0.8 V vs. SHE. Pozo et al. (2015) also worked in fed-batch mode and obtained a SRR of 188 mg SO_4^{2-}-S L^{-1} d^{-1} at a cathode potential of -0.9 V vs. SHE, lower than the obtained in this study at the same cathode potential.

5.3.4. Microbial community analysis

The microbial community of the H-BES biocathodes at different pH was analyzed at the end of their long-term operation and of the C-BES after 60 days of operation (Figure 5.7). The biocathode community was mainly composed by SRB in H-BES systems: 42% at pH 5.5, 67% at pH 7 and 60% at pH 8.5. At pH 5.5 and 7 the main genus observed was *Desulfovibrio* sp., which has one of the highest affinities for hydrogen among SRB (Laanbroek et al., 1984). However, *Desulfovibrio* sp. is not favored under alkaline pH (Stolyar et al., 2007). For this reason, *Desulfovibrio* sp. loses the competition against *Desulfonatronum* sp. at pH 8.5, since *Desulfonatronum* sp. is a genus described as hydrogenotrophic and has a broader pH growth range (between 6.7 and 10.3) with an optimum of pH between 8.0 and 9.0 (Zhilina et al., 2005). *Desulfocurvus* sp. was also detected at pH 7.0, which grows at pH values between 5.0 and 9.0, being 6.9 the optimum, and uses organic compounds as carbon and energy sources (Klouche et al., 2009). Its presence indicates the possible generation of organic matter by homoacetogenesis. *Acetobacterium* sp. should be the responsible for supplying organic compounds for *Desulfocurvus* sp. growth by transforming hydrogen and carbon dioxide to organic acids as acetate (Balch et al., 1977).

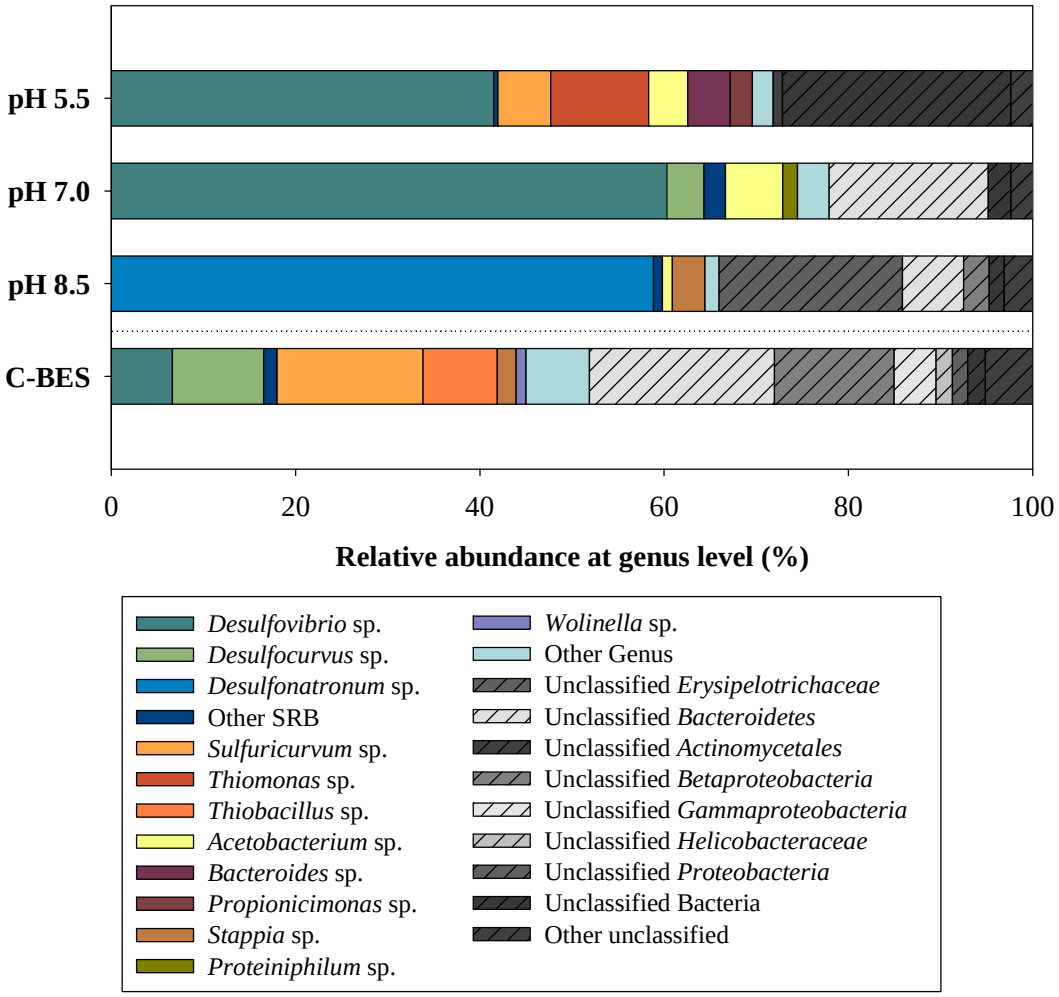

Figure 5.7. Microbial community distribution of the biocathodes of BES at different pH and of C-BES.

SOB were only detected at pH 5.5 in a percentage of 16%. SOB were mainly composed of *Thiomonas* sp., which could grow autotrophically, heterotrophically and mixotrophically at a pH range between 2.3 and 9 (Chen et al., 2004), and *Sulfuricurvum* sp. that is capable to grow under microaerophilic and anaerobic conditions (Kodama and Watanabe, 2004). Surprisingly, SOB were not detected on the cathode surface at pH 7 and 8.5 and less sulfur imbalance was detected compared with Blázquez et al. (2016), which observed a sulfur imbalance around 85% with a SOB abundance around 19%. However, SOB could grow over the BES walls and membrane, where the oxygen concentration is higher. The highest abundance of SRB was detected at pH 7, where the maximum SRR was observed. At pH 5.5, smaller abundance of *Desulfovibrio* sp. was detected since the pH could

inhibit its activity. At pH 8.5 a high abundance of SRB was also detected, although they were mostly *Desulfonatronum* sp. rather than *Desulfovibrio* sp. and *Desulfonatronum* sp. could have a smaller activity.

In C-BES, the SRB community represented about 18% and was mainly composed by *Desulfovibrio* sp. and *Desulfocurvus* sp. On the other hand, SOB represented about 24%, mainly *Sulfuricurvum* sp. and *Thiobacillus* sp. The latter is a chemolithoautotrophic sulfide-oxidizing bacterium detected in sulfur-producing reactors at high TDS loads and aerobic conditions (Visser et al., 1997). In this case, the variation of pH along the cycles and the higher oxygen transfer due to a higher relation between membrane surface and cathode volume in C-BES than in H-BES could result in a decrease of the relative abundance of SRB and an increase of the relative abundance of SOB. Otherwise, the C-BES presented high sulfate removal efficiencies. In addition, the presence of SOB explains the sulfur imbalance observed.

5.4. Conclusions

This study shows the effect of the type of membrane, pH and cathode potential on the simultaneous sulfate reduction and sulfide partial oxidation using a two-chamber BES during long-term operation.

The evaluation of adsorption and diffusion of sulfate through the membranes determined that CEM decreases better these effects (with a 0.16% of sulfate diffusion after one day and 0.0 g SO_4^{2-}-S m^{-2} of adsorption) than AEM (with a 39.4% of sulfate diffusion after one day and 5.2 g SO_4^{2-}-S m^{-2} of adsorption).

The study of the cathodic pH at a cathode potential of -0.8 vs. SHE showed a higher SRR (around 150 mg SO_4^{2-}-S L^{-1} d^{-1}) at pH 7 than at pH 5.5 and 8.5, and also a higher cathodic recovery (between 80 and 100%).

Desulfovibrio sp. was the main SRB observed at pH 7 (around 60%), which presented a high activity and abundance. At pH 5.5 also *Desulfovibrio* sp. was detected, but with lower activity because its optimal pH is neutral. At pH 8.5, *Desulfonatronum* sp. replaced *Desulfovibrio* sp. and achieved high SRR (up to

122 mg SO_4^{2-}-S L^{-1} d^{-1}) but, although the applied potential was increased, the cathodic recovery was still smaller than at pH 7.

The different cathode potentials applied showed that the lower the cathode potential was, the higher the SRR increase, achieving at -1.1 V vs. SHE a SRR of 785 ± 104 mg SO_4^{2-}-S L^{-1} d^{-1}.

However, at a cathode potential of –1.0 V vs. SHE, similar results of SRR were obtained and presented other advantages such as smaller TDS production and higher imbalances, which involves higher elemental sulfur production.

Chapter 6

Treatment of real flue gas desulfurization wastewater in an autotrophic biocathode in view of elemental sulfur recovery

The main aim of this chapter consisted of exploring how the BES previously studied would be affected by a wastewater from a chemical industry that produces pigments by elemental sulfur combustion, which has high sulfate content and lacks of electron donor. The chapter discusses thoroughly the fate of the sulfur species in the system with sulfate, sulfide and elemental sulfur as the main compounds of interest. Moreover, detailed microbiological analyses of the biomass formed in the cathode, membrane and planktonic biomass show that the higher complexity of the real flue gas desulfurization effluent, the higher the growth of sulfur oxidizing bacteria and, consequently, the higher amount of elemental sulfur that can be recovered.

Abstract

Sulfur oxide emissions can lead to acidic precipitation and health concerns. Flue gas desulfurization (FGD) systems treat these emissions generating a wastewater with high-sulfate content. The sulfate treatment and elemental sulfur recovery have been studied in a biocathode with simultaneous sulfate reduction to sulfide and partial sulfide oxidation, comparing the performance obtained with synthetic and real wastewater. A decrease of the sulfate removal rate (SRR) from 108 to 73 mg SO_4^{2-}-S L^{-1} d^{-1} was observed coupled to an increase in the elemental sulfur recovery from 1.4 to 27 mg TDS-S L^{-1} d^{-1}. This elemental sulfur recovered as a solid from the real wastewater represented a 64% of the theoretical elemental sulfur produced (the elemental sulfur corresponded to a 72% of the solid weight). In addition, microbial communities analysis of the membrane and cathode biofilms and planktonic biomass showed that the real wastewater allowed a higher growth of sulfur oxidizing bacteria (SOB) adapted to more complex waters as *Halothiobacillus* sp. while decreasing the relative abundance of sulfate reducing bacteria (SRB).

6.1. Introduction

80% of sulfur oxide (SO_x, mainly SO_2) emitted to the environment comes from anthropogenic sources, mainly industries operating with high-sulfur-containing fossil fuels or sulfur-containing raw material (e.g. pigments industry, sulfuric acid manufacturing plants, etc.) (Pandey et al., 2005). Flue gas desulfurization (FGD) technologies are implemented in order to reduce SO_2 emissions. The most widespread technology consists of the absorption of SO_2 in a neutral or lightly acidic medium producing wastewaters with a mix of sulfate and sulfite. The effluent of FGD technologies has a high concentration of sulfate due to high SO_2 concentration in flue gases (typical range between 10 and 1500 ppmv) (Zevenhoven and Kilpinen, 2001).

The biological treatment of flue gases was studied at lab-scale by Philip and Deshusses (2003) in a two-stage process consisting of a biotrickling filter followed by biological post-treatment. The SO_2 in the flue gas was recovered in the biotrickling filter as sulfite and sulfate. Then, these were reduced and partially oxidized to elemental sulfur in the post-treatment (combining anaerobic and microaerophilic conditions and supplying glucose as electron donor) with an efficiency of about 80% with respect to the total SO_2 treated. There are other reported alternative technologies for biological sulfate removal from wastewater. For example, the SANI® process (sulfate reduction, autotrophic denitrification and nitrification integrated, Hong Kong) has been implemented at full-scale for the removal of sulfur and nitrogen from saline sewage at a ratio of > 0.5 mg SO_4^{2-}-S /mg COD (Wu et al., 2016). The SULFATEQ® process (Paques B. V., The Netherlands) is a biological treatment used in metallurgical and mining industries to treat wastewater streams that contain oxidized sulfur compounds while using organic matter and H_2 as electron donor (Schröder-Wolthoorn et al., 2008). In this system, a second reactor would be needed to oxidize sulfide to elemental sulfur in case of not having enough metal content to precipitate the entire sulfide.

The use of biolectrochemical systems (BES) has also been proposed to treat high-strength sulfate wastewaters by using the H_2 produced in the cathode as electron donor. A SRB-enriched biocathode increases the bio-availability of electron donor

for the autotrophic SRB (Blázquez et al., 2016, 2017; Gacitúa et al., 2018; Pozo et al., 2017a, 2016, 2015). In this sense, Pozo et al. (2017b) recently studied a two-step configuration to treat real acid mine drainage (AMD). This new configuration avoided a potential SRB inhibition by AMD and enabled resource recovery of the inlet sulfate as elemental sulfur. Other studies, conducted in microbial fuel cells (MFC), aimed at recovering elemental sulfur from sulfate (Lee et al., 2014; Zhao et al., 2008) thanks to the spontaneous sulfide partial oxidation to elemental sulfur in the anode (Dutta et al., 2008). An external COD supply was required for the sulfate reduction to sulfide, but in this case the energy recovered and the coulombic efficiency from sulfide oxidation is lower compared with the ones that could be obtained from COD oxidation (Tice and Kim, 2014). A dual-chamber BES to recover elemental sulfur without the need of COD in the cathode was reported in our previous study (Blázquez et al., 2016). Microaerophilic conditions were achieved thanks to oxygen diffusion through the membrane which allowed the growth of both SRB and sulfide oxidizing bacteria (SOB) in the cathode.

Although there are several reported works on elemental sulfur recovery through BES, all of them were conducted using synthetic wastewater and very well controlled conditions. Hence, the aim of this work was to treat, for the first time, real high-strength sulfate wastewater from a process of FGD of a pigments industry in a biocathode of a BES recovering elemental sulfur, to further demonstrate the feasibility of this technological approach in real systems. Moreover, this work studied how real wastewater affects the microbial communities involved in its treatment.

6.2. Experimental

6.2.1. Real wastewater source and charactetization

The wastewater was collected from a chemical industry that produces pigments by elemental sulfur combustion. This combustion produces a gas with a SO_2 content of around 3000 ppmv, which are absorbed in a chemical scrubber using water with NaOH in order to keep the pH of the effluent around 6. The effluent of such FGD absorption column contained around 30 g SO_4^{2-}-S L^{-1}. This effluent is mixed with

the water used to clean the reactors of the process producing the wastewater used in this study. The composition of this wastewater is shown in Table 6.1. The wastewater was stored in a cold room at 4 ºC until its use. The real wastewater was diluted with tap water for the experiments due to its high concentration. Although sulfite is usually present at high concentration in FGD column effluents, no sulfite was detected in our wastewater because after mixing with cleaning wastewater and storing at 4 ºC for some time it was completely oxidized to sulfate.

Table 6.1. Composition of the effluent from the flue gas desulfurization absorption column.

Compound	Concentration	
TIC	1.4 ± 0.1	mg C L^{-1}
TOC	8.0 ± 0.8	mg C L^{-1}
Cl^-	1329 ± 69	mg L^{-1}
NO_2^-	0.1 ± 0.1	mg N L^{-1}
NO_3^-	0.6 ± 0.8	mg N L^{-1}
NH_4^+	92 ± 9	mg N L^{-1}
PO_4^{3-}	0.7 ± 0.4	mg P L^{-1}
SO_4^{2-}	14555 ± 137	mg S L^{-1}
$S_2O_3^{2-}$	157 ± 138	mg S L^{-1}
Mg^{2+}	20 ± 1	mg L^{-1}
Ca^{2+}	220 ± 4	mg L^{-1}

6.2.2. Experimental procedure

The whole experimental operation was divided into four different periods according to the operational conditions (Table 6.2). Each period lasted at least 4 cycles in order to determine the variability of the operational conditions. The H-BES was started up (Period I) with synthetic medium (Blázquez et al., 2017) with a cycle duration of 3 days. The H-BES was inoculated with 20 mL of sludge with

volatile suspended solids concentration around 40 g VSS L^{-1} mixed with mineral medium (up to 350 mL). The sludge was obtained from an UASB reactor enriched with SRB that treated high-strength sulfate wastewater using glycerol as electron and carbon donor. After this period, the cycle length was increased to 7 days in order to obtain a higher removal of sulfate at the end of the cycle (Period II). In Period III the synthetic wastewater was replaced for the real wastewater diluted with tap water in order to obtain an initial sulfate concentration of 750 mg SO_4^{2-}-S L^{-1} and in Period IV the real wastewater was diluted to obtain an initial sulfate concentration of 1500 mg SO_4^{2-}-S L^{-1}. The whole mineral medium was replaced for each cycle. Before each cycle, the medium was sparged with CO_2 in order to remove the oxygen of the medium and to increase the inorganic carbon content. The anodic medium contained 20 g L^{-1} of NaCl dissolved in distilled water.

Table 6.2. Operational conditions in each experimental period.

Period	Days	Wastewater	Initial sulfate concentration (mg SO_4^{2-}-S L^{-1})	Cycle length (d)
I	0-70	Synthetic	1000	3
II	71-133	Synthetic	1000	7
III	134-175	Real	750	7
IV	176-203	Real	1500	7

An abiotic control was performed in order to characterize the possible electrochemical sulfate reduction. The test was performed in duplicate with real wastewater diluted 10 times with synthetic mineral medium using the C-BES. The test lasted 7 days as the cycle length during periods II to IV. The sulfate balance was calculated according to Eq. 6.1.

$$Sulfate\ balance = 100\frac{V^{Cat}C^{Cat}_{SO_4^{2-}-S,f}+V^{An}C^{An}_{SO_4^{2-}-S,f}}{V^{Cat}C^{Cat}_{SO_4^{2-}-S,i}+V^{An}C^{An}_{SO_4^{2-}-S,i}} \quad \text{(Eq. 6.1)}$$

Where $C_{SO_4^{2-}-S,i}^{Cat}$ and $C_{SO_4^{2-}-S,f}^{Cat}$ are the initial and final sulfate concentration in the cathode, respectively, $C_{SO_4^{2-}-S,f}^{An}$ and $C_{SO_4^{2-}-S,i}^{An}$ are the same measurements in the anode.

6.3. Results and discussion

6.3.1. Sulfate removal from real wastewater

The results of sulfate removal during the long-term operation of the H-BES reactor are presented in Figure 6.1. Initial and final sulfate concentration, final total dissolved sulfide (TDS) and theoretical elemental sulfur produced are shown for the four different periods of operation. The first two periods were conducted with synthetic wastewater (Table 6.2) whereas real wastewater was used in the last two periods.

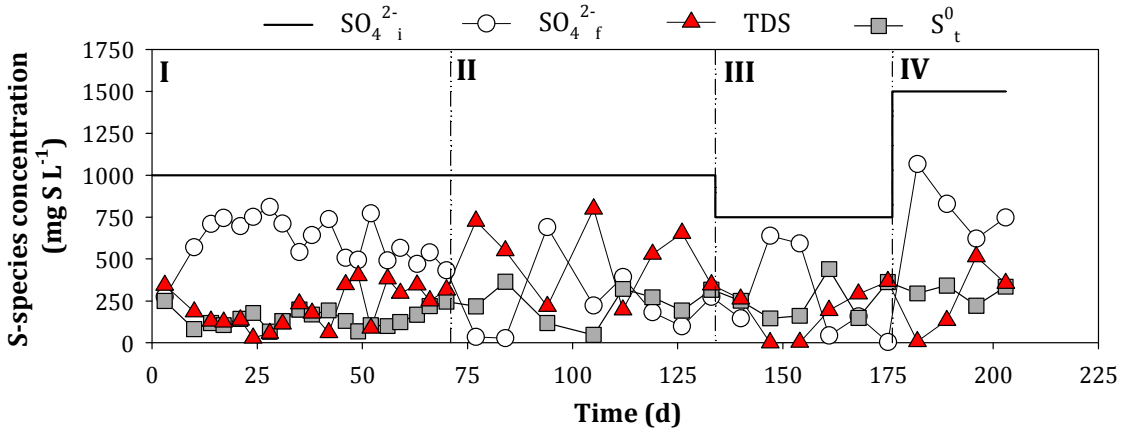

Figure 6.1. Concentration of the sulfur species for all the experimental periods: initial sulfate ($SO_4^{2-}{}_i$), and sulfate ($SO_4^{2-}{}_f$), total dissolved sulfide (TDS) and theoretical elemental sulfur ($S^0{}_t$) concentrations at the end of each cycle.

The cycle length in period I was three days and the system was not able to consume the entire sulfate obtaining a sulfate concentration at the end of the cycle between 500 and 800 mg SO_4^{2-}-S L^{-1}. For this reason, the cycle length was increased up to seven days in period II which led to a decrease in the final sulfate concentration and a consequent increase in final TDS concentration up to 502 ± 228 mg TDS-S L^{-1}.

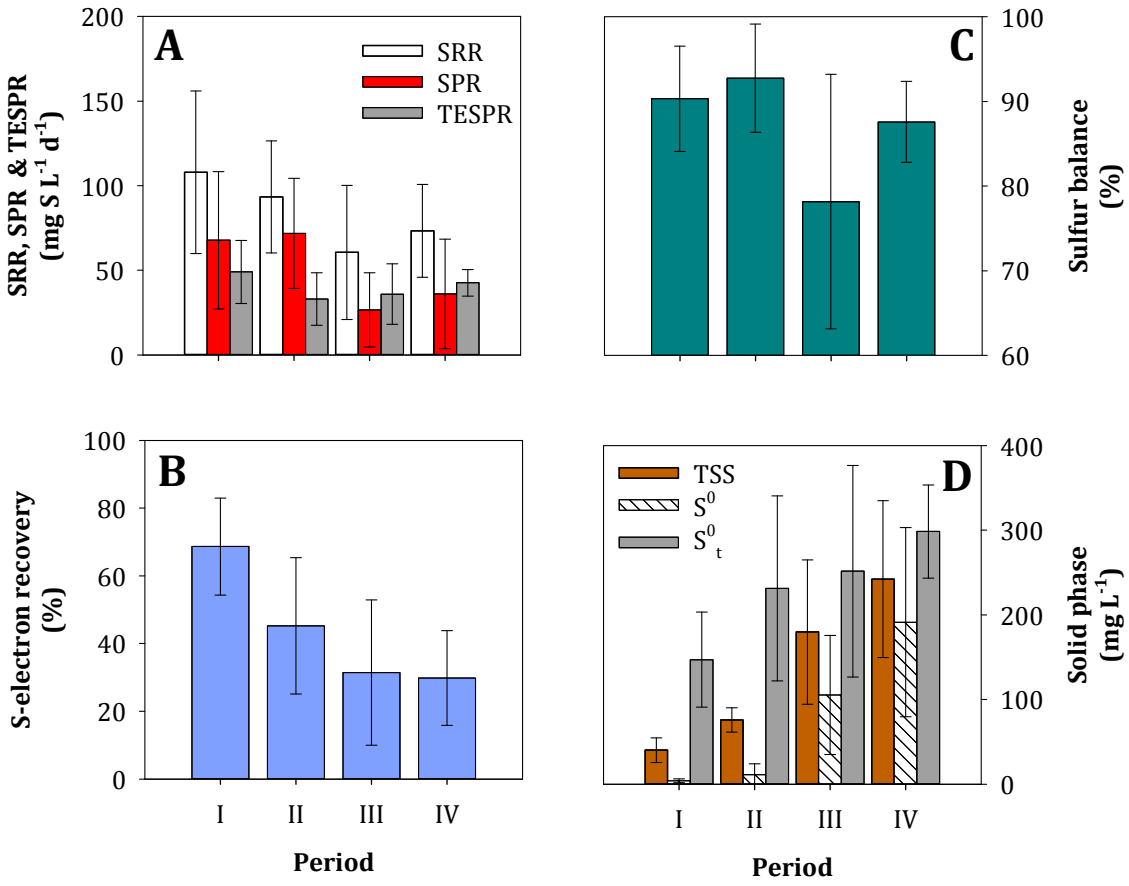

Figure 6.2. Average values of the most representative performance parameters for each operational period. A: sulfate removal rate (SRR), sulfide production rate (SPR) and theoretical elemental sulfur production rate (TESPR), B: electron recovery, C: balance of sulfur species detected at the end of the cycle respect to the beginning of the cycle and D: total suspended solids (TSS), recovered elemental sulfur (S^0) and theoretical elemental sulfur (S^0_t).

Figure 6.2 shows the average results on sulfate removal rate (SRR), sulfide production rate (SPR) and theoretical elemental sulfur production rate (TESPR) for each period (Figure 6.2A). The observed deviation was due to the replacement of the whole volume of medium between each cycle. This procedure caused periodic disturbances in the biofilm of the electrode and the removal of planktonic biomass. Increasing the cycle length from three to seven days did not have any effect on biological rates. Both SRR and SPR in both periods were very similar, e.g. SRR=108 ± 48 mg SO_4^{2-}-S L^{-1} d^{-1} in period I and SRR=93 ± 33 mg SO_4^{2-}-S L^{-1} d^{-1} in period II.

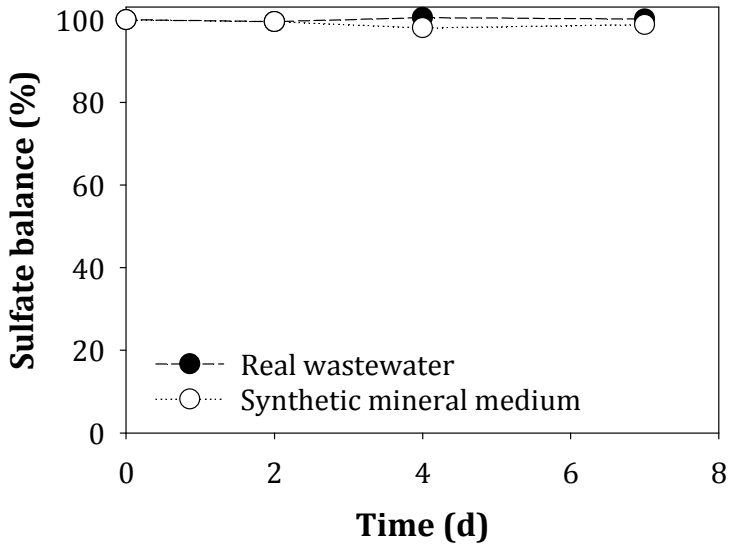

Figure 6.3. Sulfate balance of the abiotic control experiments along the cycle with real wastewater and synthetic mineral medium.

After 133 days of operation, the synthetic wastewater was replaced by the industrial effluent. This effluent was diluted (20 times for period III and 10 times for period IV) with tap water to avoid any inhibition due to the high sulfate content. The initial sulfate concentration on period III was around 750 mg SO_4^{2-}-S L^{-1} and the length of the cycle was kept at 7 days. The SRR in this period decreased down to 61 ± 40 mg SO_4^{2-}-S L^{-1} d^{-1} with a maximum SRR up to 101 mg SO_4^{2-}-S L^{-1} d^{-1}. The dilution was decreased in period IV to obtain a concentration of sulfate around 1500 mg SO_4^{2-}-S L^{-1} and to assess the performance of our system at higher sulfate concentrations. The SRR obtained was of 73 ± 27 mg SO_4^{2-}-S L^{-1} d^{-1} with a maximum SRR observed of 94 mg SO_4^{2-}-S L^{-1} d^{-1}. An abiotic control was performed with synthetic mineral medium and real wastewater (Figure 6.3). After 7 days, the sulfate balance was 100.2 ± 0.6% with the real wastewater and 98.8 ± 1.3% with the synthetic mineral medium. Thus, it can be concluded that the abiotic sulfate reduction at -0.8 V vs. SHE was negligible, for this reason, the observed sulfate removal was attributed to biological processes.

The results obtained during all the operation show much lower SRRs than other technologies. The maximum hydrogenotrophic and autotrophic sulfate removal

observed until now (around 10 g SO_4^{2-}-S L^{-1} d^{-1}) was obtained in a lab-scale gas-lift reactor which supplied H_2 externally at high flow rates (van Houten et al., 1994) which involved high losses of hydrogen. In any case, the use of biocathodes for sulfate reduction is emergent and with a high potential of improvement in many operational parameters such as the materials used. For instance, sulfate removal from synthetic wastewater using a graphite brush as biocathode was reported obtaining similar or lower results (Blázquez et al., 2016; Luo et al., 2014). Luo et al. (2014) reported sulfate reduction in a biocathode for the first time achieving SRRs around 65 mg SO_4^{2-}-S L^{-1} d^{-1} in continuous mode at pH 7. In other studies with the same configuration and also controlling the pH at 7, the SRR was also around 100 mg SO_4^{2-}-S L^{-1} d^{-1} with a length cycle around 3-4 days (Blázquez et al., 2016). Nevertheless, the maximum reported SRRs in a biocathode were obtained using carbon granules and multiwalled carbon nanotubes: SRRs over 5 g SO_4^{2-}-S L^{-1} d^{-1} at a cathode potential of -1.1 V vs. SHE were obtained (Pozo et al., 2017a). In this sense, the SRR could be increased with higher currents and higher H_2 production using more efficient electrode materials and decreasing the cathode potential. SPR would also increase but TESPR would not necessarily increase as well because it would depend on the oxygen diffusion through the membrane.

To the best of our knowledge, there are no reports on the treatment of real FGD effluents with autotrophic SRB. However, this wastewater has been used as an influent for the SANI process (Jiang et al., 2013; Qian et al., 2015b, 2015a, 2013) where organic matter (lactate, glucose and acetate) was used as electron donor and carbon source for sulfate reduction. An up-flow bed reactor was used at lab-scale in these studies and they also aimed at sulfite reduction. Sulfite reduction should theoretically be faster than sulfate reduction since sulfite is an intermediary of sulfate reduction (Jiang et al., 2013). The easy biodegradable organic matter and the use of sulfite enabled high removal rates of around 1 g S L^{-1} d^{-1}.

The cathode potential is essential to understand the biocathodic sulfate reduction presented in this work. The cathode potential during all of our operation was kept at -0.8 V vs. SHE to guarantee the continuous hydrogen production needed for the autotrophic sulfate reduction. Electron recovery is the ratio of electrons used in sulfate reduction to sulfide compared with the electrons flowing from the anode to

the cathode. The electron recovery (Figure 6.2B) decreased in period II compared to period I from 69 ± 14% to 45 ± 20% but the decrease observed in SRR was of 14%. This could be explained by the increase of the intensity from 3.82 ± 1.51 A m^{-2} in period I to 5.69 ± 1.64 A m^{-2} in period II (Figure 6.4) due to i) the enrichment of the cathodic consortium with bacteria with higher electroactivity (Pozo et al., 2015) or ii) because of the enhancement of the cathodic electroactivity due to biofilm growth (Cordas et al., 2008).

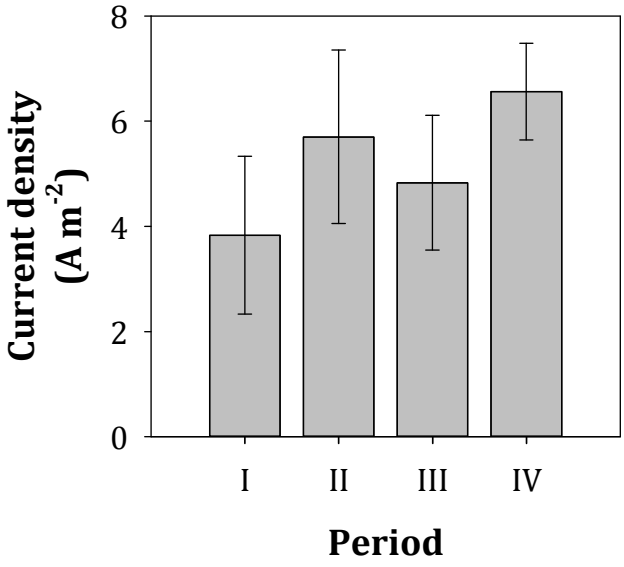

Figure 6.4. Average current density in each period.

When the synthetic wastewater was replaced by the diluted real FGD wastewater (periods III and IV), both the intensity and electron recovery decreased. The intensity decrease could be caused by a decrease of the conductivity of the medium from 8.04 mS cm^{-1} of the synthetic wastewater to 4.79 mS cm^{-1} of the real FGD wastewater diluted 20 times. Nevertheless, when the concentration of real wastewater was increased (period IV), an increase of the intensity from 4.84 ± 1.27 A m^{-2} in Period III to 6.55 ± 0.91 A m^{-2} in Period IV was observed. This increase could be attributed to biomass acclimation as well as to an increase of the catholyte conductivity from 4.79 mS cm^{-1} to 8.72 mS cm^{-1}. It seems biomass acclimation was more relevant since, comparing periods I and III, the conductivity of period III was lower but the intensity was higher. Despite the SRR also increased

from period III to IV, the electron recovery was around 30% in these two periods, which means that 30% of the electrons flowing from the anode to the cathode were used for sulfate reduction. The rest of the electrons could be wasted i) to reduce a potential excess of oxygen that diffused from the anode through the membrane to the cathode, ii) to generate an excess of hydrogen and iii) to reduce other salts of the real wastewater.

6.3.2. Elemental sulfur recovery

Figure 6.1 shows that not all the sulfate removed was transformed to TDS, sulfite or thiosulfate. This imbalance also can be observed in Figure 6.2C, which shows, for each experimental period, the average balance of the total sulfur species at the end of the cycle. As shown in a previous report, this imbalance can be linked to elemental sulfur production due to oxygen diffusion from the anode to the cathode through the membrane. However, the dissolved oxygen concentration in the cathode is close to 0 mg O_2 L^{-1} because the excess oxygen not consumed by the microorganisms is reduced to water in the cathode (Blázquez et al., 2016). In the same experimental system, Blázquez et al. (2017) reported a maximum diffusion rate for the CMI of 3.3 mmol O_2 m^{-2} h^{-1}. However, the imbalance was not the same during all the periods (Figure 6.2C). The sulfur balance in periods I and II was around 90%, indicating that the fate of around 10% of the initial sulfur as sulfate was elemental sulfur. This corresponded to a TESPR of 49.0 ± 18.7 mg S^0-S L^{-1} d^{-1} in period I and 33.0 ± 15.6 mg S^0-S L^{-1} d^{-1} in period II (Figure 6.2A). When the synthetic wastewater was replaced by real wastewater, the sulfur balance maintained in the same range: 78 ± 15% in period III and 88 ± 5% in period IV (Figure 6.2C) with also similar TESPR of 35.9 ± 17.9 mg S^0-S L^{-1} d^{-1} in period III and 42.6 ± 7.9 mg S^0-S L^{-1} d^{-1} in period IV (Figure 6.2A). Several samples of the suspended solids taken during the long-term operation showed an increase of the TSS and of the elemental sulfur recovered at the end of the cycles (Figure 6.5).

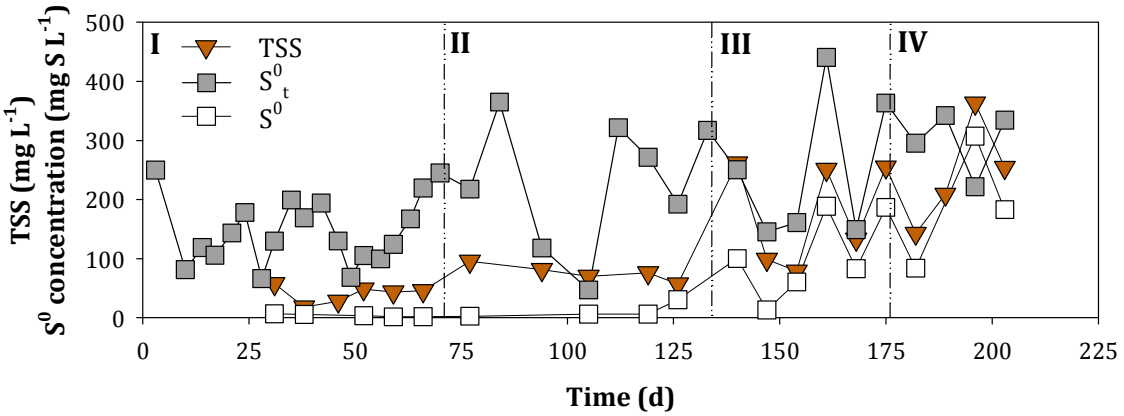

Figure 6.5. Concentration of total suspended solids (TSS), theoretical elemental sulfur (S^0_t) and recovered elemental sulfur (S^0) at the end of each cycle during the long-term operation.

The average of solids (TSS), elemental sulfur recovered (S^0) and theoretical elemental sulfur produced (S^0_t) concentrations at the end of the cycle are shown in Figure 6.2D. The S^0_t in periods I and II should be around 150 and 230 mg S^0-S L^{-1}, respectively, according to the balance. However, the average concentration of TSS at the end of the cycles were 40 ± 15 mg TSS L^{-1} in period I and 76 ± 14 mg TSS L^{-1} in period II and with a presence of S of 11.8 ± 11.7% in period I and 18.3 ± 23.6% in period II. This increase of solids from period I to period II was attributed to the increase of the cycle length which could allow more biomass growth and more sulfur production, but the elemental sulfur recovered was negligible and with a high deviation. One reason could be due to the attachment of some elemental sulfur to the walls of the cathode compartment and on the surface of the pH probe.

TESPR at the end of the cycle was quite similar when real wastewater was used (around 250 and 300 mg S^0-S L^{-1} in periods III and IV respectively), but both the TSS and the S/TSS proportion increased. The average concentration of TSS at the end of the cycles was 180 ± 85 mg L^{-1} with an S content of 56.5 ± 22.5% in period III. However, the average concentration of TSS at the end of the cycles was of 242 ± 93 mg L^{-1} with an S content of 71.8 ± 13.0% in period IV when the dilution was modified to obtain an initial sulfate concentration of 1500 mg SO_4^{2-}-S L^{-1}. Average elemental sulfur recovery was 105 ± 70 mg S^0-S L^{-1} in period III and of

191 ± 112 mg S^0-S L^{-1} in period IV, corresponding to a recovery of around 15% of initial sulfate in both periods. However, a recovery of around 42% in period III and of 64% in period IV was obtained with respect to the theoretical elemental sulfur produced. These values are still far from the recoveries with conventional aerobic and anoxic technologies (stirred tank reactors, expanded granular sludge reactors, UASB…) (Cai et al., 2017) but it is the highest elemental sulfur recovery reported until now by bioelectrochemical systems. Other authors studied the recovery from sulfide in the anodic compartment. Rabaey et al. (2006) achieved a recovery of 9 ± 4% as elemental sulfur based on sulfide dosage deposited on the anode surface (graphite granules). However, elemental sulfur passivated the electrode surface resulting in exponential decay of the current and an increase of the polarization resistance (Ateya et al., 2003). Thus, Dutta et al. (2010) tried to recover the sulfide as polysulfide in a basic solution changing the polarity of the anode, achieving a recovery of 75 ± 4% of the initial sulfide. In both studies they worked in the anodic partial oxidation of sulfide without involving sulfate reduction in the process, avoiding the requirement of external electron donor for the reduction step.

6.3.3. Microbial community analysis

The microbial evolution was analyzed comparing the Illumina sequencing results at three sampling times: inoculum, after period II and after period IV. The comparison of periods II and IV was essential to understand the differences between the use of synthetic wastewater and the real wastewater from the FGD system effluent. Moreover, samples taken from different parts of the reactor (Figure 6.6) were bacteria could grow as biofilm (on the membrane and cathode surfaces) and as planktonic in the supernatant (Table 6.3) were compared to understand possible differences among these locations. Figure 6.7 shows the relative abundances of the samples at genus level. Rarefaction curves of the samples were plotted (Figure 6.8) indicating that all of them were comparable in terms of abundance percentage and that a good coverage of diversity was reached.

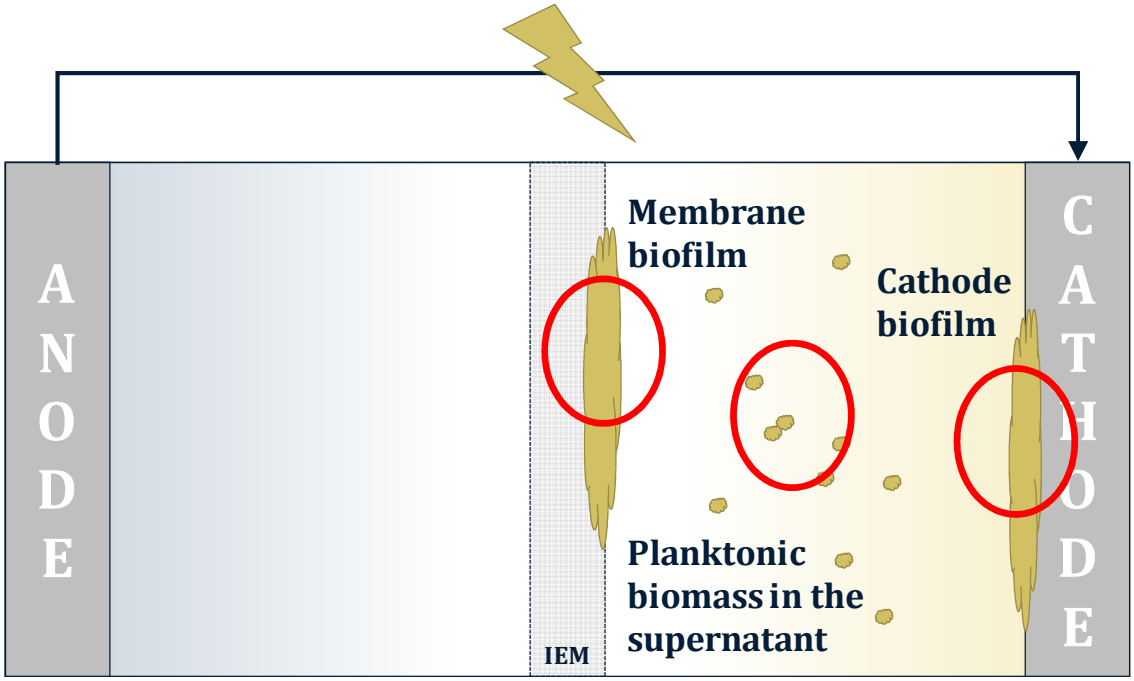

Figure 6.6. Bioelectrochemical system diagram showing the sampling points for the microbial analysis.

Table 6.3. Summary of the samples from the microbial communities analyzed.

Nomenclature	Sample	Wastewater source	n° of reads
Inoculum	Inoculum	Synthetic with glycerol	97839
Cat-PII	Cathode biofilm after period II	Synthetic	119341
Cat-PIV	Cathode biofilm after period IV	Real	116852
Mem-PII	Membrane biofilm after period II	Synthetic	126662
Mem-PIV	Membrane biofilm after period IV	Real	99797
Sup-PII	Supernatant after period II	Synthetic	98145
Sup-PIV	Supernatant after period IV	Real	109055

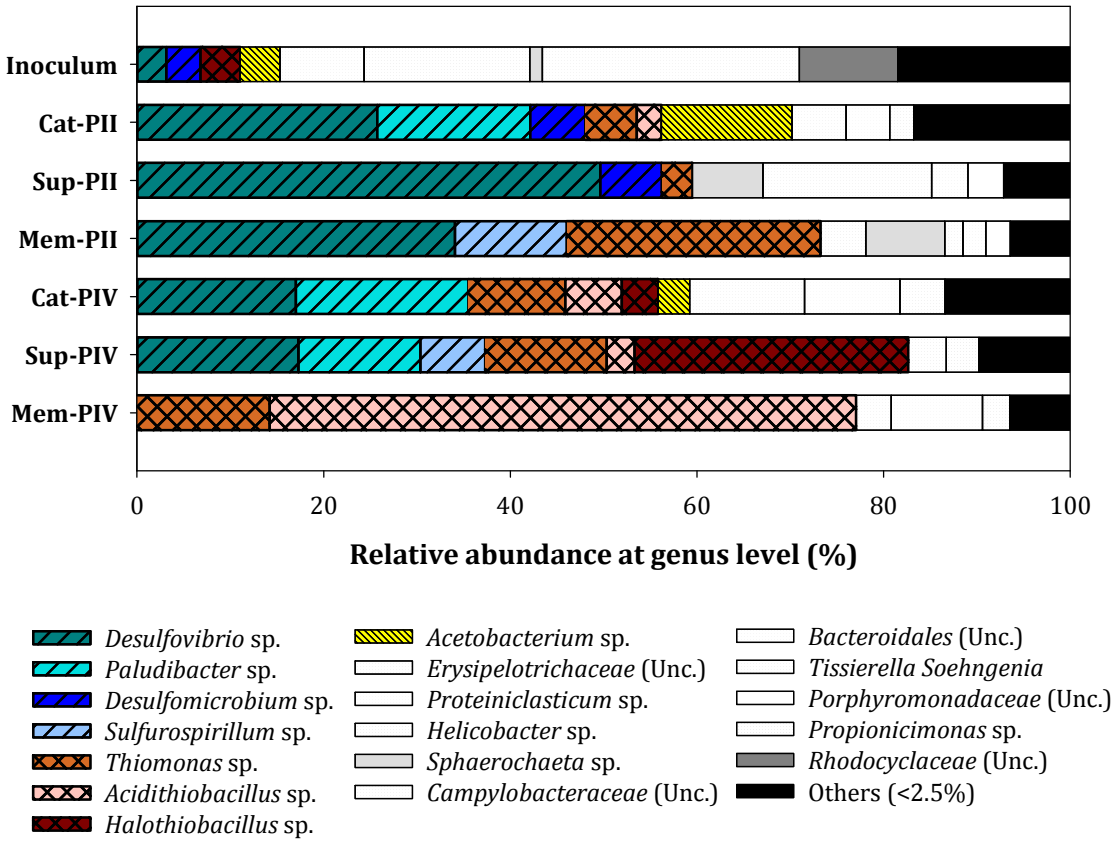

Figure 6.7. Microbial community distribution at genus level of inoculums, cathode biofilm (Cat), supernatant (Sup) and membrane biofilm (Mem) at the end of period II (PII) when synthetic wastewater was used, and at the end of period IV (PIV) when real wastewater was used.

The inoculum used to obtain an enriched population on SRB came from a reactor which treated sulfate using crude glycerol as electron donor and carbon source. The inoculum contained slightly more than a 6% of SRB, mainly *Desulfovibrio* sp. and *Desulfomicrobium* sp. *Desulfovbrio* sp. is the most studied genus of SRB and has one of the highest affinities for H_2 (Laanbroek et al., 1984). Regarding *Desulfomicrobium* sp., it has been observed that they can use either organic matter as electron donor (Copeland et al., 2009) or H_2 (Hippe et al., 2003; Thevenieau et al., 2007) depending on the species and strains. *Halothiobacillus* sp., which is a SOB that grows in high saline environments (Sievert et al., 2000), was also observed in the inoculum (>4%). *Thiomonas* sp., a SOB that could grow autotrophically, heterotrophically and mixotrophically (Chen et al., 2004), also appeared in the

inoculum (around 2%). The main genus detected in the inoculum was *Tisserella* sp. with a 27.5% of relative abundance. It has been previously detected in sewage and can grow with complex organic matter (Harms et al., 1998). Other genera were detected in a high relative abundance as *Helicobacter* sp. with a 17.8%. Both *Helicobacter* sp. and *Tisserella* sp. are involved in the degradation of organic matter.

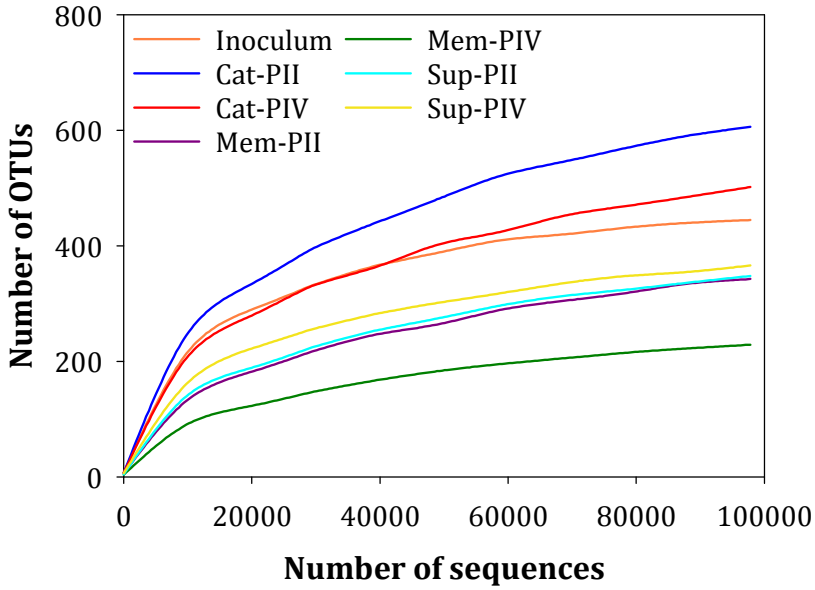

Figure 6.8. Rarefaction curves of the different samples.

Samples of the membrane (Mem-PII) and cathode (Cat-PII) biofilms and planktonic biomass of the supernatant (Sup-PII) were withdrawn after 133 days of operation (end of period II). Mem-PII and Sup-PII showed higher similarity between them as can be observed in the principal component analysis plot (Figure 6.9). A high relative abundance of SRB in both cases was observed, showing more than 46% in Mem-PII and higher than 56% in the Sup-PII. But besides *Desulfovibrio* sp. (34.1% in Mem-PII and 49.7% in Sup-PII), *Desulfomicrobium* sp. (6.6%) was detected in the Sup-PII sample and *Sulfurospirillum* sp. (11.9%) in the Mem-PII. *Sulfurospirillum* sp. is a genus of SRB that can reduce thiosulfate and sulfur using H_2 and organic matter as electron donor and can grow under microaerobic conditions (Stolz et al., 1999). Its presence in the membrane biofilm could be

explained by the oxygen diffusion and the elemental sulfur production by SOB. The relative abundance of SOB at the membrane biofilm was higher than 27% (mainly *Thiomonas* sp.), while it was quite lower in the Sup-PII sample (3.3% of *Thiomonas* sp.). Both *Helicobacter* sp. and *Tisserella* sp. did not show a high relative abundance in these samples during the BES operation due to the lack of organic matter.

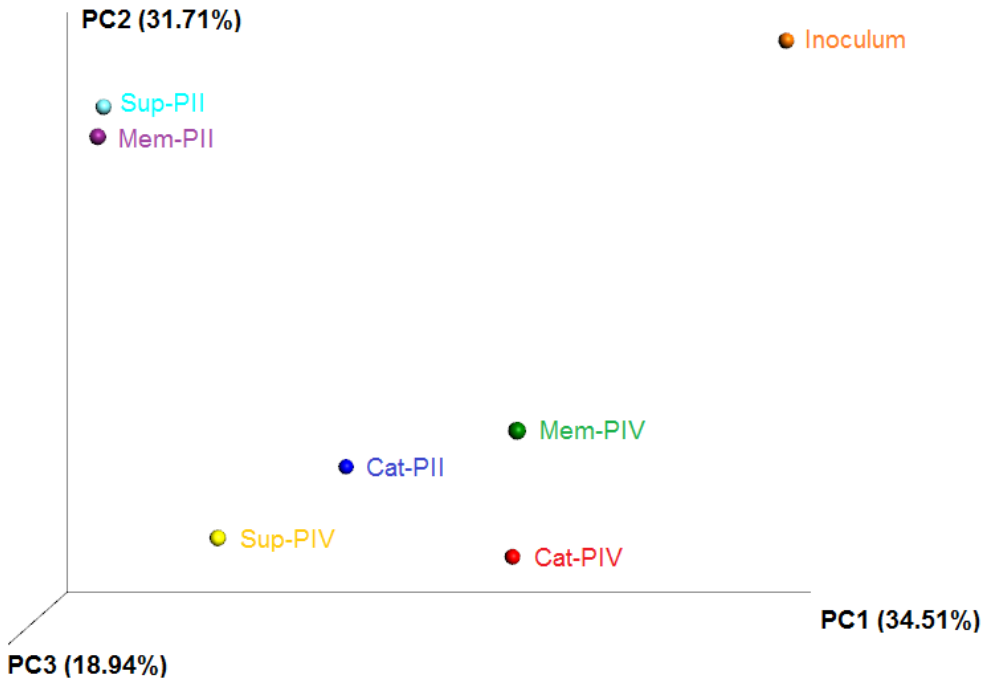

Figure 6.9. Principal component analysis: PCA based on the normalized OTUs table, where each point represents a sample.

A high relative abundance of SRB was detected in the Cat-PII (higher than 48%) consisting of *Desulfovibrio* sp. (25.8%), *Paludibacter* sp. (16.4%) and *Desulfomicrobium* sp. (5.9%). The role of *Paludibacter* sp. is not really clear. Liang et al., (2013) stated that *Paludibacter* sp. might have an important role as a sulfate reducer at acidic pH. However, *Paludibacter* sp. has been detected in this study at pH 7 and was not found in a sulfate-reducing biocathode at pH 5.5 even after long-term operation (Blázquez et al., 2017). In addition, *Paludibacter* sp. was not observed to use sulfur species as terminal electron acceptors (Qiu et al., 2014) or to produce hydrogen sulfide (Ueki et al., 2006). Also, *Acetobacterium* sp. was detected in a significant relative abundance (14.0%). It is a homoacetogenic genus

detected as dominant in a cathodic mixed culture producing acetate from CO_2 and H_2 (Kracke et al., 2015). In this case, *Acetobacterium* sp. could provide acetate as a carbon source to SRB. Finally, *Thiomonas* sp. (5.5%) and *Acidithiobacillus* sp. (2.6%) were the SOB detected.

After 133 days of operation with synthetic wastewater, the medium was replaced by real wastewater. At day 203 (end of period IV), samples of the membrane biofilm (Mem-PIV), cathode biofilm (Cat-PIV) and planktonic biomass of the supernatant (Sup-PIV) were also withdrawn in order to compare the microbial distribution between synthetic and real wastewater. The biggest differences were observed in the membrane biofilm. In Mem-PIV, SRB presence was insignificant while SOB presence increased up to more than 77%: *Acidithiobacillus* sp. (62.9%) and *Thiomonas* sp. (14.2%). The high abundance of *Acidithiobacillus* sp. was surprising since it has been observed to grow only at acidic pH (Valdés et al., 2008) and, in our experiments, the pH of the system was controlled at 7. However, protons came through the cation exchange membrane continuously and it could provide acidic local conditions to the biofilm. On the other hand, a deterioration of the membrane after more than 200 days of operation might have resulted in some anolyte diffusion causing an acidic pH in the membrane biofilm. This deterioration of the membrane could cause a prolonged acidic pH, resulting in the increase of the relative abundance of Acidithiobacillus sp. in the biofilm as has been reported in other studies with SOB biofilms (Montebello et al., 2013).

The sample Sup-PIV also showed higher relative abundance of SOB (higher than 45%) than the Sup-PII. *Halothiobacillus* sp. (29.3%) were predominant in Sup-PIV despite they had lower presence after period II. As was mentioned before, *Halothiobacillus* sp. can grow in high concentration of salts (Sievert et al., 2000), which allows the system to continuously partially oxidizing sulfide to elemental sulfur also in a real FGD system wastewater. The relative abundance of SRB decreased (around 37%) compared with the sample Sup-PII, showing an abundance of *Desulfovibrio* sp. of 17.3%, of *Paludibacter* sp. of 13.1% and of *Sulfurospirillum* of 7.0%.

The cathodic biofilm was the microbial community less influenced with the change from the synthetic to real wastewater. The SRB relative abundance was higher

than 35% in Cat-PIV. These SRB were mainly *Desulfovibrio* sp. (17.0%) and *Paludibacter* sp. (18.5%). The SOB relative abundance was higher than 20%: *Thiomonas* sp. (10.4%), *Acidithiobacillus* sp. (6.0%) and *Halothiobacillus* sp. (4.0%). In this case, the real wastewater boosted again the presence of *Halothiobacillus* sp. as in Sup-PIV. In addition, the relative abundance of *Acetobacterium* sp. decreased down to 3.3%, maybe due to the real wastewater composition which could inhibit *Acetobacterium* sp. growth, but in any case it was not a problem since *Acetobacterium* sp. is a H_2 scavenger. However, the decrease of the *Acetobacterium* sp. relative abundance could provoke the decrease of *Desulfomicrobium* sp. which was not present in any sample after period IV.

The relative abundance and role of the main genera involved in the system during the different operational periods are summarized in Table 6.4. In general terms, the change of the synthetic wastewater for the real one led to a decrease of the relative abundance of SRB and an increase of SOB in all the microbial communities studied. This could explain the decrease of SRR in periods III and IV. In addition, the real FGD systems effluent benefitted the growth of other SOB genus such as *Halothiobacillus* sp. and *Acidthiobacillus* sp. because the presence of many new compounds in low concentrations makes a much more complex scenario leading to the development of many new species playing a role in our system, which caused that higher amount of elemental sulfur could be recovered. This fact could also explain the reason why in period IV higher amount of elemental sulfur could be recovered compared with period III.

Table 6.4. Summary of relative abundance and roles of the main genera involved in the system.

Genus	Ino	Sup-PII	Mem-PII	Cat-PII	Sup-PIV	Mem-PIV	Cat-PIV	Role
Desulfovibrio sp.	3.1%	49.7%	34.1%	25.8%	17.3%	1.7%	17.0%	Mixotrophic sulfate reducing bacteria
Paludibacter sp.	<1%	<1%	<1%	16.4%	13.1%	<1%	18.5%	Sulfate reducing bacteria acidophilic
Desulfomicrobium sp.	3.7%	6.6%	1.3%	5.9%	<1%	<1%	1.0%	Heterotrophic sulfate reducing bacteria
Sulfurospirillum sp.	<1%	1.3%	11.9%	<1%	7.0%	<1%	<1%	Mixotrophic sulfur reducing bacteria
Thiomonas sp.	1.9%	3.3%	27.2%	5.5%	13.0%	14.2%	10.4%	Sulfide and sulfur oxidizing bacteria
Acidithiobacillus sp.	<1%	<1%	<1%	2.6%	3.0 %	62.9%	6.0%	Sulfide and sulfur oxidizing bacteria acidophilic
Halothiobacillus sp.	4.3%	<1%	<1%	1.8%	29.3%	1.5%	4.0%	Sulfide and sulfur oxidizing bacteria halotolerant

6.4. Conclusions

This work shows, for the first time, the effect of real wastewater from a FGD system on sulfate removal and elemental sulfur recovery using a two-chamber BES. Moreover, this study describes the influence of this real wastewater to the different microbial populations grown as biofilm and in suspension.

The sulfate removal rate decreases from 93 ± 33 mg SO_4^{2-}-S L^{-1} d^{-1} using synthetic wastewater to 73 ± 27 mg SO_4^{2-}-S L^{-1} d^{-1} using real FGD wastewater at similar conductivities. This could be due to inhibition caused by the real FGD wastewater since the current increased from 5.69 ± 1.64 A m^{-2} with the synthetic wastewater to 6.55 ± 0.91 A m^{-2} with the real one, which means higher amount of electron donor, then higher SRR would be expected.

The balance of all sulfur species was calculated at the end of the cycles and similar elemental sulfur amount was supposed to be produced. However, elemental sulfur was almost not recovered using synthetic wastewater and a 64% of elemental sulfur was recovered using real FGD wastewater respect to the theoretical elemental sulfur produced with a purity of 71.8 ± 13.0%.

The microbial population was studied with the synthetic wastewater and the real one taking samples from the membrane and cathode biofilm and from the supernatant. The results show that sulfate reducing bacteria (mainly *Desulfovibrio* sp.) and sulfide oxidizing bacteria (mainly *Thiomonas* sp.) grow with both wastewaters but more SOB appear with the real one. In addition, *Halothiobacillus* sp. proliferated due to a higher complexity of the real FGD wastewater. However, the higher amount of SOB can be found in the biofilm grown on the membrane because of oxygen diffusion from the anode through the membrane.

Chapter 7

Recovery of elemental sulfur with a novel integrated bioelectrochemical system with an electrochemical cell

The motivation of this chapter consisted in studying another configuration aiming at improving elemental sulfur production. The use of an electrochemical cell for sulfide oxidation was previously studied, but this process was not coupled in a single reactor with a BES to treat sulfate and recover elemental sulfur simultaneously. This chapter studies several conditions such as different cathode potentials and different current densities. In addition, the chapter discusses the drawbacks and benefits of this new configuration. The experimental part of this chapter was performed in the AWMC laboratories ofthe University of Queensland.

Abstract

This work proposes a new reactor configuration named BES-EC, consisting of the coupling of a BES with an electrochemical cell (EC), to treat high sulfate content wastewater and recover elemental sulfur. The reactor consisted of four electrodes: an abiotic anode and a biocathode of the BES for the autotrophic sulfate reduction and an anode of an electrochemical cell (EC) for the partial oxidation of sulfide to elemental sulfur (the cathode of the BES and the anode of the EC were placed in the same chamber) with its abiotic cathode. The results showed a high sulfate removal rate (up to 888 mg SO_4^{2-}-S L^{-1} d^{-1} at -0.9 V vs. SHE with a specific energy consumption of 9.18 ± 0.80 kWh kg^{-1} SO_4^{2-}-S). Exceptionally high theoretical elemental sulfur production rates (up to 498 mg S^0-S L^{-1} d^{-1}) were achieved with the EC controlled at a current density of 2.5 A m^{-2}. In addition, short experiments were performed at different current densities, observing that at higher current the sulfate removal did not proportionally increase according to the density applied. However, when the BES was controlled at 30 A m^{-2} and the EC at 7.5 A m^{-2}, the proportion of elemental sulfur produced corresponded to 92.9 ± 1.9% of all sulfate removed.

7.1. Introduction

Autotrophic sulfate reduction in a biocathode has been studied by several authors (Blázquez et al., 2016, 2017; Coma et al., 2013; Luo et al., 2014; Pozo et al., 2017a, 2016, 2015; Su et al., 2012; Wang et al., 2017c) because the *in-situ* production of hydrogen increases its bioavailability for sulfate reduction by SRB. In addition, several strains of *Desulfovibrio* sp. have been reported to have capability to directly exchange electrons with the cathode (Cordas et al., 2008) because of the high amount of hydrogenase observed on electrode surfaces of reactors with high abundance of *Desulfovibrio* sp. (Marshall et al., 2017), which increases the electroactivity of the biocathode (Aulenta et al., 2012). However, the main product of this reductive process is hydrogen sulfide, which requires another oxidative step to produce recoverable S^0. The recovery of S^0 as a nutrient should be taken into account in order to increase the revenue of the system as has been discussed previously in the case of nitrogen (Ledezma et al., 2015).

Sulfide oxidation in a biocathode has been observed and attributed to oxygen diffusion produced by water electrolysis from the anode chamber across the ion-exchange membrane (Blázquez et al., 2016), however this diffusion cannot be efficiently controlled to match the sulfide production rate, leading to accumulation of sulfide (if diffusion is too low) or re-formation of sulfate (if diffusion is too high). As an alternative, other previous works have instead focused on the spontaneous oxidation of sulfide in an anode (Dutta et al., 2008) and its biological improvement was also studied (Gong et al., 2013; Pham et al., 2008; Rabaey et al., 2006; Sun et al., 2009). Other investigators aimed to reduce sulfate to sulfide and oxidize sulfide to elemental sulfur in an anode (Chatterjee et al., 2017; Lee et al., 2014; Zhao et al., 2008). However, external organic matter supply was required. In these reactors, anode respiring bacteria would rather use elemental sulfur as electron acceptor than the anode, decreasing accordingly the elemental sulfur production (Dutta et al., 2009a). More recently, Pozo et al. (2017b) attempted to treat sulfate-rich acid mine drainage and recover S^0 and metals using two different bio/electrochemical reactors. The process configuration consisted of two independent cells, a BES with biocathode to reduce sulfate to sulfide and an electrochemical cell with an anode to oxidize sulfide to elemental sulfur. However, the system exhibited a relatively low

S^0 recovery and could not be operated for long-term due to competing ion-migration (Brewster et al., 2018). In addition, the use of two reactors increase the cost of the system, and the reactor cost had been estimated to be the 16% of the whole cost of the BES in a future (R. A. Rozendal et al., 2008).

Accordingly, the aim of this study was to demonstrate the possibility of simultaneous sulfate removal and elemental sulfur recovery in a single integrated reactor. The feasibility of integrating two electrochemical systems in the same chamber of one reactor was also tested for the first time: a biological system for the complete sulfate reduction and an abiotic system for the partial sulfide oxidation to elemental sulfur. This configuration allows the use of the electrons in the cathode for the reduction of sulfate avoiding the external electron donor supply and the straight production of elemental sulfur in the same chamber of one reactor. In addition, several operational conditions were tested to compare and improve sulfate removal and elemental sulfur production.

7.2. Experimental

7.2.1. Biocathode inoculation

The BES-EC reactor (Figure 3.4) was used to grow the biofilm in a previous start-up period. Carbon fiber felt of 19 * 4 * 0.25 cm (Beijing Evergrow Resources, China) was used instead of graphite granules as biocathode of the BES. This reactor was inoculated with biomass from a previous reactor containing *Desulfovibrio* sp. (Pozo et al., 2017a). The growth process lasted 66 days with the cathode potential controlled chronoamperometrically using a VMP-3 potentiostat/galvanostat (Bio-Logic, France) and was divided in three periods: *i*) a first period of 11 days without mineral medium replacement and with the cathode potential poised at -1.0 V vs. SHE, *ii*) a second stage of 14 days with continuous catholyte replacement at a HRT of 1.9 days with same applied potential and *iii*) a final 41 day phase with the same latter conditions, but with a cathode potential of -0.9 V vs. SHE because of excess of H_2 produced that was not consumed at -1.0 V vs. SHE. Recirculation at 125 mL min^{-1} was used in the cathode to ensure sufficient mixing during all experiments. The pH was not controlled during the start-up process.

Cyclic voltammetry (CV) was used in order to assess the biocathode electroactivity. Four CVs were undertaken from -0.2 to -1.2 V vs. SHE at a scan rate of 1 mV s^{-1} for 3 cycles at different days of operation, one before the inoculation (day 0; as blank) and 3 post-inoculation at days 20, 42 and 59. All CVs where performed at pH 7.3 adjusted with 1 M HCl. Moreover, the chronoamperometry was stopped 30 minutes before in order to stabilise the open circuit voltage (OCV) before the CV analysis. Once the biofilm was grown on the biocathode surface, the carbon fiber felt was cut and mixed with the graphite granules which acted as cathode of the BES along the rest of the study.

The anolyte of the BES consisted of 0.025M H_2SO_4. The mineral medium of the middle chamber and the catholyte of the EC consisted of 6 g L^{-1} Na_2HPO_4, 3 g L^{-1} KH_2PO_4, 0.1 g L^{-1} NH_4Cl, 0.5 g L^{-1} NaCl, 0.04 g L^{-1} $MgCl_2 \cdot 6H_2O$, 0.015 g L^{-1} $CaCl_2$, 1.5 g L^{-1} $NaHCO_3$, 2.2 g L^{-1} Na_2SO_4 and 1 mL L^{-1} of micronutrients as described by Jourdin et al. (2015).

7.2.2. Operational conditions

After the inoculation process, eight different periods were performed at different operational conditions and continuous mode over an experimental period of 9 months (Table 7.1). Changes were applied in response to the experimental observations, as explained in the Results and Discussion section.

In period I, the biocathode potential was fixed at -0.7 V vs. SHE. The mineral medium was supplied at 4.8 mL h^{-1} resulting in a HRT of 3.1 d while the pH was controlled at 7 by addition of 1 M HCl by a pH controller (Liquisys M CPM253; Endress+Hauser, Australia). During the periods II to V, the conditions in terms of cathode potential, hydraulic retention time (HRT) and sulfate concentration were changed to achieve a stable operation. The cathode potential was decreased to -0.8 and -0.9 V vs. SHE in order to increase the sulfate removal, the HRT was decreased to 1.1 d increasing the inlet flow up to 13.7 mL h^{-1} and the mineral medium was modified to increase the sulfate concentration up to 2000 mg SO_4^{2-}-S L^{-1} in the feed by adding up to 8.8 g L^{-1} of Na_2SO_4.

Table 7.1. Operational conditions in the reactor after the start-up period at each experimental period.

Period	Days of operation	Sulfate influent [mg S L^{-1}]	BES Cathode potential [V vs. SHE]	pH	HRT [d]	EC operation
I	0-17	500	-0.7	7.0	3.1	Off
II	17-24	500	-0.8	7.0	3.1	Off
III	24-45	500	-0.8	7.0	1.1	Off
IV	45-52	500	-0.9	7.0	1.1	Off
V	52-87	2000	-0.9	7.0	1.1	Off
VI	87-94	2000	-0.9	7.0	1.1	On
VII	94-145	2000	-0.95	7.5	1.1	On
VIII[1]	145-161	2000	-0.92 ± 0.01	7.5	1.1	On

[1] A flat rubber sheet was added as physical separation between biocathode of the BES and anode of the EC in order to try to avoid the effect of electron-shuttling compounds. The current of the BES and the EC were controlled at 10 A m^{-2} and 2.5 A m^{-2}, respectively.

Sulfide electrochemical oxidation to elemental sulfur in an anode was previously described to take place spontaneously generating elemental sulfur as the predominant final oxidation product (Dutta et al., 2008). For this reason, in period VI which started at day 87, the EC was switched on. The counter reaction at the cathode consisted of protons reduction to hydrogen. The anode potential of the EC was controlled at +0.3 V vs. SHE using a Wenking potentiostat (KP07; Bank Elektronik, Germany). This anode potential was chosen after performing a linear sweep voltammetry from OCV to +0.9 V vs. SHE at a scan rate of 1 mV s^{-1} at pH 7 and a concentration of total dissolved sulfide (TDS) of ~500 mg TDS L^{-1} (Figure 7.1) using a VMP-3 potentiostat/galvanostat (Bio-Logic, France). A peak corresponding to the sulfide oxidation reaction was observed at +0.05 V vs. SHE

but the anode potential was kept at +0.3 V vs. SHE to maximize sulfide oxidation and because it was far below the potential for oxygen evolution (Figure 7.1). Period VII started at day 94 with the pH controlled at 7.5 and the cathodic potential of the BES set at -0.95 V vs. SHE. Finally, period VIII started at day 145. A flat rubber sheet was placed between the biocathode of the BES and the anode of the EC in order to avoid the possible effects of electron-shuttling compounds. The current density output of the biocathode (BES cell) was controlled at 10 A m^{-2} while the anodic current density of the EC was set at 2.5 A m^{-2}. The current density of the BES was selected based on results obtained in the previous periods, whilst the current density of the EC was selected to ensure ¼ of the current of the BES as determined by the stoichiometry of the two reactions (see Eqs. 7.1 and 7.2).

$$SO_4^{2-} + 8e^- + 9H^+ \rightarrow HS^- + 4H_2O \quad \text{(Eq. 7.1)}$$

$$HS^- \rightarrow S^0 + 2e^- + H^+ \quad \text{(Eq. 7.2)}$$

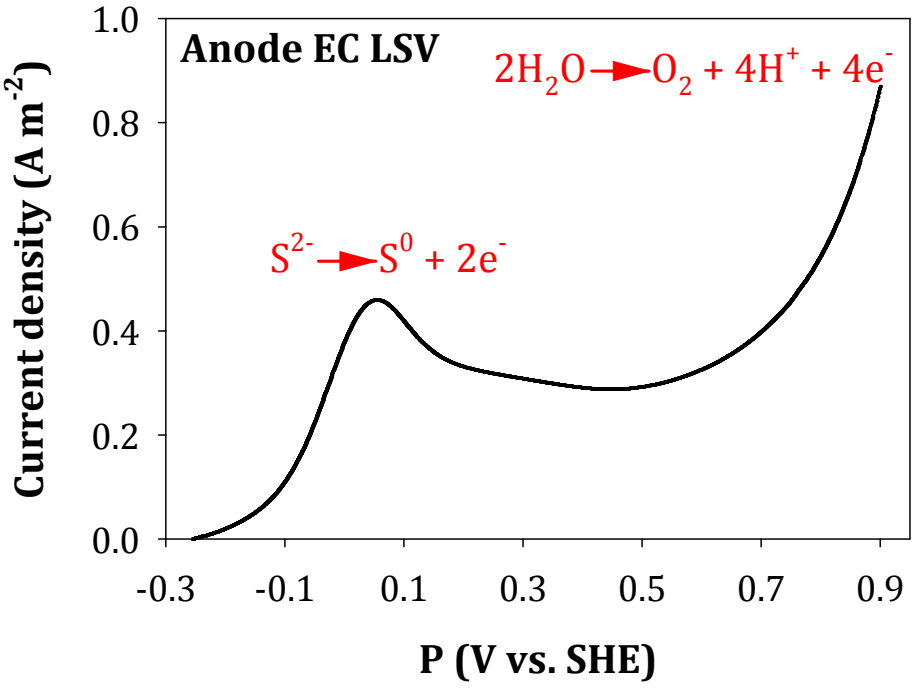

Figure 7.1. Linear Sweep Voltammetry of the EC from OCV (-0.25 V vs. SHE) to 0.9 V vs. SHE at a scan rate of 1 mV s^{-1}, pH 7 and 500 mg TDS L^{-1}.

7.2.3. BES-EC current densities controlled by galvanostat

Different current density magnitudes were tested in the same reactor using the VMP-3 galvanostat. Five periods were operated at different current densities in steps increasing by 5 A m^{-2} for the BES and 1.25 A m^{-2} the current density of the EC (Table 7.2), in accordance with current ratio 1:4 determined by the stoichiometries as previously discussed. Period A consisted of 240 hours which corresponded to the last 10 days of operation of period VIII of the last experiment. After that, the feed rate was increased to 40.1 mL h^{-1} for an HRT of 0.37 d in order to increase the sulfate loading rate (6 g SO_4^{2-}-S L^{-1} d^{-1}) because at higher currents the amount of electrons could not match with the amount of sulfate concentration in case that the electron recovery was high. Subsequently, periods B to E lasted 48 hours each. The studied current densities of the BES ranged from 10 to 30 A m^{-2} and the current densities of the EC ranged from 2.5 to 7.5 A m^{-2}. Three samples were taken from each period (from B to E) after three HRTs for each current step-change.

Table 7.2. Different current density conditions of both cells in the reactor BES-EC during the galvanostat operation.

Period	Time of operation [h]	Current density BES [A m^{-2}]	Current density EC [A m^{-2}]
A[1]	0-240	10	2.5
B	240-288	15	3.75
C	288-336	20	5
D	336-384	25	6.25
E	384-432	30	7.5

[1] This period coincided with the period VIII of the BES-EC.

7.3. Results and discussion

7.3.1. Biocathode inoculation

The BES-EC reactor was used to grow the electroactive sulfate reducing bacteria (SRB). The middle chamber was inoculated and the reactor was operated during 66 days (Figure 7.2). At the beginning of experimentation (period *i*), the mineral medium was not replaced to allow for biomass attachment onto the electrode surface. After 11 days, once the sulfate was consumed, the middle chamber was fed continuously. The average sulfate removal rate (SRR) obtained during period *ii* was 89.2 ± 31.7 mg SO_4^{2-}-S L^{-1} d^{-1} with an electron recovery of 57.0 ± 36.4%. After 14 days (period *iii*), the cathode potential of the BES was increased from -1.0 V to -0.9 V vs. SHE to maximize the electron recovery. There was an excess of H_2 produced that was not consumed in period ii. At this point, the SRR was 46.3 ± 24.8 mg SO_4^{2-}-S L^{-1} d^{-1} but the electron recovery as sulfate removed did not increase (36.8 ± 16.0%).

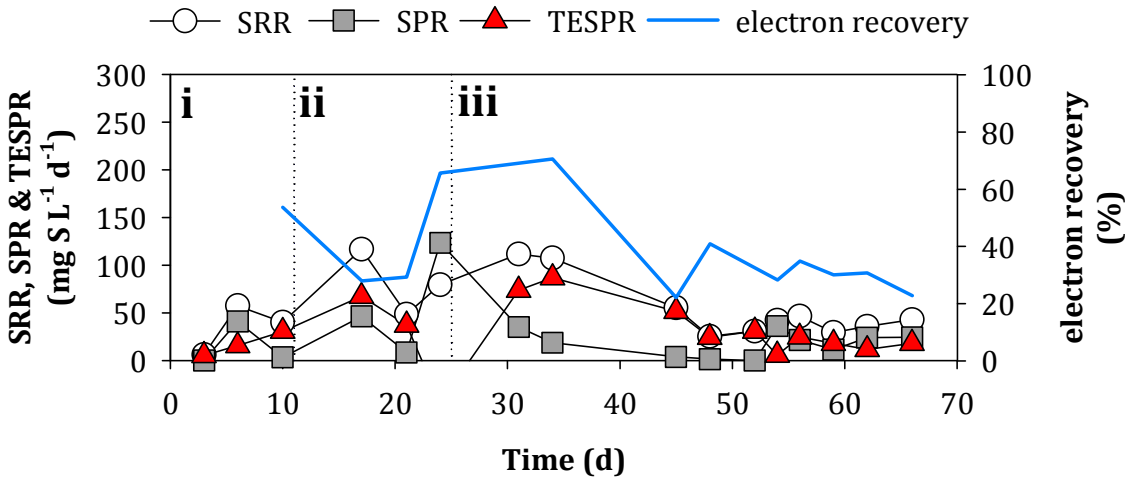

Figure7.2. Operation of the BES-EC for the start-up period.

Before inoculation a cyclic voltammetry (CV) was performed before adding the inoculum at a scan rate of 1 mV s^{-1} (day 0 in Figure 7.3) in order to characterize the electrode. After that, several CVs were performed during the inoculation period to observe the evolution of the biocathode electroactivity (Figure 7.3). The pH was not controlled during the whole start-up, for this reason pH was set to 7.3 before

each CV in order to make them repetitive between them. The CVs evolution shows how the biocathode electroactivity increased throughout the experimentation period.

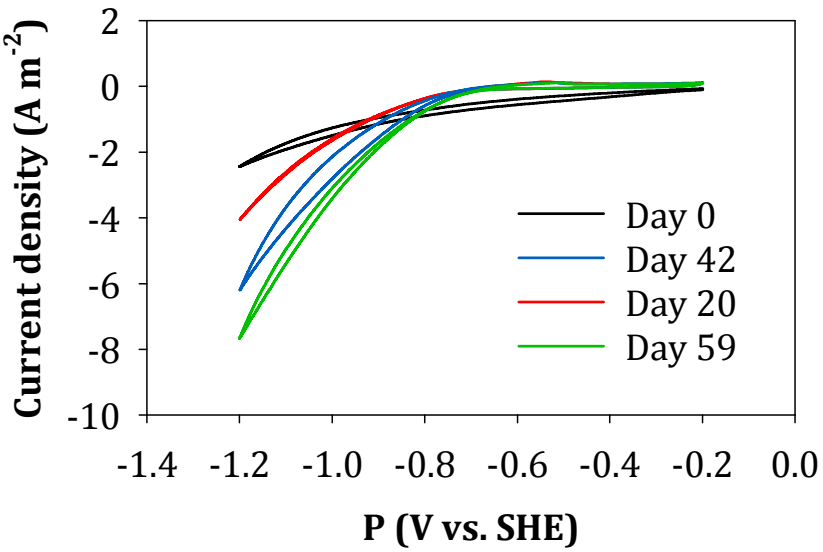

Figure 7.3. Cyclic voltammetry on abiotic carbon felt (day 0) and after 20, 42 and 59 days of operation during the start-up period. Scan rate of 1 mV s^{-1}.

7.3.2. Sulfate removal and elemental sulfur production in the autotrophic biocathode

After the inoculation process, the BES-EC reactors were operated in continuous mode for more than 160 days under different operational conditions in eight periods (from period I to V with the EC switched off and from period VI to VIII switched on) as indicated in Table 7.1. Figure 7.4 shows the concentration of the main sulfur species detected along these periods.

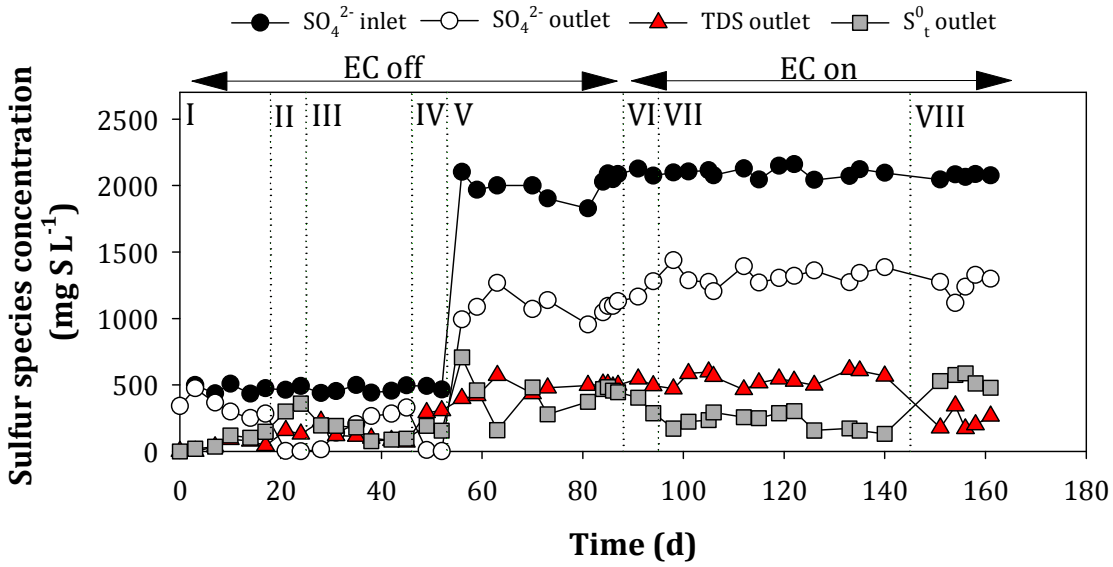

Figure 7.4. Evolution of sulfur species concentration along the BES-EC operation after the start-up period, sulfate in the inlet and outlet, total dissolved sulfide (TDS) in the outlet and theoretical elemental sulfur produced (S^0_t) in the outlet. The operational conditions of each period are explained in Table 7.1.

Figure 7.5 shows the average results on sulfate removal rate (SRR), sulfide production rate (SPR), theoretical elemental sulfur production rate (TESPR) (Figure 7.5A), elemental sulfur proportion (Figure 7.5B), current density (Figure 7.5C) and electron recovery (Figure 7.5D) for the whole operation of the BES-EC. In order to summarize these results, Figure 7.6 shows the average results of the operation with the EC switched off according to the BES cathode potential. The biocathode potential of the BES was fixed at -0.7 V vs. SHE at the beginning (period I). The sulfate was not being consumed completely with effluent concentrations around 300 mg SO_4^{2-}-S L^{-1} and a sulfate removal rate (SRR) of 46 ± 7 mg SO_4^{2-}-S L^{-1} d^{-1} (Figure 7.6A). Other authors worked at the same cathode potential in two-chamber reactors with pH controlled at 7.0 (Luo et al., 2014) and without pH control (Blázquez et al., 2017; Luo et al., 2017) but obtained much lower SRRs. In the cited studies, graphite brushes were used as cathode and tests were conducted in batch mode, which could decrease the current obtained compared with the graphite granules plus continuous operation. Moreover, no elemental sulfur production was observed in these studies meanwhile a theoretical

elemental sulfur production rate (TESPR) of 26 ± 7 mg S^0-S L^{-1} d^{-1} was observed with the BES-EC (Figure 7.6A), which means a 63.8 ± 11.7% of elemental sulfur yield from the sulfate consumed (Figure 7.6B).

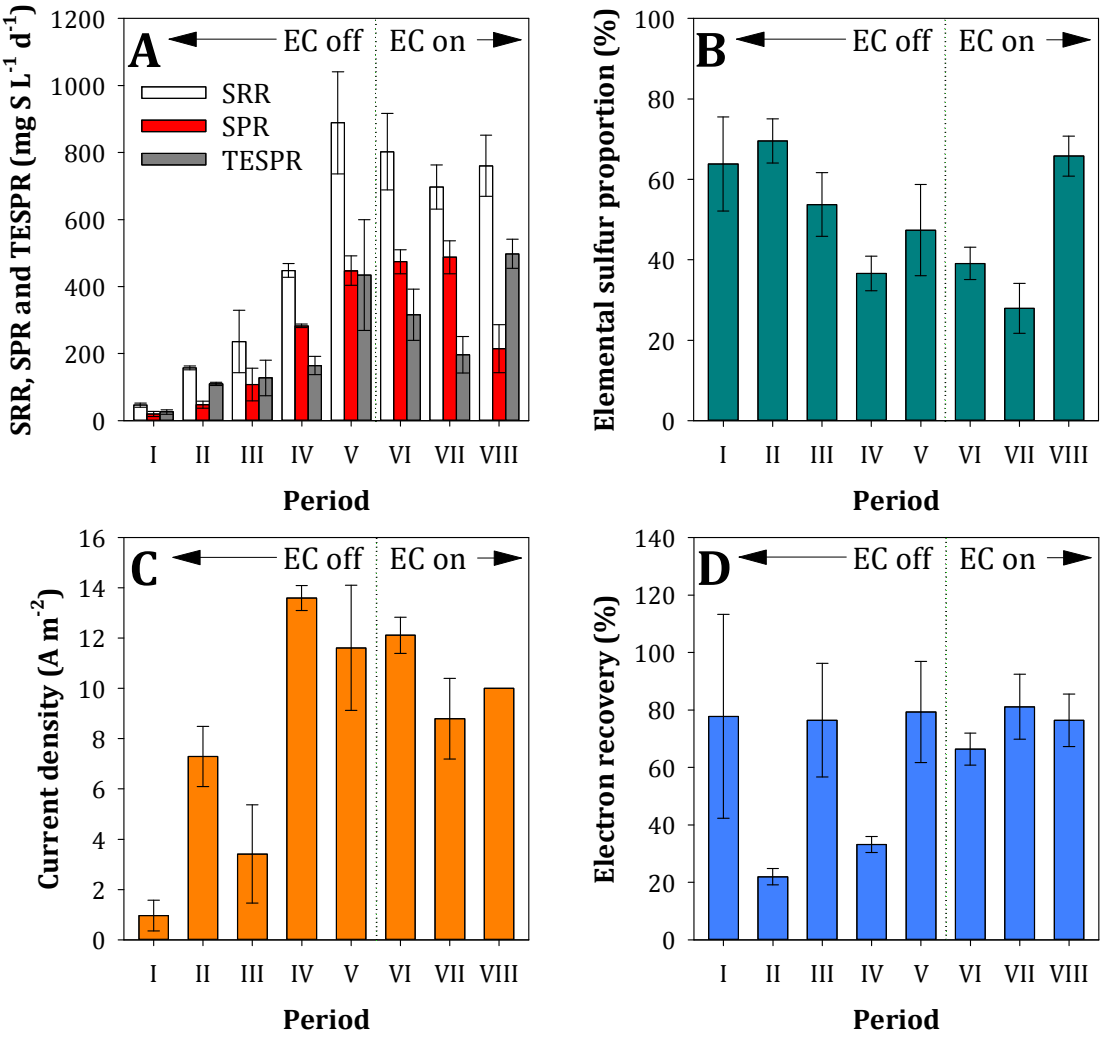

Figure 7.5. Average plots of the different operational periods of the BES-EC after the start-up on A: sulfate reduction rate (SRR) and sulfide production rate (SPR) and theoretical elemental sulfur production rate (TESPR), B: elemental sulfur proportion compared with sulfate reduced, C: current and D: electron recovery as sulfate reduced in the biocathode. The operational conditions of each period are explained in Table 7.1.

Oxygen diffusion from the anode chamber to the cathode chamber through the membrane could allow the growth of sulfide oxidizing bacteria as previously demonstrated by Blázquez et al. (2016) using the same cation exchange membrane. After 17 days, the cathode potential of the BES was decreased to -0.8 V vs. SHE in order to increase the SRR (period II), but as the sulfate was completely removed resulting in low electron recoveries –, meaning that there was H_2 excess – after 7 days the HRT was decreased down to 1.1 days. On day 24 the HRT was decreased from 3.1 days to 1.1 days in order to evaluate the maximum capacity of the system at -0.8 V vs. SHE. In period III, the SRR obtained was 236 ± 93 mg SO_4^{2-}-S L^{-1} d^{-1}, five times higher than at -0.7 V vs. SHE and the TESPR increased to 127 ± 53 mg SO_4^{2-}-S L^{-1} d^{-1} (53.8 ± 7.9% of S^0 produced from sulfate removed). This higher SRR was due to an increase of the current density from 0.96 ± 0.62 A m^{-2} in period I to 3.41 ± 1.95 A m^{-2} in period III (Figure 7.6C) with a similar electron recovery of 76.5 ± 19.7% (Figure 7.6D). Blázquez et al. (2017) also performed experiments at this cathode potential at pH 7.0 in a reactor of the same volume but in batch mode and using graphite brush as cathode. Lower SRR (147 mg SO_4^{2-}-S L^{-1} d^{-1}) and lower TESPR (91 mg S^0-S L^{-1} d^{-1}) were obtained. The higher SRR in the present work could be due to continuous mode of operation and better mass-transfer caused by the recirculation, while the higher TESPR could be due to a higher membrane surface to chamber volume: 100 cm^2 herein compared with 38.5 cm^2 in Blázquez et al. (2017). On day 45, the cathode potential of the BES was changed from -0.8 to -0.9 V vs. SHE to further enhance the SRR (period IV). As in period II, the electron recovery dropped down because all the sulfate was being consumed faster than it was being supplied, therefore after 7 days the sulfate concentration of the influent was increased in period V to 2000 mg SO_4^{2-}-S L^{-1} in order to observe the SRR capacity at -0.9 V vs. SHE. Period V started at day 52 of operation and exhibited the highest SRR observed to date in a BES with a removal rate of 888 ± 152 mg SO_4^{2-}-S L^{-1} d^{-1} at a relatively high current density (13.5 ± 0.5 A m^{-2}) and an electron recovery of 79.3 ± 17.6%, even though the sulfate concentration in the effluent was around 1000 mg SO_4^{2-}-S L^{-1}. In this period, the TESPR was of 434 ± 165 mg SO_4^{2-}-S L^{-1} d^{-1}, i.e. with an elemental sulfur production proportion of 47.4 ± 11.3% of the sulfate consumed.

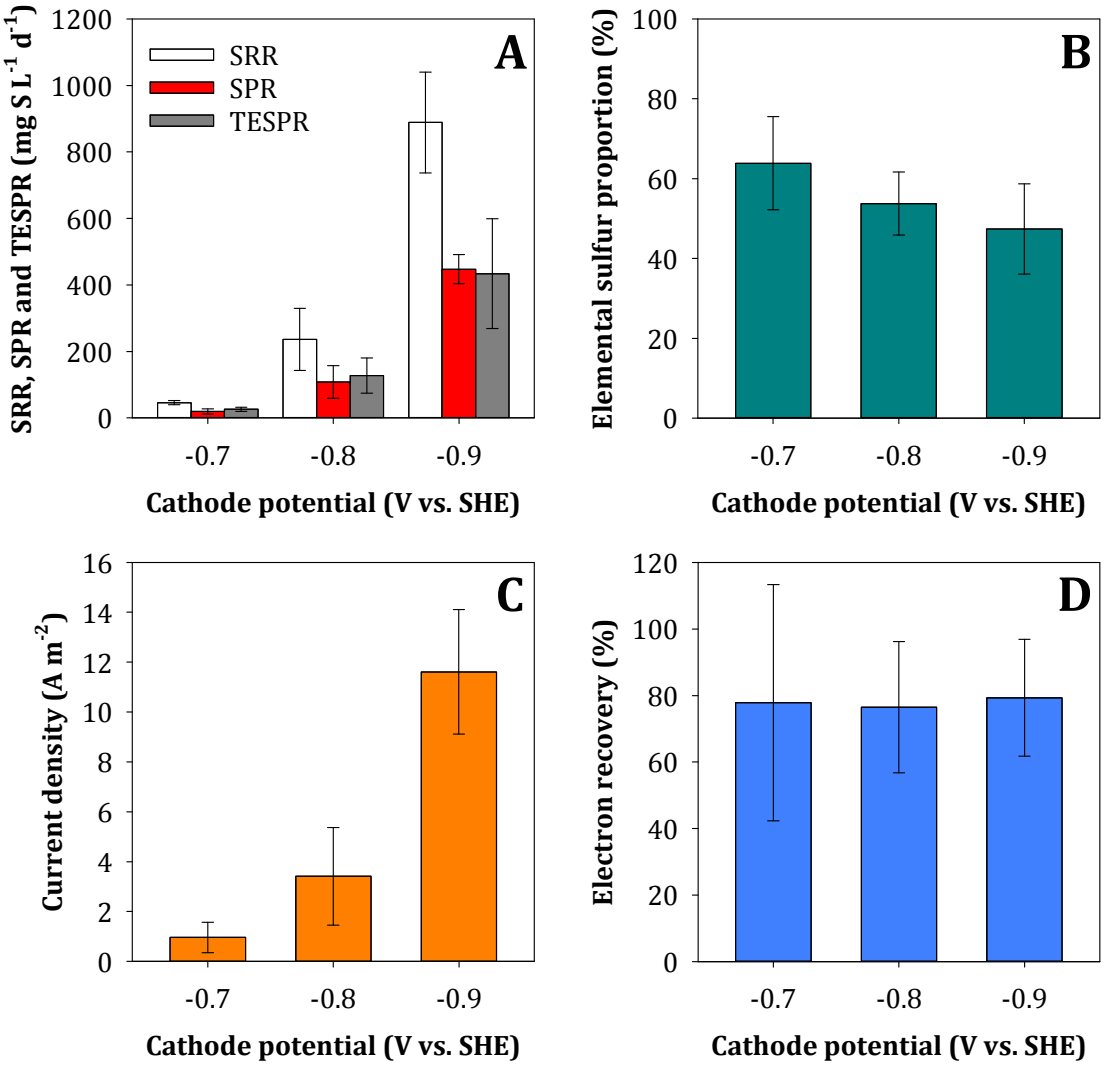

Figure 7.6. Average plots of the operational periods I, III and V at cathodes potentials of -0.7, -0.8 and -0.9 V vs. SHE respectively on A: sulfate reduction rate (SRR) and sulfide production rate (SPR) and theoretical elemental sulfur production rate (TESPR), B: elemental sulfur proportion compared with sulfate reduced, C: current and D: electron recovery as sulfate reduced in the biocathode.

No other papers have achieved this SRR at -0.9 V vs. SHE and with specific energy consumption per kilo of sulfate of 9.18 ± kWh kg^{-1} SO_4^{2-}-S. Gacitúa et al. (2018) worked with different strains of *Desulfovibrio* sp. achieving the maximum SRR of 12 mg SO_4^{2-}-S L^{-1} d^{-1}. However, the SRR was of 25.7 g SO_4^{2-}-S m^{-2} d^{-1}, a high removal per surface unit compared with the highest SRR reported until now for other authors as 36.7 g SO_4^{2-}-S m^{-2} d^{-1} (Pozo et al., 2017a), but in this case they used the

projected membrane surface area, not the real cathode area, due to the difficulty to determine the surface of the electrodes when graphite granules or graphite brushes are used. When considering the projected surface are, this study achieved a really similar SRR of 32.0 ± 5.5 g SO_4^{2-}-S m^{-2} d^{-1} in period V. Nevertheless, the real electrode surface it is not effectively comparable with the projected one, it is just an approximation. Pozo et al. (2015) also worked at -0.9 V vs. SHE in continuous mode and pH 7.3 achieving SRRs of 61 mg SO_4^{2-}-S L^{-1} d^{-1} but without elemental sulfur production. The highest SRR observed until now at -0.9 was by Blázquez et al. (2017) at 358 mg SO_4^{2-}-S L^{-1} d^{-1} and a TESPR of 221 mg S^0-S L^{-1} d^{-1}, still lower than the ones observed with our reactor in this study. Other authors studied the feasibility of the autotrophic sulfate reduction in biocathodes at lower cathode potentials. The maximum SRR observed until now was 5600 mg SO_4^{2-}-S L^{-1} d^{-1} using graphite granules at -1.1 V vs. SHE and at continuous operation in a reactor of 30 mL (Pozo et al., 2017a) but no elemental sulfur production was reported.

High SRR were observed thanks to the BES biocathode operation. However, the TESPR could be improved in order to reduce the sulfide production and increase the elemental sulfur recovery. Other studies achieved electrochemical elemental sulfur production in an anode through sulfide oxidation (Dutta et al., 2010, 2008) but in these cases they worked with a single electrochemical system because the starting contaminant was sulfide and not sulfate.

7.3.3. Microbial/electrochemical cell integration

The oxygen diffusion from the anode chamber to the cathode chamber of the BES can be responsible for the transformation of some hydrogen sulfide to elemental sulfur, but this diffusion cannot be effectively controlled and some hydrogen sulfide could remain in the solution. For this reason on day 87 (period VI) the EC was switched on, maintaining the same conditions as in period V (see details in Table 7.1) and with an anode potential at +0.3 V vs. SHE in order to boost the sulfide oxidation while avoiding water electrolysis. The anode of the EC was expected to oxidize the sulfide product of the sulfate reduction by the BES biocathode to maximize elemental sulfur production. These separate processes

(sulfate reduction in a biocathode and the sulfide oxidation in an anode) were previously described, but these processes were never integrated onto a single. Figure 7.7 shows the average results of the operation with the EC switched on (from period VI to VIII) and the last period with the EC switched off (period V) in order to compare the effect of the EC on the process. Period VII corresponds to an increase of the pH up to 7.5 and a decrease of the cathode potential down to -0.95 V vs. SHE in order to maintain a similar current density as in previous periods; and period VIII corresponds to the change of the separator by a rubber sheet, both with current densities controlled at 10 A m^{-2} in the BES and at 2.5 A m^{-2} in the EC.

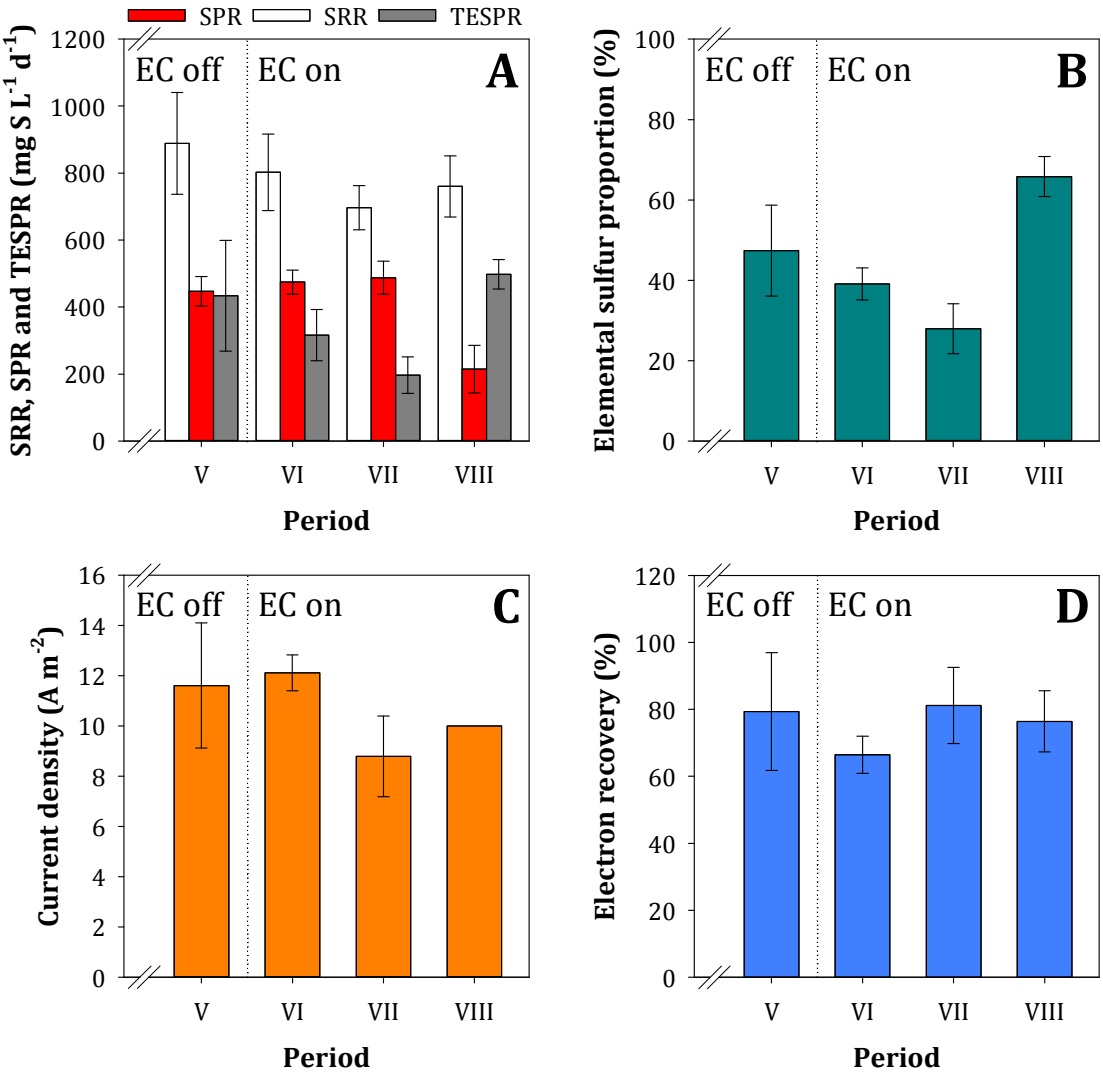

Figure 7.7. Average plots of the operational periods V (with the EC switched off), VI, VII and VII (with the EC switched on) on A: sulfate reduction rate (SRR) and sulfide production rate (SPR) and theoretical elemental sulfur production rate

(TESPR), B: elemental sulfur proportion compared with sulfate reduced, C: current and D: electron recovery as sulfate reduced in the biocathode. The operational conditions of each period are explained in Table 1.

The current density of the EC in period VI obtained was around 0.1 A m^{-2}, much lower than expected according to sulfide concentration. The current density of the EC should have been ¼ of the current density of the BES according to the stoichiometry of the reactions (Eqs. 7.1 and 7.2) but, as the electron recovery of the biocathode of the BES was not 100% and around 50% of the sulfide produced was being oxidized by oxygen diffusion across the CEM, lower current densities than the ¼ ratio were observed. The current density observed in the BES was 12.1 ± 0.7 A m^{-2} (Figure 7.7C) and the electron recovery was 66.4 ± 5.5% (Figure 7.7D). Therefore, the expected current density in the EC was around 1 A m^{-2}, however, only 0.1 A m^{-2} was observed, resulting in negligible sulfide oxidation in the EC-anode.

On day 94 (period VII), the pH control point was changed to 7.5. In the pH range of 6 – 8, there is a coexistence of H_2S and HS^-. At pH=7, the fractions are 50% - 50% based on first proton acidity constant: pKa = 7 for H_2S (Moosa and Harrison, 2006). At pH 7.5, 70% of the total S is in HS^- form, which is the charged sulfide species that can act as electron donor using the anode as electron acceptor. Moreover, pH 7.5 also lays in the optimum pH range for SRB growth, which is between 6 and 8 (Hao et al., 1996). The only drawback of this pH increase is the fact that the current drops at higher pH in the cathode (according to the Nernst equation). For this reason, the cathodic potential of the BES was decreased down to -0.95 V vs. SHE in order to maintain a similar current as in periods VI and V. Nevertheless, the current density still decreased slightly to 8.8 ± 1.6 A m^{-2} in period VII. The SRR observed in this period was of 697 ± 66 mg SO_4^{2-}-S L^{-1} d^{-1} (Figure 4A). This SRR in period VII was lower than in period V (where the EC was switched off) probably due to the lower current since the electron recovery was almost the same or even a little higher (81.2 ± 11.3%). However, the effect of the EC was not appreciable despite of increasing the current density to 0.2 – 0.3 A m^{-2} with the change of the pH. The sulfide production rate (SPR) observed was the highest of the whole operation, achieving a SPR of 485 ± 49 mg TDS-S L^{-1} d^{-1}. This means that the TESPR

was as low as 197 ± 54 mg S^0-S L^{-1} d^{-1} with a proportion of elemental sulfur of 28.0 ± 6.2% *versus* sulfate reduced (Figure 4B), the lowest of the whole operation.

The worse performance of the system when the EC was switched on was unexpected. We hypothesized that the reason was the presence of electron-shuttling compounds (such as secreted redox compounds) which are redox mediators that can reversibly be oxidized and reduced (Watanabe et al., 2009). As both electrodes were placed immediately adjacent, these redox mediators could have been repeatedly reduced and oxidized by the electrodes and/or by the microorganisms, establishing a set of redundant reaction(s) that significantly reduced and/or affected the sulfide oxidation rate. In order to test this hypothesis, on day 145 (period VIII), the plastic separator mesh between both electrodes was replaced by a rubber sheet of same dimensions, separating the electrodes completely and the recirculation was adjusted in order to have both electrode chambers properly mixed. Nevertheless, a fluidic connection remained, with the outlet of the biocathode compartment of the BES connected to the anode compartment of the EC by overflow (controlled by feed rate). Moreover, the current was kept constant by changing the potentiostat mode to galvanostat in both electrodes. The current density of the BES was controlled at 10 A m^{-2} and the current density of the EC at 2.5 A m^{-2} in order to force the ¼ stoichiometrical ratio of the reactions (Eqs. 1 and 2). The biocathode potential of the BES was -0.92 ± 0.01 V vs. SHE during this period. To maintain a constant current density of 2.5 A m^{-2} in the EC, the anode potential increased up to 0.70 ± 0.05 V vs. SHE. In this last period, the SRR achieved was 760 ± 91 mg SO_4^{2-}-S L^{-1} d^{-1} and the TESPR was 498 ± 66 mg S^0-S L^{-1} d^{-1}, the maximum TESPR achieved in all the experiments hereby presented. In this sense, the elemental sulfur proportion obtained was 65.8 ± 5.0% compared with the sulfate removed. In addition, the electron recovery was 76.4 ± 9.2%, which was a little bit lower than in previous periods.

Other studies had tried to produce elemental sulfur and energy from sulfate in a sole compartment of a microbial fuel cell (MFC). These studies were performed in single-chamber MFCs with air cathodes (Zhao et al., 2008) and in double-chamber MFCs (Chatterjee et al., 2017; Lee et al., 2014) achieving elemental sulfur recoveries up to 72%. However, an external supply of organic matter was required

as electron donor for sulfate reduction due to the lack of electron donor(s) (Liamleam and Annachhatre, 2007). Lactate and acetate were used, which could increase the operational cost. The use of autotrophic biocathodes in order to reduce sulfate allows for the treatment of these kinds of wastewaters because the electrons and/or hydrogen can be taken directly by the biofilm. Pozo et al. (2017b) first attempted to use two different cells in order to remove sulfate and recover elemental sulfur and metals (because the feed was sulfate-rich acid mine drainage, AMD). The SRR that was achieved in that system was 946 ± 18 mg SO_4^{2-}-S L^{-1} d^{-1} at a cathode potential of -1.1 V vs. SHE, and the sulfide oxidizing rate (which could be assumed to be the TESPR) in the electrochemical cell was 324 ± 20 mg TDS-S L^{-1} d^{-1}. The BES-EC configuration hereby presented allows for the treatment of AMD and other sulfate-rich wastewaters if it is fed in the EC cathodic chamber and, according to the results obtained, it could have significantly higher the SRR and the TESPR, increasing the techno-economic viability of the proposed process according to the estimated cost of the reactor (R. A. Rozendal et al., 2008) which was estimated to be the 16% in a future. In addition, the results obtained show that BES-EC configuration can achieve similar SRR at -0.9 V vs. SHE than the SRR at -1.1 V vs. SHE achieved by Pozo et al. (2017b), which means lower specific energy consumption (9.18 kWh kg^{-1} SO_4^{2-}-S *versus* of 10 kWh kg^{-1} SO_4^{2-}-S), and higher production rates of elemental sulfur, decreasing the amount of sulfide remaining in the effluent. However, the energy consumption obtained with the EC switched on in terms of kg of elemental sulfur produced was 18.74 ± 1.81 kWh kg^{-1} S^0-S.

7.3.4. BES-EC feasibility at higher current densities

The galvanostat mode (controlling the BES and EC current densities) increased the TESPR. Hence, we tested the effect of applying higher current densities to the BES-EC but always maintaining the ¼ ratio and following the steps shown in Table 7.2. The sulfur species concentration and the currents steps along time are shown in the Figure 7.8 and the average results are shown in Figure 7.9. Period A refers to the last 10 days of period VIII discussed in the previous section. Subsequently, the supply rate was increased for an HRT of 0.37 d in order to compensate for a

possible increase in SRR. However, in period B, once the current density was increased to 15 A m^{-2} in the BES and 3.75 A m^{-2} in the EC, the SRR and the TESPR did not increase as much as expected.

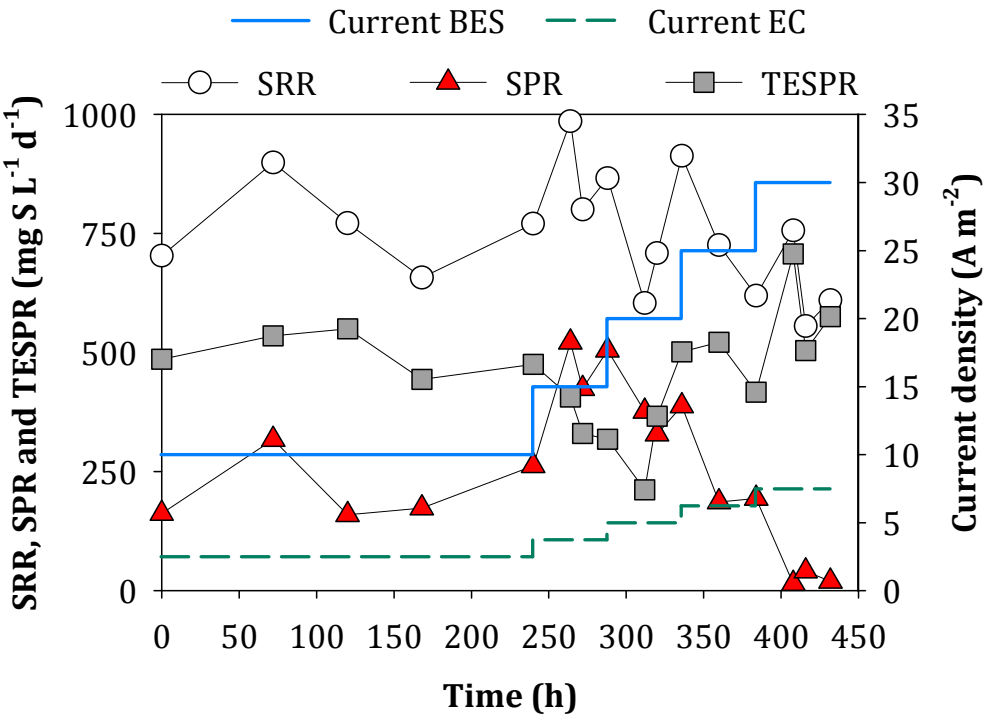

Figure 7.8. Sulfate removal rate (SRR), sulfide production rate (SPR), theoretical elemental sulfur production rate (TESPR) and different currents of BES and EC along the BES-EC operation of different currents in galvanostat mode.

The SRR achieved was 884 ± 94 mg SO_4^{2-}-S L^{-1} d^{-1} and the TESPR was 351 ± 48 mg S^0-S L^{-1} d^{-1} (Figure 7.9A). This caused the lowest elemental sulfur proportion of the whole periods of this experiment (39.7 ± 2.6%, Figure 7.9B) and a decrease of the electron recovery down to 59.2 ± 6.3% (Figure 7.9C).

48 h later the current density in the BES was increased to 20 A m^{-2} and in the EC to 5 A m^{-2} (period C). The SRR decreased instead of increasing achieving 742 ± 157 mg SO_4^{2-}-S L^{-1} d^{-1} and the TESPR was 359 ± 145 mg S^0-S L^{-1} d^{-1}. The elemental sulfur proportion increased up to 47.2 ± 10.7%, but the electron recovery decreased down to 37.3 ± 7.9%. In period D, when the current densities were increased to 25 A m^{-2} in the BES and 6.25 A m^{-2} in the EC the same behavior

was observed, a slightly decrease of SRR (672 ± 75 mg SO_4^{2-}-S L^{-1} d^{-1}), an increase of the TESPR (469 ± 74 mg S^0-S L^{-1} d^{-1}) which meant an increase of the sulfur proportion up to 69.6 ± 3.3% and a decrease of the electron recovery down to 27.0 ± 3.0%. In the last experimental phase (period E), when the current density was increased up to 30 A m^{-2} in the BES and 7.5 A m^{-2} in the EC, the SRR decreased also to 640 ± 104 mg SO_4^{2-}-S L^{-1} d^{-1} but the SPR was really low achieving a result of 25 ± 14 mg TDS-S L^{-1} d^{-1}. This meant a TESPR of 595 ± 103 mg S^0-S L^{-1} d^{-1}, which meant that the elemental sulfur produced proportion compared with the sulfate removed was of 92.9 ± 1.9%, the highest obtained in the whole study. However the electron recovery decreased down to 21.4 ± 3.5%. The biofilm possibly could not achieve higher SRR with these short periods of 48 h which led to an excess of hydrogen production in the cathode of the BES. In addition, as the current of the EC was also being increased and the sulfate was not completely reduced, the anode possibly produced enough oxygen to fully oxidize sulfide or elemental sulfur to sulfate again, given that the SRR did not increase after each step. The high elemental sulfur production is nevertheless a very favorable result when compared with the recoveries of systems which reduced sulfate using acetate and lactate (Chatterjee et al., 2017; Lee et al., 2014), but the low electron recovery shows a significant inefficiency in the direct use of electrical energy for sulfate removal. In addition, at 7.5 A m^{-2} in the EC the anode potential increased up to +2 V vs. SHE and operated unstably with some peaks up to +6 V vs. SHE. This could be due to RVC oxidation at this current. At current densities lower than 7.5 A m^{-2}, the anode potentials were never above +1 V vs. SHE. According to the overall results, at higher current densities the SRR decreased causing a drop in electron recovery, but the TESPR increases. Accordingly, the best conditions for the sulfate treatment were the current densities of 10 A m^{-2} in the BES and 2.5 A m^{-2} in the EC. But if the main target were elemental sulfur recovery, the best conditions of current densities were 30 A m^{-2} in the BES and 7.5 A m^{-2} in the EC. However, the issue of excess sulfide oxidation in the anode of the EC requires further investigation by *e.g.* increasing the surface of the electrode or changing it for an improved material, which could allow for higher current densities without oxygen evolution nor electrode corrosion (*e.g.* dimensionally-stable electrodes such as boron-doped diamond).

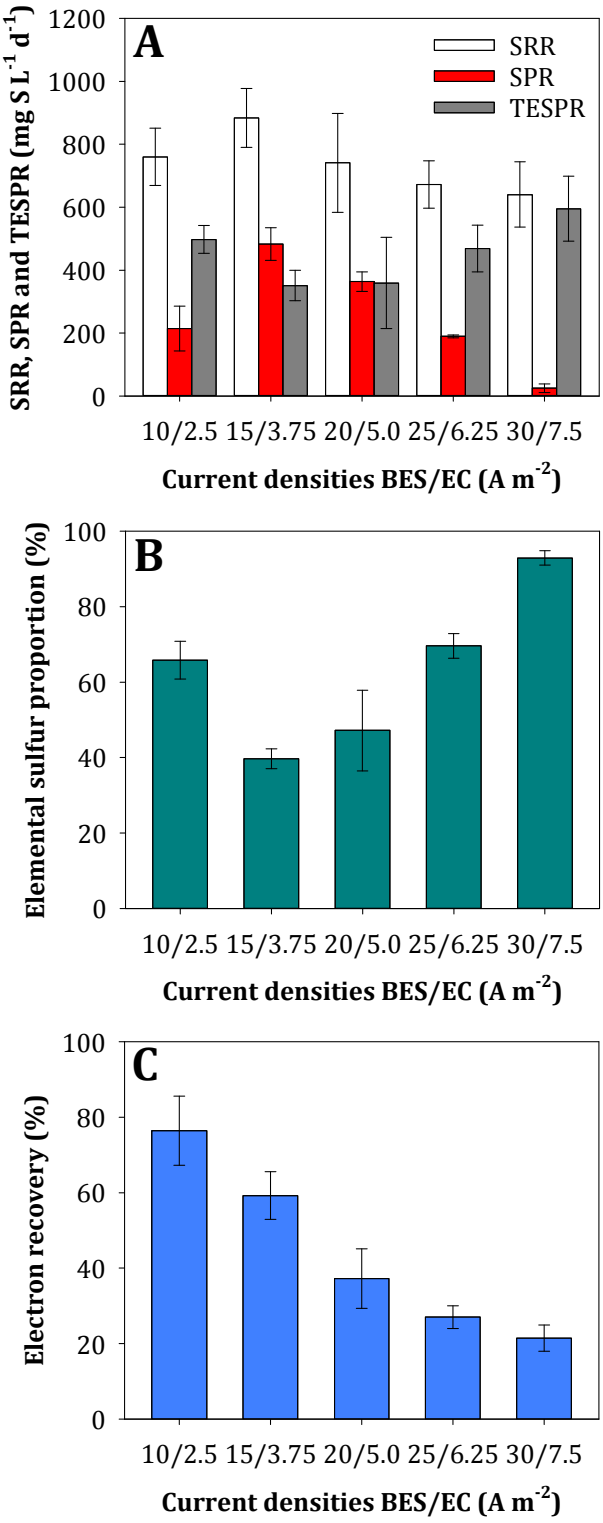

Figure 7.9. Average plots of the different periods in the study of the feasibility of higher current in the BES-EC on A: sulfate reduction rate (SRR) and sulfide production rate (SPR) and theoretical elemental sulfur production rate (TESPR), B: elemental sulfur proportion compared with sulfate reduced and C: electron recovery as sulfate reduced in the biocathode.

7.4. Conclusions

The study shows the capability of the BES-EC to treat synthetic wastewater with high sulfate content. High sulfate removal rates of up to 888 mg SO_4^{2-}-S L^{-1} d^{-1} at -0.9 V vs. SHE were achieved with the BES biocathode when the electrochemical cell was switched off, the highest SRR observed at this cathode potential to date with a specific energy consumption of 9.18 ± 0.80 kWh kg^{-1} SO_4^{2-}-S. Moreover, the configuration of the bioelectrochemical system coupled to an electrochemical cell in a single reactor was studied for the first time, achieving a high recovery of elemental sulfur (up to 498 mg S^0-S L^{-1} d^{-1}) corresponding to 66% recovery efficiency with the EC switched on. A decrease of the electron recovery was observed when higher currents densities were studied in galvanostatic mode, probably caused by the redundant complete oxidation of sulfide to sulfate or because of excess hydrogen production. For this reason, in terms of sulfate removal the best current densities observed with the BES-EC reactor were 10 A m^{-2} in the BES and 7.5 A m^{-2} in the EC. However, when the BES was operated at 30 A m^{-2} and the EC at 7.5 A m^{-2}, the efficiency of elemental sulfur produced was 92.9 ± 1.9%, but at the expense of lower electron recovery.

Chapter 8

Effect of an air-cathode in an integrated bioelectrochemical system for sulfate treatment, sulfide abatement and elemental sulfur recovery

The motivation of this chapter consisted in studying another configuration aiming at improving elemental sulfur production. The use of a fuel cell for sulfide anodic oxidation was previously demonstrated to be spontaneous allowing the reduction of the energy expenses for sulfur recovery, but this process has not coupled yet in a single reactor with a BES in order to treat sulfate simultaneously. This chapter studies the integration of a fuel cell with air-cathode to a bioelectrochemical system with biocathode for sulfate reduction. It also studies several operational conditions and the effect of the extra entrance of oxygen through the air-cathode. In addition, the chapter discusses the drawbacks and benefits of this new configuration. The experimental part of this chapter was performed in the AWMC laboratories of the University of Queensland.

Abstract

This study proposes a novel configuration of a BES (for sulfate reduction at the cathode) coupled with a fuel cell (FC) with air-cathode in order to improve the elemental sulfur production. High sulfate removal rates (up to 768 mg SO_4^{2-}-S L^{-1} d^{-1} at -0.9 V vs. SHE) were achieved. In addition, an elemental sulfur production rate of up to 386 mg S^0-S L^{-1} d^{-1} was achieved. A maximum of 65% of the sulfate removed was recovered as elemental sulfur using the oxygen diffused through the air-cathode and the fuel cell operation. This improvement compared with the use of an electrochemical cell is translated into a 12% lower energy consumption per kg of sulfur produced (16.50 ± 0.19 kWh kg^{-1} S^0-S).

8.1. Introduction

There is a wide range of studies involving S-species and BES (Blázquez et al., 2019b) as, for example, anodic sulfide oxidation (Dutta et al., 2010; Gong et al., 2013; Rabaey et al., 2006; Sun et al., 2010, 2009; Zhao et al., 2008) obtaining elemental sulfur as the predominant oxidation product. Complete heterotrophic sulfate reduction and partial sulfide anodic oxidation to sulfur in a single reactor (Chatterjee et al., 2017; Lee et al., 2014) has also been reported at expenses of external organic matter supply. Pozo et al. (2017b) achieved autotrophic sulfate reduction in a biocathode and subsequent elemental sulfur production from sulfide in a two-cell configuration where the anodic sulfide oxidation was conducted in an electrochemical cell.

In *Chapter 7*, an electrochemical cell (EC) was integrated into a BES in order to reduce the energy losses and to improve the elemental sulfur production with a chamber containing both the biocathode for sulfate reduction and the anode for sulfide oxidation. Good elemental sulfur production (up to 93% of sulfate reduced converted into elemental sulfur) was observed when the current of the EC was controlled at 7.5 A m^{-2}, but at expenses of low electron recoveries. However, the power density expenses for elemental sulfur production could be reduced by using a fuel cell in a new configuration according to the work of Dutta et al. (2008), who demonstrated that sulfide could be spontaneously oxidized in an anode of a MFC producing elemental sulfur as predominant final oxidation product.

The aim of this study was to integrate a BES for autotrophic sulfate reduction with an air-cathode fuel cell for anodic elemental sulfur recovery in a unique reactor configuration in view of reducing energy requirements. Studying the effect of the extra oxygen coming through the air-cathode and reducing the energy consumption per kg of sulfur produced were the main targets of this work.

8.2. Experimental

8.2.1. Operational conditions

The system was inoculated with biomass from a previous reactor containing *Desulfovibrio* sp. (Pozo et al., 2017a) and was enriched as described in *Chapter 7*.

The anolyte of the BES consisted of 0.025 M H_2SO_4. The reactor used in this chapter consisted of the BES-FC (Figure 3.5). The mineral medium of the middle (biocathode) chamber simulated a high-sulfate content wastewater and consisted of 6 g L^{-1} Na_2HPO_4, 3 g L^{-1} KH_2PO_4, 0.1 g L^{-1} NH_4Cl, 0.5 g L^{-1} NaCl, 0.04 g L^{-1} $MgCl_2 \cdot 6H_2O$, 0.015 g L^{-1} $CaCl_2$, 1.5 g L^{-1} $NaHCO_3$, 2.2 g L^{-1} Na_2SO_4 and 1 mL L^{-1} of micronutrients as described by Jourdin et al. (2015). The operation was conducted at room temperature (22 ± 2 ºC). The chambers were recirculated at 125 mL min^{-1} in order to guarantee a proper mix.

Table 8.1. Operational conditions in each experimental period.

Period	Days of operation	Sulfate influent [mg S L^{-1}]	BES cathode potential [V vs. SHE]	pH	HRT [d]	FC operation
I	0-17	500	-0.7	7.0	3.1	Off
II	17-24	500	-0.8	7.0	3.1	Off
III	24-45	500	-0.8	7.0	1.1	Off
IV	45-52	500	-0.9	7.0	1.1	Off
V	52-87	2000	-0.9	7.0	1.1	Off
VI	87-94	2000	-0.9	7.0	1.1	On
VII[1]	94-145	2000	-0.95	7.5	1.1	On
VIII[2]	145-161	2000	-0.98 ± 0.01	7.5	1.1	On

[1] Air-cathode of the FC replacement.

[2] A piece of rubber was added as physical separation between biocathode and anode. The current density of the BES started to be controlled at 10 A m^{-2}.

After the inoculation, eight different periods were studied at different operational conditions (Table 8.1) of sulfate load, BES-cathode potential, pH and operation of the fuel cell (FC). Period I started with a (bio)cathodic potential of -0.7 V vs. SHE

with a hydraulic retention time (HRT) of 3.1 d (mineral medium supply at 4.8 mL h^{-1}) and controlling the pH at 7.0 by addition of 1 M HCl by a pH controller (Liquisys M CPM253; Endress+Hauser, Australia). During the periods II to V, the conditions in terms of cathode potential, HRT and sulfate concentration were changed to achieve a stable operation. The cathode potential was decreased to -0.8 and -0.9 V vs. SHE, the HRT was decreased to 1.1 d increasing the inlet flow (13.7 mL h^{-1}) in period III and changing the concentration of Na_2SO_4 in order to obtain a concentration of 2000 mg SO_4^{2-}-S L^{-1} in the feed in period V.

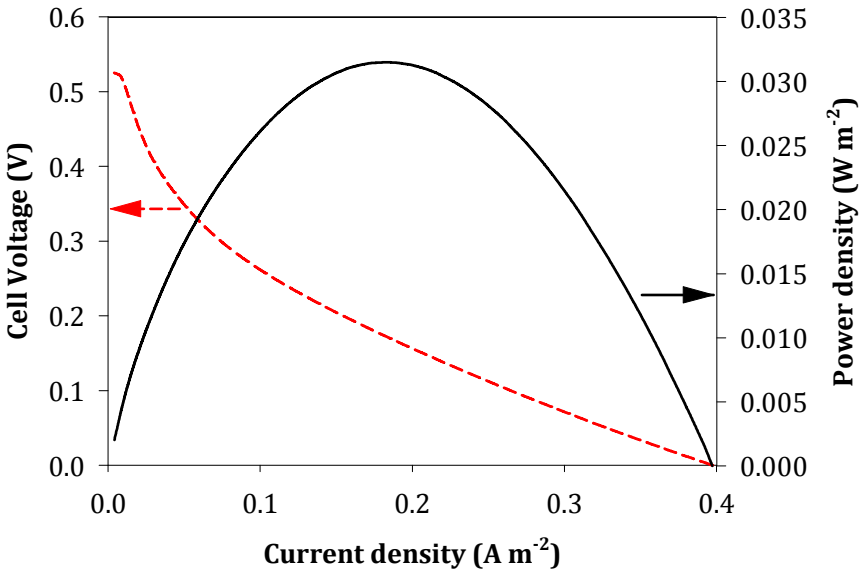

Figure 8.1. Polarization curve of the FC. Scan rate of 1 mV s^{-1}.

The FC was switched on in period VI. The external resistance used in the FC was of 95 Ω which was the optimum according to the polarization curve (Figure 8.1). The polarization curve was performed with a VMP-3 potentiostat/galvanostat (Bio-Logic, France) from the open circuit voltage to 0 V at 1 mV s^{-1} of scan rate. The current was recorded every 60 s using an Agilent 34970A data acquisition unit. Period VII started at day 94 with the pH controlled at 7.5 and the cathodic potential of the BES at -0.95 V vs. SHE. In addition, the air-cathode was replaced for a new one in order to improve its operation and was characterized by cyclic voltammetry (CV) from -0.2 to +0.5 V vs. SHE at a scan rate of 1 mV s^{-1} (Figure 8.2). In period VIII, a flat rubber sheet was placed between the biocathode of the BES

and the anode of the FC in order to avoid the possible effect of electron-shuttling compounds and the current density output of the BES was controlled at 10 A m^{-2}.

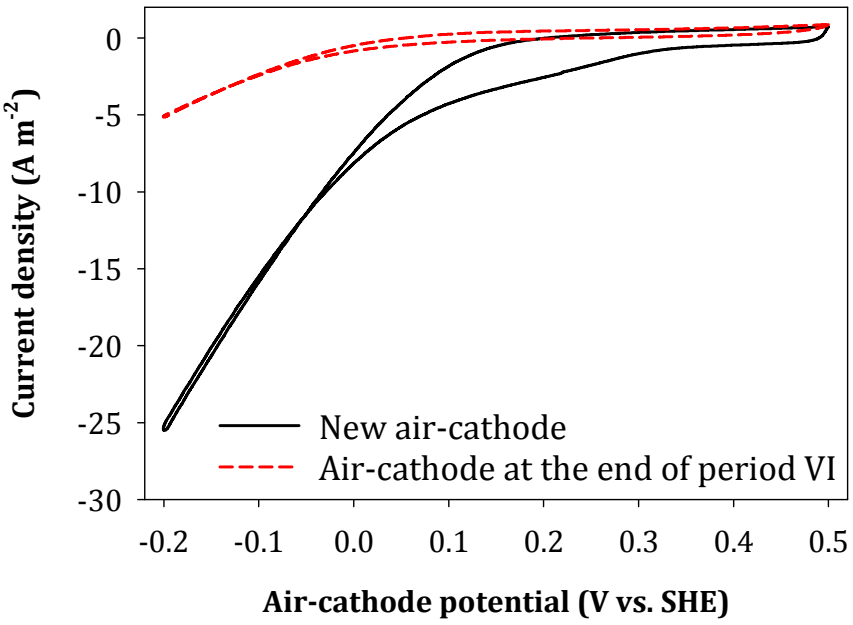

Figure 8.2. Cyclic voltammetry of the air-cathode at the end of period VI and of a new piece of air-cathode. Scan rate of 1 mV s^{-1}.

8.3. Results and discussion

8.3.1. Effect of the additional oxygen input on the autotrophic biocathode

The BES-FC reactor was operated for 161 days under continuous mode and under different operational conditions (Figure 8.3). Water electrolysis took place in the anode of the BES in order to supply the electrons for the sulfate reduction in the cathode of the BES. Eight different periods were performed: from period I to V with the FC switched off and from VI to VIII with the FC switched on (Table 8.1). The BES-FC reactor introduced an extra input of oxygen to the middle chamber of the reactor during the whole operation (both when the FC was switched on and off). This was because the modified carbon cloth used as air-cathode allowed oxygen diffusion into the reactor. The extra oxygen was apart from the oxygen diffusion

from the anode of the BES to the cathode through the membrane described by Blázquez et al. (2016).

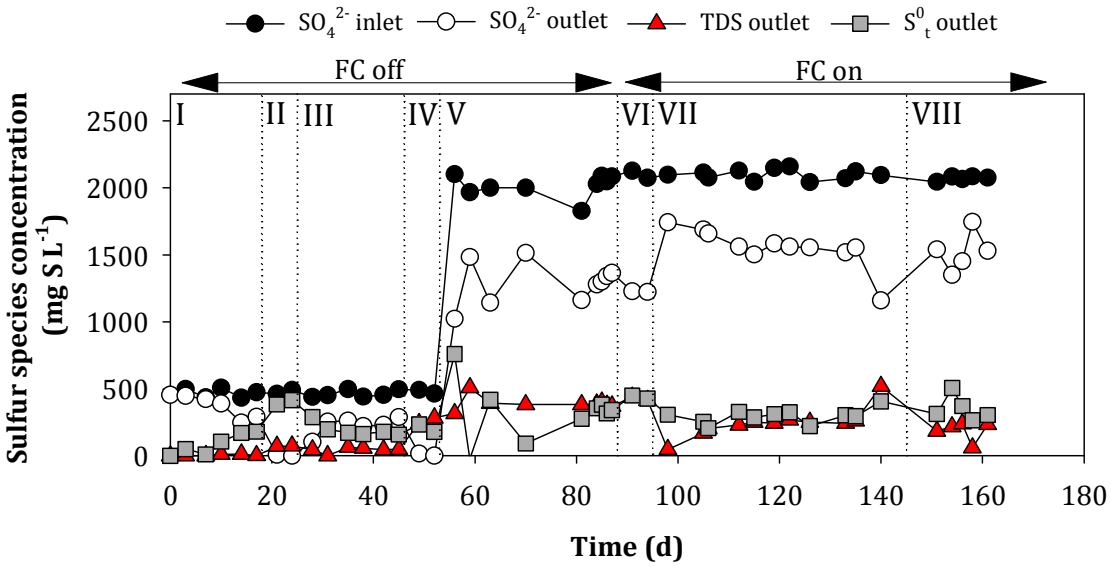

Figure 8.3. Evolution of sulfur species concentration along the BES-EC operation after the start-up period, sulfate in the inlet and outlet, total dissolved sulfide (TDS) in the outlet and theoretical elemental sulfur produced (S^0_t) in the outlet. The operational conditions of each period are explained in Table 8.1.

From period I to V the operational conditions were changed in order to increase the sulfate removal rate (SRR). The effect of the extra oxygen entrance through the carbon cloth (coupled with the oxygen diffusion from the anode chamber through the membrane) was evaluated without the FC on. In period I, the cathode potential of the BES was -0.7 V vs. SHE and the SRR observed was 26 ± 13 mg SO_4^{2-}-S L^{-1} d^{-1}, but the sulfide production rate (SPR) observed was just 2.0 ± 1.7 mg TDS-S L^{-1} d^{-1} (Figure 8.4A), which meant that up to 94.1 ± 4.3% of sulfate reduced was putatively converted to elemental sulfur (Figure 8.4B). However, the electron recovery observed was 42.5 ± 18.4% (Figure 8.4D), indicating that there was an extra electron sink besides sulfate reduction. This electron flow could be used for i) excess H_2 production, or ii) reduction of oxygen reaching the biocathode via leakages through the membrane or from the carbon cloth. The possible excess of oxygen reaching the biocathode chamber could be also used to re-oxidize sulfide to

sulfate as observed previously (Blázquez et al., 2019a). This last fact could explain the low SRR and SPR observed.

The cathode potential was decreased to -0.8 V vs. SHE in period II in order to increase the SRR. Sulfate was completely removed and the electron recoveries decreased, which meant that there was excess H_2 production. After 7 days, the HRT was decreased down to 1.1 days (period III) in order to have more sulfate available and observe the improvement on SRR at -0.8 V vs. SHE.

The SRR observed in period III increased up to 214 ± 39 mg SO_4^{2-}-S L^{-1} d^{-1} with a really low SPR (40 ± 21 mg TDS-S L^{-1} d^{-1}) achieving a high putative elemental sulfur proportion of 81.6 ± 9.9%. The SRR values obtained were close to that obtained in Chapter 7 with a BES with an electrochemical cell under the same conditions of sulfate load and cathode potential, but the production of elemental sulfur was higher because of the extra entrance of oxygen through the carbon cloth.

The cathode potential was decreased again down to -0.9 V vs. SHE at day 45 (period IV) in order to increase the SRR but, as in period II, sulfate was completely removed with low electron recoveries. For this reason, the inlet sulfate concentration after 7 days was increased up to 2000 mg SO_4^{2-}-S L^{-1} (period V) to have more sulfate available and to improve SRR at -0.9 V vs. SHE.

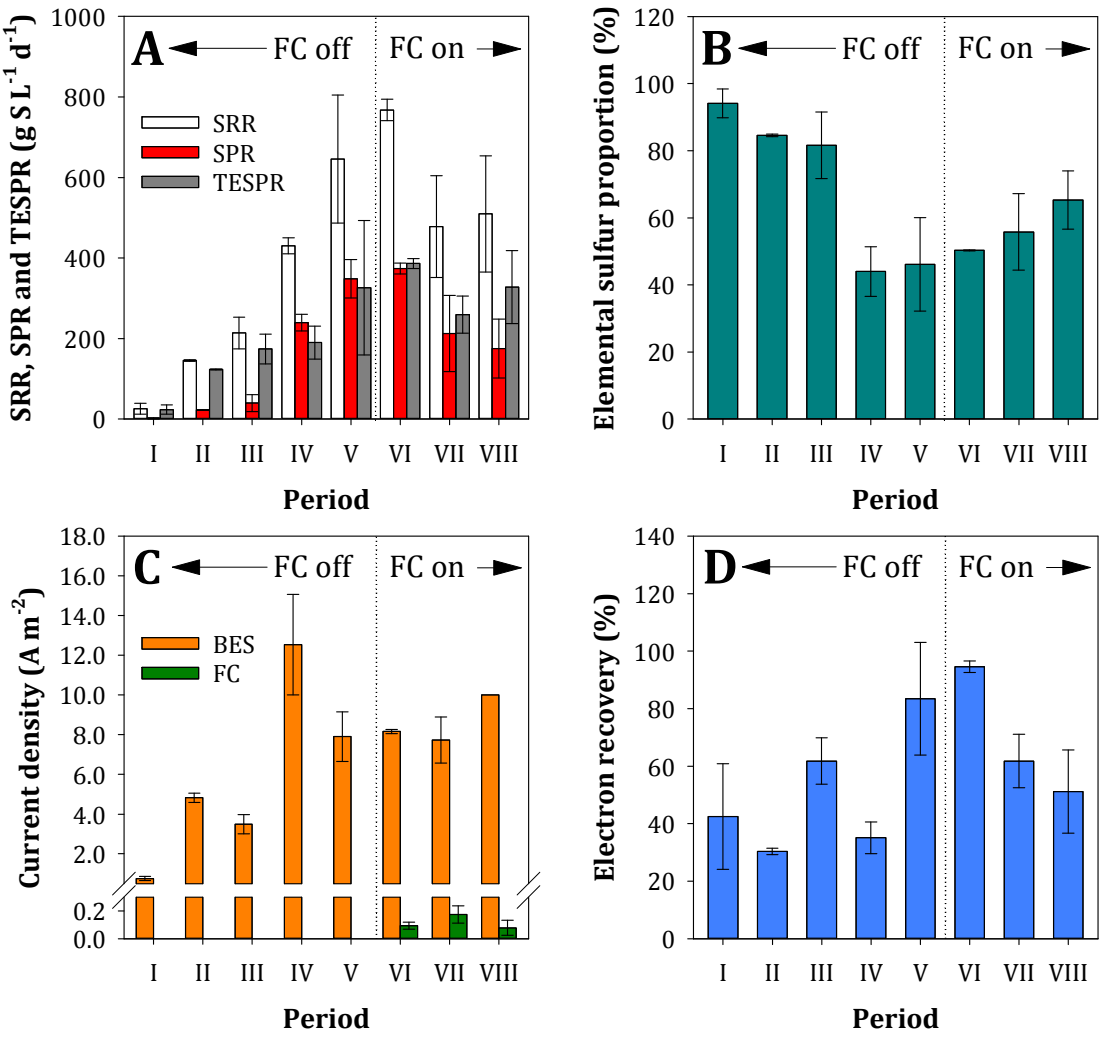

Figure 8.4. Average plots of the different operational periods of the BES-EC after the start-up on A: sulfate reduction rate (SRR) and sulfide production rate (SPR) and theoretical elemental sulfur production rate (TESPR), B: elemental sulfur proportion compared with sulfate reduced, C: current and D: electron recovery as sulfate reduced in the biocathode. The operational conditions of each period are explained in Table 8.1.

Period V started on day 52 achieving a SRR of 646 ± 159 mg SO_4^{2-}-S L^{-1} d^{-1}. In this period, the SPR increased up to 348 ± 48 mg TDS-S L^{-1} d^{-1} which meant a putative proportion of elemental sulfur of 46.1 ± 13.9%. At this cathode potential, the sulfate reduction was so high that the oxygen entrance was too low to oxidize the whole amount of sulfide to elemental sulfur. In addition, the electron recovery observed was 83.5 ± 19.6% (Figure 8.4C), which corroborated the fact that there

was no oxygen excess compared with periods I and III. Therefore, the SRR was much higher than other systems working at the same cathode potential such as Pozo et al. (2015), who achieved 63 mg SO_4^{2-}-S L^{-1} d^{-1} in continuous mode, pH 7.3 and graphite granules as biocathode material, and Blázquez et al. (2017), who achieved 358 mg SO_4^{2-}-S L^{-1} d^{-1} in batch mode without pH control and graphite fibers brush as biocathode material. During the whole operation of our system, the use of carbon cloth allowed for an extra route of oxygen intrusion, which declined the SRR, but at the same time it improved the TESPR comparing the results with the BES-EC reported in Chapter 7. As oxygen can be reduced in the BES-cathode to water, the electron recovery is expected to be lower if there is an excess of oxygen. However, the electron recovery in period V was higher than 80%, indicating that microorganisms and/or elemental sulfur were attached to the carbon cloth provoking a lower entrance of oxygen. The decrease of oxygen diffusion through the air-cathode because of microorganisms growth was previously described by Montpart et al. (2018). The oxygen diffusion from the BES-anode chamber and through the membrane cannot be controlled. Thus, the elemental sulfur production could be improved by an anode in order to achieve sulfide partial oxidation.

8.3.2. Microbial/ fuel cell air-cathode integration

The FC was switched on at day 87 (period VI) to evaluate its influence on sulfate treatment, elemental sulfur production and electron recovery. Figure 8.5 shows the current production in the FC. In period VI, the current density obtained in the FC was 0.09 ± 0.03 A m^{-2}, which was negligible compared with the current density of the BES (8.2 ± 0.1 A m^{-2}) and, thus, the FC was not able to oxidize the sulfide produced. The SRR increased up to 767 ± 26 mg SO_4^{2-}-S L^{-1} d^{-1} and the TESPR up to 386 ± 12 mg S^0-S L^{-1} d^{-1} which corresponded to a proportion of elemental sulfur of 50.3 ± 0.1% and achieving an electron recovery of 94.6 ± 2.1%.

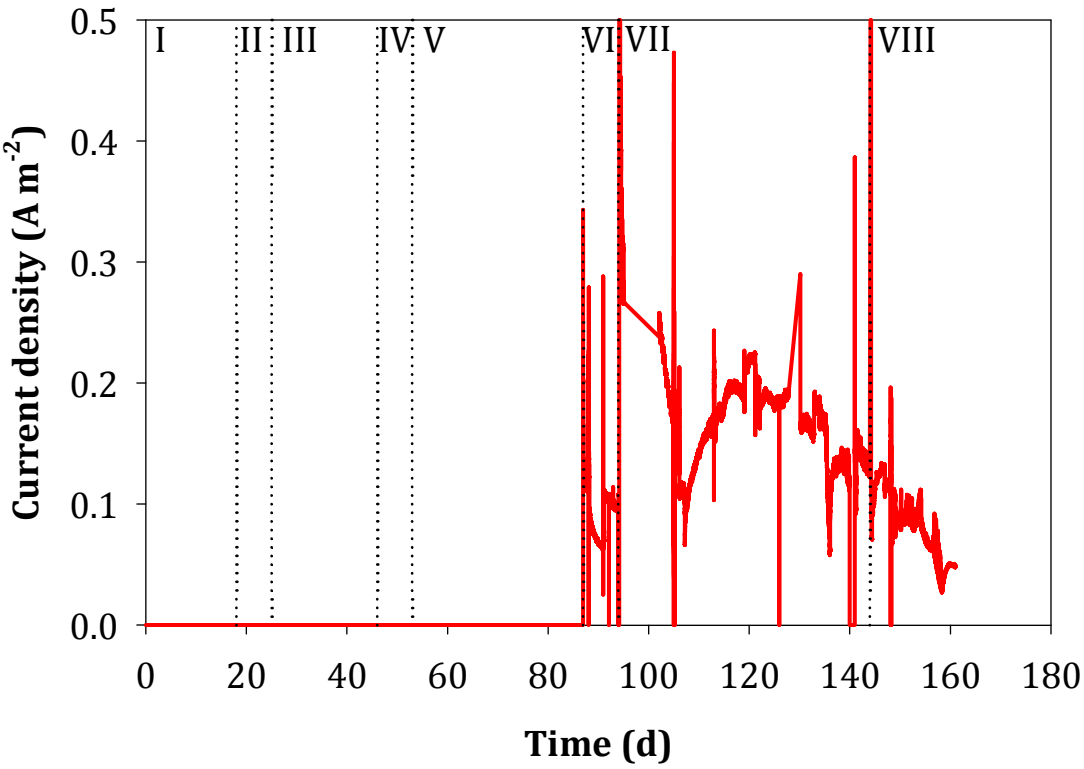

Figure 8.5. Current density of the FC during the whole operation.

The unexpected low improvement observed on the TESPR with the FC switched on could be due to i) a low reaction of TDS with the FC-anode or ii) an inactivation of the FC electrodes because of elemental sulfur precipitated on the air-cathode surface or by inactivation of the catalyst (platinum) by sulfide. The elemental sulfur precipitated on the air-cathode could block the entrance of oxygen. In order to check if the low improvement was due to the low reaction of TDS with the FC-anode, the pH was increased up to 7.5 in period VII (day 94) to increase the HS^- proportion from 50% to 70% (the first proton acidity constant for H_2S is pKa=7) (Moosa and Harrison, 2006). A pH of 7.5 was still in the optimum pH range for SRB growth (between pH 6 and 8 (Hao et al., 1996)). Increasing the pH in the cathode has a negative effect since hydrogen production is less favorable according to the Nernst equation and this leads to a current production decrease. Thus, the cathode potential of the BES was decreased down to -0.95 V vs. SHE to balance the effects of the pH increase.

A CV of the air-cathode was performed in order to know if there was an inactivation of the FC electrodes because of elemental sulfur precipitated on air-

cathode surface blocking the entrance of oxygen or by inactivation of the catalyst (platinum) by sulfide (Figure 8.2). The CV showed that, after 94 days of operation of the reactor with the FC switched off, the air-cathode was inactivated since much lower current density was observed at the same air-cathode potential. For this reason, period VII started with a new air-cathode.

In period VII, the current density of the FC was almost double than in period VI (0.17 ± 0.06 A m^{-2}), but the SRR decreased to 478 ± 126 mg SO_4^{2-}-S L^{-1} d^{-1} and also the SPR and TESPR decreased significantly. As the current density of the BES was almost the same (7.7 ± 1.2 A m^{-2}), the decrease on the SRR, SPR and TESPR compared with periods V and VI might be caused by the new air-cathode that allowed a high entrance of oxygen and led to a complete sulfide and elemental sulfur oxidation to sulfate again. However, the current of the FC was still really low and this poor performance was hypothesized to be caused by the effect of electron-shuttling compounds which are redox mediators that can be repeatedly oxidized and reduced by the electrodes and the microorganisms (Watanabe et al., 2009). To minimize this possible effect, the plastic mesh that separated the BES-cathode from the FC-anode was replaced by a rubber separating completely both electrodes on period VIII (day 145). However, both chambers were still connected because the outlet of the BES-cathode chamber was connected to the FC-anode chamber by overflow. Moreover, recirculation was adapted in order to properly mix both electrode chambers separately. In addition, the current density of the BES was controlled at 10 A m^{-2} using the galvanostat mode, in order to avoid fluctuations in the BES performance in period VIII and keeping a similar current density compared with the previous periods.

All these changes in the operation did not result in a high SRR improvement (510 ± 144 mg SO_4^{2-}-S L^{-1} d^{-1}) but the SPR decreased (175 ± 73 mg TDS-S L^{-1} d^{-1}) and the TESPR increased (328 ± 90 mg S^0-S L^{-1} d^{-1}), which meant an increase on the proportion of elemental sulfur up to 65.3 ± 8.7%. However, the current density of the FC decreased again to 0.08 ± 0.05 A m^{-2}. Figure 6 shows that, from mid period VII to the end, the current of the FC started to decrease and the air-cathode could be inactivated again.

In our study, we integrated an air-cathode fuel cell in a BES in order to improve SRR and elemental sulfur recovery. However, the FC integration did not improve the system performance as expected mainly because of a deterioration of the air-cathode along time. The biofilm grown over the air-cathode surface reduced drastically the presence of dissolved oxygen in the bulk liquid (Montpart et al., 2018) and in addition better columbic efficiencies and current production were observed (Montpart et al., 2018; Ou et al., 2016). For this reason, the biofilm attached to the air cathode was not detrimental and did not decline the FC performance. The poor performance of the FC might be caused by the elemental sulfur attached to the air-cathode surface or by inactivation of the air-cathode platinum catalyst as observed in other metal-based catalysts (Rabaey et al., 2006).

There are few reports in the literature studying sulfide oxidation in an anode for elemental sulfur recovery using a fuel cell with air-cathode. Sun et al. (2009) observed elemental sulfur conversion to sulfate in the case of microorganisms presence in a microbial fuel cell for sulfide oxidation but did not report any inactivation of the air-cathode. However, Zhao et al. (2008) studied the sulfate removal using organic matter and sulfide oxidation in an anode improving the configuration by the addition of a membrane of Nafion next to the air-cathode in order to avoid an excess of oxygen entrance and the possible inactivation of the air-cathode. The membrane next to the air-cathode could be a solution for this problem at expenses of higher internal resistance. Other studies tried to remove sulfate heterotrophically and then oxidize the sulfide in the anode of a single reactor, achieving proportions of elemental sulfur between 60 and 75% of the initial sulfate (Chatterjee et al., 2017; Lee et al., 2014) but at lower SRR and at expenses of an external electron donor supply.

The FC improved the production of elemental sulfur. This improvement could be just due to the extra entrance of oxygen once the air-cathode was replaced for a new one that was not blocked by attached elemental sulfur nor inactivated by sulfide. In comparison to Chapter 7, the FC improved significantly the proportion of elemental sulfur but with lower SRR and electron recoveries. The BES-FC achieved also similar SRR than Pozo et al. (2017b) which operated the BES at -1.1 V vs. SHE instead of at -0.9 V vs. SHE as in our study. However, in terms of energy

consumption for sulfur recovery, the BES-FC supposes an improvement compared with the BES-EC. In Chapter 7 energy consumption per kg of sulfate removed of 9.18 ± 0.80 kWh kg^{-1} SO_4^{2-}-S was reported taking into account the maximum SRR. Converting this result into kg of sulfur recovered and adding the energy consumption of the EC, it showed an energy consumption of 18.74 ± 1.81 kWh kg^{-1} S^0-S. The energy consumption for sulfate removed in the case of our BES-FC was slightly higher (10.61 ± 0.12 kWh kg^{-1} SO_4^{2-}-S) because, as mentioned before, the extra oxygen entrance could cause the re-oxidation of sulfide to sulfate. However, as the FC was not consuming energy, the total energy consumption for sulfur production was of 16.50 ± 0.19 kWh kg^{-1} S^0-S. Therefore, the BES-FC allows a 12% better elemental sulfur production in terms of energy consumption than the use of a BES-EC.

8.4. Conclusions

This work demonstrates that the BES-FC can treat synthetic wastewater with high sulfate content obtaining sulfate removal rates up to 768 mg SO_4^{2-}-S L^{-1} d^{-1} at -0.9 V vs. SHE. In addition, the BES-FC allowed reducing a 12% the energy consumption per kg of elemental sulfur recovered compared with a BES with an electrochemical cell instead of the FC with an air-cathode, which allow spontaneous sulfide oxidation to elemental sulfur. However, the oxygen diffusion through the carbon cloth decreased the sulfate removal rates because of complete re-oxidation of sulfide to sulfate. The FC improved the proportion of elemental sulfur produced compared with an electrochemical cell but at expenses of lower sulfate removals. Further studies are required in order to avoid the inactivation of the air-cathode catalyst by the sulfide and the elemental sulfur produced in the reactor.

Chapter 9

General conclusions and future work

The main objective of this thesis was to treat wastewaters with high sulfate content at the biocathode of bioelectrochemical systems towards the recovery of elemental sulfur. This section summarizes the main achievements and conclusions that can be drawn from this thesis. Some future research directions are also suggested, in order to further develop bioelectrochemical systems in different ways and improving the sulfate removal and elemental sulfur recovery.

9.1. General conclusions

This thesis shows for the first time the treatment of high-strength sulfate wastewater using bioelectrochemical systems with the possibility to recover elemental sulfur and without any external electron donor dosage. The process is characterized by microaerophilic conditions in the biocathode compartment due to oxygen diffusion through the membrane during water electrolysis in the anode. This configuration allows the development of a microbial community with a mixture of SRB and SOB able to reduce sulfate to sulfide and partially oxidize sulfide to elemental sulfur in an autotrophic biocathode.

The study of the cathodic pH at a cathode potential of -0.8 vs. SHE showed a higher SRR at pH 7 than at pH 5.5 and 8.5, and also a higher electron recovery. The problem with alkaline pH lays on the lower hydrogen production at the same cathode potential, while pH 5.5 is out of range of the optimum pH for SRB.

Different cathode potentials were studied showing that the lower the cathode potential was, the higher the SRR. However, the cathode material and BES configuration are key factors that can also influence the SRR.

This thesis also shows, for the first time, the treatment of real wastewater from a FGD system in a BES, and its effect on sulfate removal and elemental sulfur recovery. The influence of this real wastewater on the different microbial populations grown as biofilm and in suspension was also studied. The sulfate removal rate decreased using real FGD wastewater compared with synthetic wastewater at similar conductivities. This could be due to inhibition caused by the real FGD wastewater since the current increased, which meant higher amount of electron donor. Therefore, higher SRR would be expected with the real

wastewater. The microbial population was studied with the synthetic wastewater and the real one taking samples from the membrane and cathode biofilm and from the supernatant. The results show that sulfate reducing bacteria and sulfide oxidizing bacteria grow with both wastewaters but more SOB appear with the real one. In addition, high salt concentration tolerant SOB proliferated due to a higher complexity of the real FGD wastewater. However, the higher amount of SOB can be found in the biofilm grown on the membrane because of the oxygen diffusion from the anode through the membrane.

Two different configurations were also studied in order to improve the elemental sulfur recovery. These configurations consisted in the integration of a BES for cathodic sulfate reduction with an electrochemical cell (EC) and a fuel cell (FC) with air cathode for the anodic sulfide partial oxidation. Higher removal rates were obtained with the electrochemical cell than with the fuel cell because the extra entrance of oxygen through the air-cathode in the second case caused the complete sulfide oxidation to sulfate. However, the proportion of elemental sulfur recovered was higher with the BES coupled with the FC than coupled with the EC. In addition, as sulfide can be spontaneously oxidized in an anode, the BES-FC allowed reducing energy costs for kg of elemental sulfur produced.

9.2. Future work

BESs are opening up the possibility of creating new processes related to the sulfur cycle. The link between the sulfur cycle and BES has recently gained the attention of many researchers according to the number of publications in the topic. Moreover, some works have shown how part of the sulfur compounds treated can be recovered as elemental sulfur fitting thus in the new paradigm of environmental engineering: resource recovery in addition to treatment.

Some studies deal on the optimization of BES configuration in view of successful sulfate removal and sulfur recovery BES. One of the main limiting factors is the low reaction rates in BES that cannot compete with the treatment capacities attained in conventional systems reactors such as Continued Stirred Tank Reactors (CSTR) or Upflow Anaerobic Sludge Blanket (UASB).

Another common drawback in all bioelectrochemical systems is the cost of materials for BES construction. Many studies show that use of certain materials and diverse methodologies may improve BES performance as well as that not all materials are appropriated for biofilm growth.

Thus, the first approach to be investigated in order to improve the use of BES on sulfate treatment is the materials used for the electrodes. Some advances have been performed (for example, graphite granules allow producing high currents for lower material cost than metal based electrodes such as platinum), but the results obtained on sulfate treatment with carbon based biocathodes are not properly comparable due to the wide amount of different BES configurations and electrode surfaces utilized.

In addition, some authors have observed that *Desulfovibrio* sp. can produce hydrogen using the electrons from the cathode. In this thesis, it was observed that the growth of SRB mainly composed by *Desulfovibrio* sp. on the cathode allowed the improvement of current production. Therefore, the use of *Desulfovibrio* sp. and other SRB species on biocathodes should be further studied in order to properly understand their mechanisms of electron transfer.

If the electrode materials and the mechanisms of electron transfer could be improved, the costs for the biological sulfate removal in biocathodes would be reduced making it a more competitive technology.

In the case of elemental sulfur recovery, the use of the oxygen diffused through the membrane has been observed to be not enough. The use of the EC and FC coupled to the BES did not work as expected, thus, several improvements could be performed. First of all, the use of separated cells continuously fed should be tested in order to achieve the good performance of both processes. In addition, the performance of the air-carhode in the case of the FC should be improved using nonmetal-based catalysts or adding a separator between the anode and the cathode.

Chapter 10

References

Adlem, C.J.L., Maree, J.P., Plessis, P. DU, 1991. Treatment of sulphate-rich mining effiuents with the barium hydroxide process and recovery of valuable by-products. 4th Int. Miner. Water Assoc. Congr. 211–222.

Ambler, J.R., Logan, B.E., 2011. Evaluation of stainless steel cathodes and a bicarbonate buffer for hydrogen production in microbial electrolysis cells using a new method for measuring gas production. Int. J. Hydrogen Energy 36, 160–166.

American Public Health Association, A.P.H.A., 2005. Standard methods for the examination of water & wastewater., 19th ed. American Public Health Association, Washington DC.

Ateya, B.G., AlKharafi, F.M., Al-Azab, A.S., 2003. Electrodeposition of Sulfur from Sulfide Contaminated Brines. Electrochem. Solid-State Lett. 6, C137.

Auguet, O., Pijuan, M., Guasch-Balcells, H., Borrego, C.M., Gutierrez, O., 2015. Implications of Downstream Nitrate Dosage in anaerobic sewers to control sulfide and methane emissions. Water Res. 68, 522–532.

Aulenta, F., Catapano, L., Snip, L., Villano, M., Majone, M., 2012. Linking bacterial metabolism to graphite cathodes: Electrochemical insights into the H2-producing capability of desulfovibrio sp. ChemSusChem 5, 1080–1085.

Balch, W.E., Schoberth, S., Tanner, R.S., Wolfe, R.S., 1977. Acetobacterium, a New Genus of Hydrogen-Oxidizing, Carbon Dioxide-Reducing, Anaerobic Bacteria. Int. J. Syst. Bacteriol. 27, 355–361.

Barr, A., 2001. Sulphate removal by nanofiltration. Filtr. Sep. 38, 18–20.

Batlle-Vilanova, P., Puig, S., Gonzalez-Olmos, R., Vilajeliu-Pons, A., Balaguer, M.D., Colprim, J., 2015. Deciphering the electron transfer mechanisms for biogas upgrading to biomethane within a mixed culture biocathode. RSC Adv. 5, 52243–52251.

Bijmans, M.F.M., Dopson, M., Ennin, F., Lens, P.N.L., Buisman, C.J.N., 2008. Effect of sulfide removal on sulfate reduction at pH 5 in a hydrogen fed gas-lift bioreactor. J. Microbiol. Biotechnol. 18, 1809–1818.

Blázquez, E., Baeza, J.A., Gabriel, D., Guisasola, A., 2019a. Treatment of real flue gas desulfurization wastewater in an autotrophic biocathode in view of elemental sulfur recovery: Microbial communities involved. Sci. Total Environ. 657, 945–952.

Blázquez, E., Gabriel, D., Baeza, J.A., Guisasola, A., 2017. Evaluation of key parameters on simultaneous sulfate reduction and sulfide oxidation in an autotrophic biocathode. Water Res. 123.

Blázquez, E., Gabriel, D., Baeza, J.A., Guisasola, A., 2017. Evaluation of key parameters on simultaneous sulfate reduction and sulfide oxidation in an autotrophic biocathode. Water Res. 123, 301–310.

Blázquez, E., Gabriel, D., Baeza, J.A., Guisasola, A., 2016. Treatment of

high-strength sulfate wastewater using an autotrophic biocathode in view of elemental sulfur recovery. Water Res. 105, 395–405.

Blázquez, E., Guisasola, A., Gabriel, D., Baeza, J.A., 2019b. Application of Bioelectrochemical Systems for the Treatment of Wastewaters With Sulfur Species. Microb. Electrochem. Technol. 641–663.

Bosman, D.J., Clayton, J.A., Maree, J.P., Adlem, C.J.L., 1990. Removal of Sulphate From Mine Water. Int. J. mine water 9, 149–163.

Bowell, R.J., 2004. A review of sulfate removal options from mine waters, in: Jarvis, A.P., Dudgeon, B.A., Younger, P.L. (Eds.), Proceedungs International Mine Water Association Symposium 2. Newcastle upon Tyne (University of Newcastle), pp. 75–91.

Boyd, D.A., 2016. Sulfur and Its Role In Modern Materials Science. Angew. Chemie - Int. Ed. 55, 15486–15502.

Brewster, E.T., Pozo, G., Batstone, D.J., Freguia, S., Ledezma, P., 2018. A modelling approach to assess the long-term stability of a novel microbial / electrochemical system for the treatment of acid mine drainage †. RSC Adv. 8, 18682–18689.

Brimblecombe, P., 2015. BIOGEOCHEMICAL CYCLES | Sulfur Cycle. Encycl. Atmos. Sci. 187–193.

Brown, M., Barley, B., Wood, H., 2002. Minewater treatment: technology, application and policy. IWA Pub.

Cai, J., Zheng, P., Qaisar, M., Zhang, J., 2017. Elemental sulfur recovery of biological sulfide removal process from wastewater: A review. Crit. Rev. Environ. Sci. Technol. 3389, 1–21.

Chatterjee, P., Ghangrekar, M.M., Rao, S., Kumar, S., 2017. Biotic conversion of sulphate to sulphide and abiotic conversion of sulphide to sulphur in a microbial fuel cell using cobalt oxide octahedrons as cathode catalyst. Bioprocess Biosyst. Eng. 40, 759–768.

Chen, X.G., Geng, A.L., Yan, R., Gould, W.D., Ng, Y.L., Liang, D.T., 2004. Isolation and characterization of sulphur-oxidizing Thiomonas sp. and its potential application in biological deodorization. Lett. Appl. Microbiol. 39, 495–503.

Cheng, S., Liu, H., Logan, B.E., 2006a. Increased performance of single-chamber microbial fuel cells using an improved cathode structure. Electrochem. commun. 8, 489–494.

Cheng, S., Liu, H., Logan, B.E., 2006b. Power densities using different cathode catalysts (Pt and CoTMPP) and polymer binders (Nafion and PTFE) in single chamber microbial fuel cells. Environ. Sci. Technol. 40, 364–369.

Cheng, S., Logan, B.E., 2007. Sustainable and efficient biohydrogen production via electrohydrogenesis. Proc. Natl. Acad. Sci. U. S. A. 104, 18871–3.

Cheng, S., Xing, D., Call, D.F., Logan, B.E., 2009. Direct biological conversion of electrical current into methane by electromethanogenesis. Environ. Sci. Technol. 43, 3953–3958.

Chung, W.J., Griebel, J.J., Kim, E.T., Yoon, H., Simmonds, A.G., Ji, H.J., Dirlam, P.T., Glass, R.S., Wie, J.J., Nguyen,

N.A., Guralnick, B.W., Park, J., Somogyi, Á., Theato, P., Mackay, M.E., Sung, Y.-E., Char, K., Pyun, J., 2013. The use of elemental sulfur as an alternative feedstock for polymeric materials. Nat. Chem. 5, 518–524.

Claesson, M.J., O'Sullivan, O., Wang, Q., Nikkilä, J., Marchesi, J.R., Smidt, H., de Vos, W.M., Ross, R.P., O'Toole, P.W., 2009. Comparative Analysis of Pyrosequencing and a Phylogenetic Microarray for Exploring Microbial Community Structures in the Human Distal Intestine. PLoS One 4, e6669.

Clair, N., Perry, L., Gene, F., 2003. Chemistry for environmental engineering and science. Mcgraw-Hill, New York.

Clauwaert, P., Ha, D. van der, Boon, N., Verbeken, K., Verhaege, M., Rabaey, K., Verstraete, W., 2007. Open Air Biocathode Enables Effective Electricity Generation with Microbial Fuel Cells. Environ. Sci. Technol. 41, 7564–7569.

Cole, J.R., Wang, Q., Cardenas, E., Fish, J., Chai, B., Farris, R.J., Kulam-Syed-Mohideen, A.S., McGarrell, D.M., Marsh, T., Garrity, G.M., Tiedje, J.M., 2009. The Ribosomal Database Project: improved alignments and new tools for rRNA analysis. Nucleic Acids Res. 37, D141–D145.

Coma, M., Puig, S., Pous, N., Balaguer, M.D., Colprim, J., 2013. Biocatalysed sulphate removal in a BES cathode. Bioresour. Technol. 130, 218–223.

Cope, G., 2012. The calm before the storm. Hydrocarb. Eng. 10, 82–87.

Copeland, A., Spring, S., Göker, M., Schneider, S., Lapidus, A., del Rio, T.G., Tice, H., Cheng, J.F., Lucas, S., Chen, F., Nolan, M., Bruce, D., Goodwin, L., Pitluck, S., Ivanova, N., Mavromatis, K., Ovchinnikova, G., Pati, A., Chen, A., Palaniappan, K., Land, M., Hauser, L., Chang, Y.J., Jeffries, C.C., Meincke, L., Sims, D., Brettin, T., Detter, J.C., Han, C., Chain, P., Bristow, J., Eisen, J.A., Markowitz, V., Hugenholtz, P., Kyrpides, N.C., Klenk, H.P., Lucas, S., 2009. Complete genome sequence of Desulfomicrobium baculatum type strain (X T). Stand. Genomic Sci. 1, 29–37.

Cordas, C.M., Guerra, L.T., Xavier, C., Moura, J.J.G., 2008. Electroactive biofilms of sulphate reducing bacteria. Electrochim. Acta 54, 29–34.

Cusick, R.D., Kiely, P.D., Logan, B.E., 2010. A monetary comparison of energy recovered from microbial fuel cells and microbial electrolysis cells fed winery or domestic wastewaters. Int. J. Hydrogen Energy 35, 8855–8861.

Davidova, I., Stams, A., 1996. Sulfate reduction with methanol by a thermophilic consortium obtained from a methanogenic reactor. Appl. Microbiol. Biotechnol.

Dominguez-Benetton, X., Varia, J.C., Pozo, G., Modin, O., Ter Heijne, A., Fransaer, J., Rabaey, K., 2018. Metal recovery by microbial electro-metallurgy. Prog. Mater. Sci. 94, 435–461.

Doughty, T., Littlejohn, P., 2015. Sulf-IX ™: Water Treatment Utilizing Fluidized Resin Beds 1–3.

Dutta, P.K., Keller, J., Yuan, Z., Rozendal, R.A., Rabaey, K., 2009a. Role of

sulfur during acetate oxidation in biological anodes. Environ. Sci. Technol. 43, 3839–3845.

Dutta, P.K., Rabaey, K., Yuan, Z., Keller, J., 2008. Spontaneous electrochemical removal of aqueous sulfide. Water Res. 42, 4965–4975.

Dutta, P.K., Rabaey, K., Yuan, Z., Rozendal, R.A., Keller, J., 2010. Electrochemical sulfide removal and recovery from paper mill anaerobic treatment effluent. Water Res. 44, 2563–2571.

Dutta, P.K., Rozendal, R.A., Yuan, Z., Rabaey, K., Keller, J., 2009b. Electrochemical regeneration of sulfur loaded electrodes. Electrochem. commun. 11, 1437–1440.

Finster, K., Liesack, W., Tindall, B.J., 1997. Sulfurospirillum arcachonense sp. nov., a new microaerophilic sulfur- reducing bacterium. Int J Syst Bacteriol 47, 1212–1217.

Fortin, D., Davis, B., Beveridge, T.J., 1996. Role of Thiobacillus and sulfate-reducing bacteria in iron biocycling in oxic and acidic mine tailings. FEMS Microbiol. Ecol. 21, 11–24.

Gacitúa, M.A., Muñoz, E., González, B., 2018. Bioelectrochemical sulphate reduction on batch reactors: Effect of inoculum-type and applied potential on sulphate consumption and pH. Bioelectrochemistry 119, 26–32.

Gazea, B., Adam, K., Kontopoulos, A., 1996. A review of passive systems for the treatment of acid mine drainage. Miner. Eng. 9, 23–42.

Gibert, O., Rötting, T., Cortina, J.L., de Pablo, J., Ayora, C., Carrera, J., Bolzicco, J., 2011. In-situ remediation of acid mine drainage using a permeable reactive barrier in Aznalcóllar (Sw Spain). J. Hazard. Mater. 191, 287–295.

Gil, G.-C., Chang, I.-S., Kim, B.H., Kim, M., Jang, J.-K., Park, H.S., Kim, H.J., 2003. Operational parameters affecting the performannce of a mediator-less microbial fuel cell. Biosens. Bioelectron. 18, 327–334.

Gildemyn, S., Rozendal, R.A., Rabaey, K., 2017. A Gibbs Free Energy-Based Assessment of Microbial Electrocatalysis. Trends Biotechnol. 35, 393–406.

Goar, B.G., Fenderson, S., 1996. Fundamentals of Sulfur Recovery by the Claus Process, in: The Laurance Reid Gas Conditioning Conference. Norman, Oklahoma.

Gong, Y., Ebrahim, A., Feist, A.M., Embree, M., Zhang, T., Lovley, D., Zengler, K., 2013. Sulfide-driven microbial electrosynthesis. Environ. Sci. Technol. 47, 568–573.

Groudev, S., Kontopoulos, A., Spasova, I., Komnitsas, K., Angelov, A., Georgiev, P., 1998. In situ treatment of groundwater at Burgas Copper Mines, Bulgaria, by enhancing microbial sulphate reduction. IAHS Publ. 249–255.

Guan, F., Zhai, X., Duan, J., Zhang, M., Hou, B., 2016. Influence of sulfate-reducing bacteria on the corrosion behavior of high strength steel eq70 under cathodic polarization. PLoS One 11, 1–22.

Handley, K.M., Bartels, D., O'Loughlin, E.J., Williams, K.H., Trimble, W.L., Skinner, K., Gilbert, J.A., Desai, N., Glass, E.M., Paczian, T., Wilke, A., Antonopoulos, D., Kemner, K.M., Meyer, F., 2014. The complete genome sequence for putative H2- and S-oxidizer Candidatus Sulfuricurvum sp., assembled de novo from an aquifer-derived metagenome. Environ. Microbiol. 16, 3443–3462.

Hao, O.J., Chen, J.M., Huang, L., Buglass, R.L., 1996. Sulfate-reducing bacteria. Crit. Rev. Environ. Sci. Technol. 26, 155–187.

Harms, C., Schleicher, A., Collins, M.D., Andreesen, J.R., 1998. Tissierella creatinophila sp . nov ., a Gram-positive , anaerobic , non-spore-f orming , creatinine-f errnent ing organism. Int. J. Syst. Bacteriol. 48, 983–993.

Harnisch, F., Aulenta, F., Schröder, U., 2011. Microbial Fuel Cells and Bioelectrochemical Systems: Industrial and Environmental Biotechnologies Based on Extracellular Electron Transfer, Second Edi. ed, Comprehensive Biotechnology. Elsevier B.V.

Harnisch, F., Rabaey, K., 2012. The diversity of techniques to study electrochemically active biofilms highlights the need for standardization. ChemSusChem 5, 1027–1038.

Heijnen, J.J., 1999. Bioenergetics of microbial growth, in: Encyclopedia of Bioprocess Technology. Wiley Online Library.

Hippe, H., Vainshtein, M., Gogotova, G.I., Stackebrandt, E., 2003. Reclassification of Desulfobacterium macestii as Desulfomicrobium macestii comb. nov. Int. J. Syst. Evol. Microbiol. 53, 1127–1130.

Hlabela, P., Maree, J., Bruinsma, D., 2007. Barium carbonate process for sulphate and metal removal from mine water. Mine Water Environ. 26, 14–22.

Houten, R.T. Van, Poi, L.W.H., Lettinga, G., Soils, C., 1994. Biological Sulphate Reduction Using Gas-Lift Reactors Fed with Hydrogen and Carbon Dioxide as Energy and Carbon Source.

Hulshoff, L.W., Lens, P.N.L., Weijma, J., Stams, A.J.M., 2001. New developments in reactor and process technology for sulfate reduction. Water Sci. Technol. 44, 67–76.

Islander, R.L., Devinny, J.S., Mansfeld, F., Postyn, A., Shih, H., 1991. Microbial Ecology of Crown Corrosion in Sewers. J. Environ. Eng. 117, 751–770.

Jadhav, D.A., Ghosh Ray, S., Ghangrekar, M.M., 2017. Third generation in bio-electrochemical system research – A systematic review on mechanisms for recovery of valuable by-products from wastewater. Renew. Sustain. Energy Rev. 76, 1022–1031.

Janneck, E., Cook, M., Kunze, C., Sommer, K., Dinu, L., 2012. Ettringite Precipitation vs. Nano-Filtration for Efficient Sulphate Removal from Mine Water. Int. Mine Water Assoc.

Annu. Conf. 206I-R.

Jiang, F., Zhang, L., Peng, G.-L., Liang, S.-Y., Qian, J., Wei, L., Chen, G.-H., 2013. A novel approach to realize SANI process in freshwater sewage treatment – Use of wet flue gas desulfurization waste streams as sulfur source. Water Res. 47, 5773–5782.

Johnson, D.B., 2000. Biological removal of sulfurous compounds from inorganic wastewaters, in: Environmental Technologies to Treat Sulfur Pollution: Principles and Engineering. IWA Publishing, London (UK), pp. 175–205.

Johnson, D.B., Jameson, E., Rowe, O.F., Wakeman, K., Hallberg, K.B., 2009. Sulfidogenesis at Low pH by Acidophilic Bacteria and its Potential for the Selective Recovery of Transition Metals from Mine Waters. Adv. Mater. Res. 71–73, 693–696.

Jourdin, L., Freguia, S., Donose, B.C., Keller, J., 2015. Autotrophic hydrogen-producing biofilm growth sustained by a cathode as the sole electron and energy source. Bioelectrochemistry 102, 56–63.

Julián, E., Roldán, M., Sánchez-Chardi, A., Astola, O., Agustí, G., Luquin, M., 2010. Microscopic cords, a virulence-related characteristic of Mycobacterium tuberculosis, are also present in nonpathogenic mycobacteria. J. Bacteriol. 192, 1751–60.

Kaksonen, A.H., Puhakka, J.A., 2007. Sulfate reduction based bioprocesses for the treatment of acid mine drainage and the recovery of metals. Eng. Life Sci. 7, 541–564.

Keller-Lehmann, B., Corrie, S., Ravn, R., Yuan, Z., Keller, J., 2006. Preservation and simultaneous analysis of relevant soluble sulfur species in sewage samples. Proc. Second Int. IWA Conf. Sewer Oper. Maint. 26, 28.

Klouche, N., Basso, O., Lascourreges, J.F., Cayol, J.L., Thomas, P., Fauque, G., Fardeau, M.L., Magot, M., 2009. Desulfocurvus vexinensis gen. nov., sp. nov., a sulfate-reducing bacterium isolated from a deep subsurface aquifer. Int J Syst Evol Microbiol 59, 3100–3104.

Kodama, Y., Watanabe, K., 2004. Sulfuricurvum kujiense gen. nov., sp. nov., a facultatively anaerobic, chemolithoautotrophic, sulfur-oxidizing bacterium isolated from an underground crude-oil storage cavity. Int. J. Syst. Evol. Microbiol. 54, 2297–2300.

Kondaveeti, S.K., Seelam, J.S., Mohanakrishna, G., 2018. Anodic Electron Transfer Mechanism in Bioelectrochemical Systems, in: Microbial Fuel Cell. Springer International Publishing, Cham, pp. 87–100.

Kracke, F., Vassilev, I., Krömer, J.O., 2015. Microbial electron transport and energy conservation - The foundation for optimizing bioelectrochemical systems. Front. Microbiol. 6, 1–18.

Laanbroek, H.J., Geerligs, H.J., Sijtsma, L., Veldkamp, H., 1984. Competition for sulfate and ethanol among *Desulfobacter*, *Desulfobulbus*, and

Desulfovibrio species isolated from intertidal sediments. Appl. Environ. Microbiol. 47, 329–34.

Ledezma, P., Kuntke, P., Buisman, C.J.N., Keller, J., Freguia, S., 2015. Source-separated urine opens golden opportunities for microbial electrochemical technologies. Trends Biotechnol. 33, 214–220.

Lee, D.J., Liu, X., Weng, H.L., 2014. Sulfate and organic carbon removal by microbial fuel cell with sulfate-reducing bacteria and sulfide-oxidising bacteria anodic biofilm. Bioresour. Technol. 156, 14–19.

Lens, P., Pol, L., 2015. Environmental Technologies to Treat Sulfur Pollution - Principles and Applications. Water Intell. Online 4, 9781780403038–9781780403038.

Liamleam, W., Annachhatre, A.P., 2007. Electron donors for biological sulfate reduction. Biotechnol. Adv. 25, 452–463.

Liang, F., Xiao, Y., Zhao, F., 2013. Effect of pH on sulfate removal from wastewater using a bioelectrochemical system. Chem. Eng. J. 218, 147–153.

Liang, P., Fan, M., Cao, X., Huang, X., 2009. Evaluation of applied cathode potential to enhance biocathode in microbial fuel cells. J. Chem. Technol. Biotechnol. 84, 794–799.

Loka Bharathi, P.A., 2008. Sulfur Cycle. Encycl. Ecol. 3424–3431.

Luo, H., Fu, S., Liu, G., Zhang, R., Bai, Y., Luo, X., 2014. Autotrophic biocathode for high efficient sulfate reduction in microbial electrolysis cells. Bioresour. Technol. 167, 462–468.

Luo, H., Teng, W., Liu, G., Zhang, R., Lu, Y., 2017. Sulfate reduction and microbial community of autotrophic biocathode in response to acidity. Process Biochem. 54, 120–127.

Mao, Z., Anani, A., White, R.E., Srinivason, S., Appleby, A.J., 1991. A Modified Electrochemical Process for the Decomposition of Hydrogen Sulfide in an Aqueous Alkaline Solution. J. Electrochem. Soc. 138, 1299.

Mariam, S., Hong, B., Ghasemi, M., Ramli, W., Daud, W., 2015. Separators used in microbial electrochemical technologies: Current status and future prospects. Bioresour. Technol. 195, 170–179.

Marshall, C.W., Ross, D.E., Handley, K.M., Weisenhorn, P.B., Edirisinghe, J.N., Henry, C.S., Gilbert, J.A., May, H.D., Norman, R.S., 2017. Metabolic reconstruction and modeling microbial electrosynthesis. Sci. Rep. 7, 1–12.

Mokhatab, S., Poe, W.A., Mak, J.Y., 2018. Sulfur Recovery and Handling, Handbook of Natural Gas Transmission and Processing.

Montebello, A.M., Mora, M., López, L.R., Bezerra, T., Gamisans, X., Lafuente, J., Baeza, M., Gabriel, D., 2014. Aerobic desulfurization of biogas by acidic biotrickling filtration in a randomly packed reactor. J. Hazard. Mater. 280, 200–208.

Montpart, N., Rago, L., Baeza, A., Guisasola, A., 2018. Oxygen barrier and catalytic effect of the cathodic biofilm in single chamber microbial fuel cells. J. Chem. Technol. Biotechnol.

Montpart, N., Ribot-Llobet, E., Garlapati, V.K., Rago, L., Baeza, J.A., Guisasola, A., 2014. Methanol opportunities for electricity and hydrogen production in bioelectrochemical systems. Int. J. Hydrogen Energy 39, 770–777.

Moosa, S., Harrison, S.T.L., 2006. Product inhibition by sulphide species on biological sulphate reduction for the treatment of acid mine drainage. Hydrometallurgy 83, 214–222.

Muyzer, G., Stams, A.J.M., 2008. The ecology and biotechnology of sulphate-reducing bacteria. Nat. Rev. Microbiol. 6, 441–454.

Nevin, K.P., Hensley, S.A., Franks, A.E., Summers, Z.M., Ou, J., Woodard, T.L., Snoeyenbos-West, O.L., Lovley, D.R., 2011. Electrosynthesis of Organic Compounds from Carbon Dioxide Is Catalyzed by a Diversity of Acetogenic Microorganisms. Appl. Environ. Microbiol. 77, 2882–2886.

Ou, S., Zhao, Y., Aaron, D.S., Regan, J.M., Mench, M.M., 2016. Modeling and validation of single-chamber microbial fuel cell cathode biofilm growth and response to oxidant gas composition. J. Power Sources 328, 385–396.

Pandey, R. a., Biswas, R., Chakrabarti, T., Devotta, S., 2005. Flue Gas Desulfurization: Physicochemical and Biotechnological Approaches. Crit. Rev. Environ. Sci. Technol. 35, 571–622.

Pham, T.H., Boon, N., Aelterman, P., Clauwaert, P., De Schamphelaire, L., Vanhaecke, L., De Maeyer, K., Höfte, M., Verstraete, W., Rabaey, K., 2008. Metabolites produced by Pseudomonas sp. enable a Gram-positive bacterium to achieve extracellular electron transfer. Appl. Microbiol. Biotechnol. 77, 1119–1129.

Philip, L., Deshusses, M.A., 2003. Sulfur Dioxide Treatment from Flue Gases Using a Biotrickling Filter–Bioreactor System. Environ. Sci. Technol. 37, 1978–1982.

Piao, J., An, J., Ha, P.T., Kim, T., Jang, J.K., Moon, H., Chang, I.S., 2013. Power density enhancement of anion-exchange membrane-installed microbial fuel cell under bicarbonate-buffered cathode condition. J. Microbiol. Biotechnol. 23, 36–39.

Pohanish, R.P., 2008. Sittig's Handbook of Toxic and Hazardous Chemicals and Carcinogens. William Andrew.

Pol, L.W.H., Lens, P.N.L., Stams, A.J.M., Lettinga, G., 1998a. Anaerobic treatment of sulphate-rich wastewaters. Biodegradation 9, 213–224.

Pol, L.W.H., Lens, P.N.L., Stams, A.J.M., Lettinga, G., 1998b. Anaerobic treatment of sulphate-rich wastewaters 213–224.

Potter, M.C., 1910. On the difference of potential due to the vital activity of microorganisms. Proc. Univ. Durham Phil. Soc. 3, 245–249.

Pous, N., Puig, S., Dolors Balaguer, M., Colprim, J., 2015. Cathode potential and anode electron donor evaluation for a suitable treatment of nitrate-contaminated

groundwater in bioelectrochemical systems. Chem. Eng. J. 263, 151–159.

Pozo, G., Jourdin, L., Lu, Y., Keller, J., Ledezma, P., Freguia, S., 2016. Cathodic biofilm activates electrode surface and achieves efficient autotrophic sulfate reduction. Electrochim. Acta 213, 66–74.

Pozo, G., Jourdin, L., Lu, Y., Ledezma, P., Keller, J., Freguia, S., 2015. Methanobacterium enables high rate electricity-driven autotrophic sulfate reduction. RSC Adv. 5, 89368–89374.

Pozo, G., Lu, Y., Pongy, S., Keller, J., Ledezma, P., Freguia, S., 2017a. Selective cathodic microbial biofilm retention allows a high current-to-sulfide efficiency in sulfate-reducing microbial electrolysis cells. Bioelectrochemistry 118, 62–69.

Pozo, G., Pongy, S., Keller, J., Ledezma, P., Freguia, S., 2017b. A novel bioelectrochemical system for chemical-free permanent treatment of acid mine drainage. Water Res. 126, 411–420.

Preuß, V., Riedel, C., Koch, T., Thűrmer, K., Domańska, M., 2012. Nanofiltration as an effective tool of reducing sulphate concentration in mine water. Archit. Civ. Eng. Environ. 3/2012, 127–132.

Qian, J., Jiang, F., Chui, H.K., Van Loosdrecht, M.C.M., Chen, G.H., 2013. Industrial flue gas desulfurization waste may offer an opportunity to facilitate SANI® application for significant sludge minimization in freshwater wastewater treatment. Water Sci. Technol. 67, 2822–2826.

Qian, J., Liu, R., Wei, L., Lu, H., Chen, G., 2015a. System evaluation and microbial analysis of a sulfur cycle-based wastewater treatment process for Co-treatment of simple wet flue gas desulfurization wastes with freshwater sewage. Water Res. 80, 189.

Qian, J., Lu, H., Jiang, F., Ekama, G.A., Chen, G.H., 2015b. Beneficial co-treatment of simple wet flue gas desulphurization wastes with freshwater sewage through development of mixed denitrification-SANI process. Chem. Eng. J. 262, 109–118.

Qiu, Y.L., Kuang, X.Z., Shi, X.S., Yuan, X.Z., Guo, R.B., 2014. Paludibacter jiangxiensis sp. nov., a strictly anaerobic, propionate-producing bacterium isolated from rice paddy field. Arch. Microbiol. 196, 149–155.

Rabaey, K., Rozendal, R.A., 2010. Microbial electrosynthesis — revisiting the electrical route for microbial production. Nat. Rev. Microbiol. 8, 706–716.

Rabaey, K., Van de Sompel, K., Maignien, L., Boon, N., Aelterman, P., Clauwaert, P., De Schamphelaire, L., Pham, H.T., Vermeulen, J., Verhaege, M., Lens, P., Verstraete, W., 2006. Microbial Fuel Cells for Sulfide. Env. Sci Technol 40, 5218–5224.

Rabaey, K., Verstraete, W., 2005. Microbial fuel cells: Novel biotechnology for energy generation. Trends Biotechnol. 23, 291–298.

Rago, L., Guerrero, J., Baeza, J.A.,

Guisasola, A., 2015. 2-Bromoethanesulfonate degradation in bioelectrochemical systems. Bioelectrochemistry 105, 44–49.

Reinsel, M.A., 1999. A New Process for Sulfate Removal From Industrial Waters. J. Am. Soc. Min. Reclam. 546–550.

Reyes-Alvarado, L.C., Rene, E.R., Esposito, G., Lens, P.N.L., 2018. Bioprocesses for Sulphate Removal from Wastewater. Springer, Singapore, pp. 35–60.

Rosenbaum, M., Aulenta, F., Villano, M., Angenent, L.T., 2011. Cathodes as electron donors for microbial metabolism: Which extracellular electron transfer mechanisms are involved? Bioresour. Technol. 102, 324–333.

Rozendal, R. a., Hamelers, H.V.M., Buisman, C.J.N., 2006. Effects of Membrane Cation Transport on pH and Microbial Fuel. Environ. Sci. Technol. 40, 5206–5211.

Rozendal, R. a, Jeremiasse, a W., Hamelers, H.V.M., Buisman, C.J.N., 2008. Hydrogen production with a microbial biocathode. Environ. Sci. Technol. 42, 629–634.

Rozendal, R.A., Hamelers, H.V.M., Molenkamp, R.J., Buisman, C.J.N., 2007. Performance of single chamber biocatalyzed electrolysis with different types of ion exchange membranes. Water Res. 41, 1984–1994.

Rozendal, R.A., Hamelers, H.V.M., Rabaey, K., Keller, J., Buisman, C.J.N., 2008. Towards practical implementation of bioelectrochemical wastewater treatment. Trends Biotechnol. 26, 450–459.

Runtti, H., Tolonen, E.T., Tuomikoski, S., Luukkonen, T., Lassi, U., 2018. How to tackle the stringent sulfate removal requirements in mine water treatment—A review of potential methods. Environ. Res. 167, 207–222.

Saha, B., Saha, S., Roy, P.D., Padhan, D., Pati, S., Hazra, G.C., 2018. Microbial Transformation of Sulphur: An Approach to Combat the Sulphur Deficiencies in Agricultural Soils, in: Role of Rhizospheric Microbes in Soil. Springer Singapore, Singapore, pp. 77–97.

Schröder-Wolthoorn, A., Kuitert, S., Dijkman, H., Huisman, J.L., 2008. Application of sulfate reduction for the biological conversion of anglesite (PbSO4) to galena (PbS). Hydrometallurgy 94, 105–109.

Sheridan, C., Akcil, A., Kappelmeyer, U., Moodley, I., 2018. A Review on the Use of Constructed Wetlands for the Treatment of Acid Mine Drainage. Constr. Wetl. Ind. Wastewater Treat. 249–262.

Shih, Y.S., Lee, J.L., 1986. Continuous Solvent Extraction of Sulfur from the Electrochemical Oxidation of a Basic Sulfide Solution in the CSTER System. Ind. Eng. Chem. Process Des. Dev. 25, 834–836.

Sievert, S.M., Heidorn, T., Kuever, J., 2000. Halothiobacillus kellyi sp . nov ., a mesophilic , obligately chemolithoautotrophic , sulfur-oxidizing bacterium isolated from a shallow- water hydrothermal vent in the Aegean Sea , Halothiobacillus. Int. J. Syst. Evol. Microbiol. 1229–1237.

Sigalevich, P., Baev, M. V., Teske, A.,

Cohen, Y., 2000. Sulfate reduction and possible aerobic metabolism of the sulfate-reducing bacterium Desulfovibrio oxyclinae in a chemostat coculture with Marinobacter sp. strain MB under exposure to increasing oxygen concentrations. Appl. Environ. Microbiol. 66, 5013–5018.

Speece, R.E., 1983. Anaerobic biotechnology for industrial wastewater treatment. Environ. Sci. Technol. 17, 416A–427A.

Srivastava, R.K., Jozewicz, W., 2001. Flue Gas Desulfurization: The State of the Art. J. Air Waste Manage. Assoc. 51, 1676–1688.

Stolyar, S., He, Q., Joachimiak, M.P., He, Z., Zamin, K.Y., Borglin, S.E., Joyner, D.C., Huang, K., Aim, E., Hazen, T.C., Zhou, J., Wall, J.D., Arkin, A.P., Stahl, D.A., 2007. Response of Desulfovibrio vulgaris to alkaline stress. J. Bacteriol. 189, 8944–8952.

Stolz, J.F., Ellis, D.J., Blum, J.S., Ahmann, D., Lovley, D.R., Oremland, R.S., 1999. Note: Sulfurospirillum barnesii sp. nov. and Sulfurospirillum arsenophilum sp. nov., new members of the Sulfurospirillum clade of the -Proteobacteria. Int. J. Syst. Bacteriol. 49, 1177–1180.

Su, W., Zhang, L., Tao, Y., Zhan, G., Li, D., Li, D., 2012. Sulfate reduction with electrons directly derived from electrodes in bioelectrochemical systems. Electrochem. commun. 22, 37–40.

Sun, M., Mu, Z.X., Chen, Y.P., Sheng, G.P., Liu, X.W., Chen, Y.Z., Zhao, Y., Wang, H.L., Yu, H.Q., Wei, L., Ma, F., 2009. Microbe-assisted sulfide oxidation in the anode of a microbial fuel cell. Environ. Sci. Technol. 43, 3372–3377.

Sun, M., Tong, Z.-H., Sheng, G.-P., Chen, Y.-Z., Zhang, F., Mu, Z.-X., Wang, H.-L., Zeng, R.J., Liu, X.-W., Yu, H.-Q., Wei, L., Ma, F., 2010. Microbial communities involved in electricity generation from sulfide oxidation in a microbial fuel cell. Biosens. Bioelectron. 26, 470–476.

Tang, K., Baskaran, V., Nemati, M., 2009. Bacteria of the sulphur cycle: An overview of microbiology, biokinetics and their role in petroleum and mining industries. Biochem. Eng. J. 44, 73–94.

Teng, W., Liu, G., Luo, H., Zhang, R., Xiang, Y., 2016. Simultaneous sulfate and zinc removal from acid wastewater using an acidophilic and autotrophic biocathode. J. Hazard. Mater. 304, 159–165.

Thevenieau, F., Fardeau, M.L., Ollivier, B., Joulian, C., Baena, S., 2007. Desulfomicrobium thermophilum sp. nov., a novel thermophilic sulphate-reducing bacterium isolated from a terrestrial hot spring in Colombia. Extremophiles 11, 295–303.

Tice, R.C., Kim, Y., 2014. Energy efficient reconcentration of diluted human urine using ion exchange membranes in bioelectrochemical systems. Water Res. 64, 61–72.

Tichý, R., Lens, P., Grotenhuis, J.T.C., Bos, P., 1998. Solid-State Reduced Sulfur Compounds: Environmental Aspects and Bio-Remediation. Crit. Rev. Environ. Sci. Technol. 28, 1–40.

Ueki, A., Akasaka, H., Suzuki, D., Ueki, K., 2006. Paludibacter propionicigenes gen. nov., sp. nov., a novel strictly anaerobic, Gram-negative, propionate-producing bacterium isolated from plant residue in irrigated rice-field soil in Japan. Int. J. Syst. Evol. Microbiol. 56, 39–44.

Valdés, J., Pedroso, I., Quatrini, R., Dodson, R.J., Tettelin, H., Blake, R., Eisen, J.A., Holmes, D.S., 2008. Acidithiobacillus ferrooxidans metabolism: From genome sequence to industrial applications. BMC Genomics 9, 1–24.

van Houten, R.T., Pol, L.W., Lettinga, G., 1994. Biological sulphate reduction using gas-lift reactors fed with hydrogen and carbon dioxide as energy and carbon source. Biotechnol. Bioeng. 44, 586–94.

Visser, J.M., Stefess, G.C., Robertson, L.A., Kuenen, J.G., 1997. Thiobacillus sp. W5, the dominant autotroph oxidizing sulfide to sulfur in a reactor for aerobic treatment of sulfidic wastes. Antonie van Leeuwenhoek, Int. J. Gen. Mol. Microbiol. 72, 127–134.

von Gemmingen, U., Lahne, U., 1994. The Linde Clinsulf® process for sulfur recovery: Modelling and simulation. Gas Sep. Purif. 8, 241–246.

Wang, K., Cao, Z., Chang, J., Sheng, Y., Cao, H., Yan, K., Zhang, Y., 2017a. Promoted bioelectrocatalytic activity of microbial electrolysis cell (MEC) in sulfate removal through the synergy between neutral red and graphite felt. Chem. Eng. J. 327, 183–192.

Wang, K., Sheng, Y., Cao, H., Yan, K., Zhang, Y., 2017b. Impact of applied current on sulfate-rich wastewater treatment and microbial biodiversity in the cathode chamber of microbial electrolysis cell (MEC) reactor. Chem. Eng. J. 307, 150–158.

Wang, K., Sheng, Y., Cao, H., Yan, K., Zhang, Y., 2017c. A novel microbial electrolysis cell (MEC) reactor for biological sulfate-rich wastewater treatment using intermittent supply of electric field. Biochem. Eng. J. 125, 10–17.

Watanabe, K., Manefield, M., Lee, M., Kouzuma, A., 2009. Electron shuttles in biotechnology. Curr. Opin. Biotechnol. 20, 633–641.

Waybrant, K.R., Blowes, D.W., Ptacek, C.J., 1998. Selection of Reactive Mixtures for Use in Permeable Reactive Walls for Treatment of Mine Drainage. Environ. Sci. Technol. 32, 1972–1979.

Weijma, J., Gubbels, F., Hulshoff Pol, L.W., Stams, A.J., Lens, P., Lettinga, G., 2002. Competition for H2 between sulfate reducers, methanogens and homoacetogens in a gas-lift reactor. Water Sci. Technol. 45, 75–80.

Wright, E.S., Yilmaz, L.S., Noguera, D.R., 2012. DECIPHER, a Search-Based Approach to Chimera Identification for 16S rRNA Sequences. Appl. Environ. Microbiol. 78, 717–725.

Wu, D., Ekama, G.A., Chui, H.K., Wang, B., Cui, Y.X., Hao, T.W., van Loosdrecht, M.C.M., Chen, G.H., 2016. Large-scale demonstration of the sulfate reduction autotrophic

denitrification nitrification integrated (SANI®) process in saline sewage treatment. Water Res. 100, 496–507.

Yu, L., Duan, J., Zhao, W., Huang, Y., Hou, B., 2011. Characteristics of hydrogen evolution and oxidation catalyzed by Desulfovibrio caledoniensis biofilm on pyrolytic graphite electrode. Electrochim. Acta 56, 9041–9047.

Zevenhoven, R., Kilpinen, P., 2001. Flue gases and fuel gases. Control Pollut. Flue Gases Fuel Gases 2.1-2.12.

Zhang, L., Hirai, M., Shoda, M., 1991. Removal characteristics of dimethyl sulfide, methanethiol and hydrogen sulfide by Hyphomicrobium sp. 155 isolated from Peat Biofilter. J. Ferment. Bioeng. 72, 392–396.

Zhang, Y., Angelidaki, I., 2014. Microbial electrolysis cells turning to be versatile technology: Recent advances and future challenges. Water Res. 56, 11–25.

Zhao, F., Rahunen, N., Varcoe, J.R., Chandra, A., Roberts, A.J., Avignone-Rossa, C., Thumser, A.E., Slade, R.C.T., 2008. Activated Carbon Cloth as Anode for Sulfate Removal in a Microbial Fuel Cell. Environ. Sci. Technol. 42, 4971–4976.

Zhilina, T.N., Zavarzina, D.G., Kuever, J., Lysenko, A.M., Zavarzin, G.A., 2005. Desulfonatronum cooperativum sp. nov., a novel hydrogenotrophic, alkaliphilic, sulfate-reducing bacterium, from a syntrophic culture growing on acetate. Int. J. Syst. Evol. Microbiol. 55, 1001–1006.

List of contributions

Publications

Blázquez, E., Guisasola, A., Gabriel, D., Baeza, J.A., 2019. *Application of Bioelectrochemical Systems for the Treatment of Wastewaters With Sulfur Species*. Microb. Electrochem. Technol. 641–663. doi:10.1016/B978-0-444-64052-9.00026-1 (Book chapter)

Blázquez, E., Baeza, J.A., Gabriel, D., Guisasola, A., 2019. *Treatment of real flue gas desulfurization wastewater in an autotrophic biocathode in view of elemental sulfur recovery: Microbial communities involved*. Sci. Total Environ. 657, 945–952. doi:10.1016/J.SCITOTENV.2018.12.037 (IF journal: 4.610)

Blázquez, E., Gabriel, D., Baeza, J.A., Guisasola, A., 2017. *Evaluation of key parameters on simultaneous sulfate reduction and sul fi de oxidation in an autotrophic biocathode*. Water Res. 123, 301–310. doi:10.1016/j.watres.2017.06.050 (IF journal: 7.051)

Blázquez, E., Gabriel, D., Baeza, J.A., Guisasola, A., 2016. *Treatment of high-strength sulfate wastewater using an autotrophic biocathode in view of elemental sulfur recovery*. Water Res. 105, 395–405. doi:10.1016/j.watres.2016.09.014 (IF journal: 7.051)

Blázquez, E., Baeza, J.A., Gabriel, D., Guisasola, A., Freguia, S., Ledezma, P. *Recovery of elemental sulfur with a novel integrated bioelectrochemical system with an electrochemical cell*. Submitted at: Sci. Total Environ.

Blázquez, E., Baeza, J.A., Gabriel, D., Guisasola, A., Ledezma, P., Freguia, S. *Effect of an air-cathode in an integrated bioelectrochemical system for sulfate treatment, sulfide abatement and elemental sulfur recovery.* Under preparation.

Conference contributions

Blázquez, E., Guisasola, A., Baeza, J. A., Gabriel, D., Freguia, S., Ledezma, P. *Recovery of elemental sulfur and metals from acid mine drainage as trace nutrients for next-generation fertilizer formulations*. IWA: Nutrient Removal and Recovery 2018, Brisbane, Australia, 18/11/2018 – 21/11/2018. (Oral presentation)

Blázquez, E., Gabriel, D., Baeza, J. A., Guisasola, A. *Bioelectrochemical Treatment of Sulfate Wastewater Towrds Sulfur Recovery*. IWA World Water Conference 2018, Tokyo, Japan, 16/09/2018 – 21/09/2018. (Poster)

Blázquez, E., Gabriel, D., Baeza, J. A., Guisasola, A. *Opportunities of BES for sulfate wastewater treatment: potential sulfur recovery*. ISMET6, Lisbon, Portugal, 03/10/2017 – 06/10/2017. (Oral presentation)

Blázquez, E., Guisasola, A., Baeza, J. A., Gabriel, D. *Effect of pH on the treatment of high-strength sulphate wastewaters in bioelectrochemical systems for elemental Sulphur recovery*. Biotechniques 2017, Coruña, Spain, 19/07/2017 – 21/07/2017. (Oral presentation)

Blázquez, E., Gabriel, D., Baeza, J. A., Guisasola, A. *Simultaneous autotrophic sulfate reduction and sulfide oxidation to elemental sulfur in a BES cathode*. IWA: EcoSTP16, Cambridge, United Kingdom, 27/06/2016 – 30/06/2016. (Oral presentation)

Blázquez, E., Baeza, J. A., Gabriel, D., Guisasola, A. *Promoting autotrophic sulfate reduction in bioelectrochemical systems*. Biotechniques 2015, Ghent, Belgium, 02/09/2015 – 04/09/2015. (Oral presentation)